



Cairo University

**A NOVEL COMPANDING TECHNIQUE TO REDUCE HIGH PEAK TO AVERAGE
POWER RATIO IN OFDM SYSTEM**

Submitted by

Abdulwahid Mohammed Abdulwahid Mohammed

A Thesis Submitted to the

Faculty of Engineering at Cairo University

in Partial Fulfillment of the

Requirements for the Degree of

Master of Science

in

ELECTRONICS AND COMMUNICATIONS ENGINEERING

FACULTY OF ENGINEERING, CAIRO UNIVERSITY

GIZA, EGYPT

2019

**A NOVEL COMPANDING TECHNIQUE TO REDUCE HIGH PEAK TO AVERAGE
POWER RATIO IN OFDM SYSTEM**

Submitted by

Abdulwahid Mohammed Abdulwahid Mohammed

A Thesis Submitted to the
Faculty of Engineering at Cairo University
in Partial Fulfillment of the
Requirements for the Degree of
Master of Science

in

ELECTRONICS AND COMMUNICATIONS ENGINEERING

Under the Supervision of

Amin Nassar

Professor of Communications Engineering
Electronics and Communications Department
Faculty of Engineering, Cairo University

Hassan Mostafa

Associate Professor of Electronics Engineering
Electronics and Communications Department
Faculty of Engineering, Cairo University

FACULTY OF ENGINEERING, CAIRO UNIVERSITY

GIZA, EGYPT

2019

**A NOVEL COMPANDING TECHNIQUE TO REDUCE HIGH PEAK TO AVERAGE
POWER RATIO IN OFDM SYSTEM**

Submitted by

Abdulwahid Mohammed Abdulwahid Mohammed

A Thesis Submitted to the
Faculty of Engineering at Cairo University
in Partial Fulfillment of the
Requirements for the Degree of

Master of Science

in

ELECTRONICS AND COMMUNICATIONS ENGINEERING

Approved by the Examining Committee		Signature
Prof. Dr. Amin Nassar	Thesis main Advisor
<hr/>		
Prof. Dr. Hassan Mostafa	Advisor
<hr/>		
Prof. Dr. Ahmed Hussain Khalil	Internal Examiner
<hr/>		
Prof. Dr. Al-sayed Mustafa Saad	External Examiner

(Professor in Faculty of Engineering, Helwan University)

FACULTY OF ENGINEERING, CAIRO UNIVERSITY

GIZA, EGYPT

2019

Engineer's Name : Abdulwahid Mohammed Abdulwahid
Date of Birth : 01 March 1985
Nationality : Yemeni
Email : abdulwahid1520121@eng1.cu.edu.eg
Mobile : +201150747206
Address : Faisal King Street, Giza, Egypt
Registration Date : 01 October 2015
Awarding Date :/...../ 2019
Degree : Master of science
Department : Electronics and Communications Engineering
Supervisors :



Prof. Amin Nassar
Prof. Hassan Mostafa

Examiners :

Prof. Dr. Amin Nassar Thesis main Advisor
Prof. Dr. Hassan Mostafa Advisor
Prof. Dr. Ahmed Hussain Khalil Internal Examiner
Prof. Dr. Al-sayed Mustafa Saad External Examiner
(Professor in Faculty of Engineering, Helwan University)

Title of Thesis:

A Novel companding technique to reduce high peak to average power ratio in OFDM system.

Key Words:

Orthogonal frequency division multiplexing (OFDM), peak-to-average-power-ratio (PAPR) and image adjustment (IMADJS).

Summary:

In the presented work, new companding technique is used to reduce high peak to average power ratio (PAPR) in orthogonal frequency division multiplexing (OFDM) systems. The new companding technique (IMADJS) is used in image processing to do enhancement for pictures. This technique is applied on the OFDM signal to reduce the high PAPR problem. Then, the results of the new technique will be compared with some existing companding methods. The simulation results using Matlab proves that the best results in PAPR, BER and PSD can be achieved by using the new technique (IMADJS).

Disclaimer

I hereby declare that this thesis is my own original work and that no part of it has been submitted for a degree qualification at any other university or institute.

I further declare that I have appropriately acknowledged all sources used and have cited them in the references section

Name : Abdulwahid Mohammed

Date : / / 2019

Signature :

A handwritten signature in blue ink, appearing to be 'Abdulwahid Mohammed', written over a horizontal line.

Acknowledgments

First and foremost, I am thankful to God, the most gracious most merciful for helping me finishing this work.

It is a pleasure to acknowledge my supervisors that have profoundly endued me with guidance and support. I wish to express my sincere thanks to Prof. Amin Nassar, Cairo University, for his valuable supervision, continuous encouragement, useful suggestions, and active help during the course of this work. I would like to thank my supervisor, Prof. Hassan Mostafa, Cairo University, for the patient guidance, encouragement and advice he has provided throughout my time as his student. I have been extremely lucky to have a supervisor who cared so much about my work, and who responded to my questions and queries so promptly.

I also extend my gratitude to Prof Dr. Erzsébet Csereklye from Eötvös University, Hungary for her valuable revision, which greatly improved my technical writing skills.

Finally, I am indebted to my father, my mother and my wife, who are always beside me in all happy as well as hard times.

List of Published Papers

Published Papers

Accepted

1. Mohammed, A., M. Shehata, H. Mostafa, and A. Nassar, "Peak-to-Average Power Ratio Suppression Using Companding Schemes in OFDM Systems", IEEE International Midwest Symposium on Circuits and Systems (MWSCAS 2018), Windsor, Ontario, Canada, pp. 933-936, 2018.
2. Mohammed, A., M. Shehata, A. Nassar, and H. Mostafa, "Performance Comparison of Companding-Based PAPR Suppression Techniques in OFDM Systems", IEEE International Conference on Modern Circuits and Systems Technologies (MOCAS 2019), Thessaloniki, Greece.

Under review

1. A. Mohammed, A. Nassar, and H. Mostafa, "A Novel Companding Technique to Reduce High Peak to Average Power Ratio in OFDM Systems"

Contents

Disclaimer	i
Acknowledgements	ii
List of Published Papers	iii
List of Figures	vii
List of Tables	ix
List of Abbreviations	x
1 Overview and transmission impairment types	1
1.1 Transmission impairments	1
1.1.1 Attenuation	1
1.1.2 Distortion	2
1.1.3 Noise	3
1.2 Signal to Noise Ratio (SNR)	3
1.3 Multi-path transmission	4
1.4 Inter-symbol interference (ISI)	5
1.5 Single-carrier and multi-carrier modulation	5
1.5.1 Single-carrier modulation	5
1.5.2 Multi-carrier Modulation	6
2 Basic principles of OFDM system	7
2.1 Introduction	7
2.2 Orthogonal Frequency Division Multiplexing	8
2.3 The Concept of Orthogonality	9
2.4 The advantages of OFDM systems	11
2.5 Major problems of OFDM system	11
2.6 Basic Concept of the OFDM	13
2.7 Block Diagram of OFDM System	13
2.7.1 Modulation	14
2.7.2 Serial to Parallel Conversion (S/P)	15
2.7.3 OFDM Modulation	15

2.7.4	Implementation of FFT	16
2.7.5	Cyclic Prefix Extension	17
2.8	Base-band and Pass-band signals	19
2.9	Modeling of the channel	21
2.10	Modeling of the receiver	22
3	Peak to average power ratio (PAPR)	24
3.1	Introduction	24
3.2	Definition of the PAPR	24
3.3	Complementary cumulative distribution function	27
3.4	Non-linear Power Amplifier effects	28
3.5	PAPR reduction schemes	29
3.5.1	Distortion based techniques	29
3.5.2	Non-distortion techniques	30
3.5.3	Hybrid techniques	30
3.6	Criteria for Selection of PAPR Reduction Techniques	30
4	Comanding techniques	32
4.1	A-law companding technique	33
4.2	μ -law companding	35
4.3	Absolute exponential (AEXP) companding technique	36
4.4	Non-linear error function (NERF) companding technique	37
4.5	Proposed companding technique (IMADJS)	38
5	Simulation Results and Analysis	41
5.1	Simulation results of companding techniques	41
5.1.1	Simulation results for A-law companding technique	42
5.1.2	Simulation results for μ -law companding technique	44
5.1.3	Simulation results for AEXP companding technique	45
5.1.4	Simulation results for NERF companding technique	46
5.2	Simulation results for the new companding technique	46
5.2.1	The effect of changing the <i>low-in</i> parameter on PAPR and BER	48
5.2.2	The effect of changing the <i>low-out</i> parameter on PAPR and BER	50
5.2.3	The effect of changing the <i>high-out</i> parameter on PAPR and BER	53
5.2.4	The effect of changing the <i>high-in</i> parameter on PAPR and BER	57
5.2.5	The effect of changing the degree of companding (γ) on PAPR and BER in IMADJS technique	59
5.3	Performance comparison of companding-based PAPR suppression techniques using multi-path channel.	62
5.3.1	Comparing IMADJS technique with the existing companding techniques based on the PAPR and BER.	62
5.3.2	Comparing IMADJS technique with the existing companding techniques based on the average power.	65
5.3.3	Comparing IMADJS technique with the existing companding techniques based on PSD.	66

5.3.4	Comparing IMADJS technique with the existing companding techniques based on execution time.	67
6	Conclusion and future work	68
6.1	Conclusion	68
6.2	Future work	70
	Bibliography	71

List of Figures

1.1	Impairment types.	1
1.2	Attenuation of signal [1].	2
1.3	Distortion of signal [1].	2
1.4	Noise effect on the signal [1].	3
1.5	A wireless channel with multipath propagation [2].	4
1.6	Basic structure of a single carrier system [3].	5
1.7	Basic structure of a multi-carrier system [3].	6
2.1	Representation of OFDM: (a) Conventional multi-carrier technique (FDM), (b) Orthogonal multi-carrier modulation technique (OFDM) [4].	8
2.2	Frequency response of 3 sub-carriers of OFDM signal.	9
2.3	Orthogonality among the sub-carriers in time domain [5].	10
2.4	Effects of carrier frequency offset [6].	12
2.5	One OFDM symbol in time domain.	12
2.6	Block Diagram of OFDM System [4].	14
2.7	QPSK, 16-QAM, and 64-QAM constellation [4].	14
2.8	Serial to Parallel Conversion [7].	15
2.9	OFDM Modulator [7].	16
2.10	The ISI due to multi-path propagation [4].	17
2.11	OFDM symbol with cyclic extension [4].	18
2.12	OFDM symbol with cyclic prefix (CP) [4].	18
2.13	Base-band versus pass-band: (a) base-band to pass-band conversion, and (b) pass-band to base-band conversion [8].	20
3.1	Power amplifier transfer function.	25
3.2	An example illustrating effects of clipping [9].	26
3.3	CCDF of PAPR for N=64, 256, 1024 and 4096 sub-carriers.	28
3.4	Effects of non-linear power amplifier on: (a) signal spectrum, (b) signal constellation, (c) amplifier response and (d) bit error rate.	29
4.1	Bloc diagram of companding technique for an OFDM system	33
4.2	Transfer function of A-law companding technique	34
4.3	Transfer function of μ -law companding technique	35
4.4	Plots of AEXP transfer function	37
4.5	Plots of NERF transfer function	38

4.6	The IMADJS function with $\gamma=1$, $\gamma < 1$ and $\gamma > 1$	39
4.7	Plots of IMADJS transfer function	40
5.1	The effect of changing the parameter A on: (a) PAPR and (b) BER.	42
5.2	The effect of changing the parameter A on the average power and constellation points	43
5.3	The effect of changing the parameter μ on: (a) PAPR and (b) BER.	44
5.4	The effect of changing the parameter d on: (a) PAPR and (b) BER.	45
5.5	Plots of PAPR & BER for NERF companding technique: (a) PAPR and (b) BER	46
5.6	An OFDM signal with high PAPR.	47
5.7	Plot of PAPR & BER for the OFDM signal: (a) PAPR and (b) BER.	47
5.8	The effect of changing the <i>low-in</i> parameter on: (a) PAPR and (b) BER	48
5.9	Transfer function of IMADJS companding technique with the change of <i>low-in</i> parameter.	49
5.10	IMADJS technique with the change of <i>low-in</i> parameter: (a) PAPR and (b) BER	50
5.11	The effect of changing the <i>low-out</i> parameter on: (a) PAPR and (b) BER	51
5.12	Transfer function of IMADJS companding technique with the change of <i>low-out</i> parameter.	52
5.13	IMADJS technique with the change of <i>low-out</i> parameter: (a) PAPR and (b) BER	53
5.14	The effect of changing the <i>high-out</i> parameter on: (a) PAPR and (b) BER	54
5.15	Transfer function of IMADJS companding technique with the change of <i>high-out</i> parameter.	55
5.16	IMADJS technique with the change of <i>high-out</i> parameter: (a) PAPR and (b) BER	56
5.17	The effect of changing the <i>high-in</i> parameter on: (a) PAPR and (b) BER	57
5.18	Transfer function of IMADJS companding technique with the changing of <i>high-in</i> parameter.	58
5.19	IMADJS technique with the change of <i>high-in</i> parameter: (a) PAPR and (b) BER	59
5.20	Effect of decreasing the γ value on the IMADJS technique with (a): PAPR and (b): BER.	60
5.21	Product of the PAPR curve and the BER curve	61
5.22	Transfer function of IMADJS technique with the change of γ parameter.	61
5.23	Comparing the different companding techniques based on BER when they have same PAPR: (a) same PAPR and (b) BER.	63
5.24	Comparing the different companding techniques based on PAPR when they have same BER: (a) same BER and (b) PAPR.	64
5.25	Comparing the different companding techniques based on the average power: (a) IMADJS technique, (b) NERF technique, (c) EXP technique and (d) μ -law technique.	65
5.26	PSD for Original signal versus companded signals by using different companding techniques: μ -law, NERF, AEXP and IMADJS.	66

List of Tables

5.1	Simulation Parameters	41
5.2	Performance comparison for different values of parameter A	42
5.3	Performance comparison for different values of parameter μ	44
5.4	Performance comparison for different values of parameter d	45
5.5	Channel Power-Delay profile [10].	62
5.6	Execution time for four companding techniques	67

List of Abbreviations

A

3G	Third Generation
3GPP	3rd Generation Partnership Project
4G	Fourth Generation
A/D	Analog-to-digital
ACI	Adjacent channel interference
AWGN	Additive white Gaussian noise
AEXP	Absolute Exponential
Avg	Average

B

BER	Bit error rate
BPSK	Binary PSK

C

CCDF	Complementary cumulative distribution function
CDF	Cumulative distribution function
CPM	Continuous phase modulation
CFO	Carrier frequency offsets

D

DAB	Digital audio broadcasting
D/A	Digital-to-analog
DFT	Discrete Fourier transform
DSL	Digital subscriber lines
DVB-T	Terrestrial digital video broadcasting
DL	Downlink
DCT	Discrete cosine transform
DST	Discrete sine transform
DHT	Discrete Hartley transform

E

ERF	Error function
-----	----------------

F

FDE	Frequency domain equalization
FDM	Frequency division multiplexing
FFT	Fast Fourier transform
FIR	Finite impulse response

G

GPRS	General packet radio service
GSM	Global system for mobile communications

I

IBI	Inter-block interference
IBO	Input power back off
ICI	Inter-carrier interference
IDFT	Inverse discrete Fourier transform
IFFT	Inverse fast Fourier transform
i.i.d.	Identically distributed
ISI	Inter-symbol interference
IQ	In phase and quadrature
IMADJS	Image adjustment

L

LTE	Long term evolution
LTE-A	Long term evolution advanced

M

MCM	Multi-carrier modulation
-----	--------------------------

N

NERF	Non-linear error function
------	---------------------------

O

OFDM	Orthogonal frequency division multiplexing
OOB	Out of band
OBO	Output back off

P

PA	Power amplifier
PAM	Pulse amplitude modulation
PAPR	Peak-to-average power ratio
PLC	Power line communication
PTS	Partial transmit sequences

Q

QAM	Quadrature amplitude modulation
QPSK	Quadrature phase shift keying

R

RMS	Root-mean-square
-----	------------------

S

SI	Side information
SLM	Selective mapping
SNR	Signal-to-noise ratio
S/P	Serial-to-parallel
SC	Sub-carrier
SCs	Sub-carriers

T

tanh	Hyperbolic tangent
------	--------------------

W

WLAN	Wireless local area network
WLANs	Wireless local area networks
WiMAX	Worldwide interoperability for microwave access
WHT	Walsh-Hadamard Transform

Abstract

Orthogonal frequency division multiplexing (OFDM) is a striking multi-carrier transmission technique for wide-band communications because it efficiently converts the frequency selective fading channel into a flat fading channel. Therefore, OFDM provides better resistance to multi-path fading and impulsive noise, and reduces the need for complicated equalizers. OFDM could be utilized at the core of well-known systems such as asymmetric digital subscriber line (ADSL) internet, digital television/radio broadcasting, wireless local area network (WLANs), and Long Term Evolution (LTE). However, OFDM communication systems have two main disadvantages. The first drawback is the high sensitivity to carrier frequency offsets (CFO) and phase noise, while the second and main aspect is the high peak-to-average power ratio (PAPR) of the transmitted signals. The high PAPR makes OFDM sensitive to non-linear distortion caused by the transmitter power amplifier (PA), and correspondingly, leads to degradation in the system performance.

This thesis is divided into three key parts. The first part provides a complete overview of an OFDM system and the PAPR problem in multi-carrier systems. This is followed by the companding schemes, one of the most popular non-linear techniques, due to its good system performance including PAPR reduction and BER, low implementation complexity and no bandwidth expansion.

The second part explains the performance of the companding techniques including: A -law, μ -law, absolute exponential (AEXP) and non-linear error function (NERF) companding techniques. In this part, new companding technique (IMADJS) is considered to reduce high PAPR. The complementary cumulative distribution function (CCDF) and the bit error rate (BER) is used here as the performance metrics of interest. The main goal of this part is to show the improvement in PAPR and the degradation in BER for each technique separately.

The third part shows the comparative study of the performance of the companding techniques including: μ -law, absolute exponential (AEXP), non-linear error function (NERF) and new technique (IMADJS). The comparative study is based on: the improvement in PAPR, the degradation in BER, average power (Avg-pw) and power spectral density (PSD). At the same PAPR for all technique, the best technique based on BER and PSD is the proposed technique (IMADJS).

Overview and transmission impairment types

1.1 Transmission impairments

In any communication system, the received signal is never identical to the transmitted one due to the transmission impairments. As the transmission media is not perfect, it causes changes in the transmitted signal. When a transmitted signal passes through a transmission medium, the transmitted signal at the source and the received signal at the destination are not the same. In other words, what is sent is not what is received [11, 12]. There are various kinds of transmission impairments, the most significant impairments include: attenuation, distortion and noise, as shown in Figure 1.1.

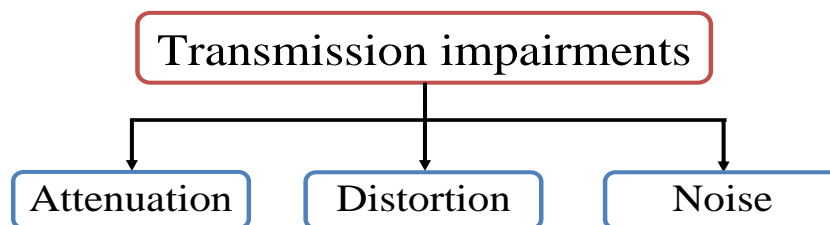


Figure 1.1: Impairment types.

1.1.1 Attenuation

As Stallings (1997) described, attenuation means a loss of energy. The strength of a signal attenuates with increasing the distance which causes the loss of energy. When a signal travels through a medium, it loses some of its energy in overcoming the resistance of the medium. To compensate this loss, amplifiers are used to amplify the signal. Figure 1.2 shows the effect of attenuation and amplification. The received signal strength must be high enough to be detected by the electronic circuitry in the receiver. Moreover, it must be sufficiently higher than noise to be received without error. Attenuation decides the signal to noise ratio (SNR), and therefore the quality of the received signal [11]. Attenuation in decibel (dB) is given as:

$$Attenuation(dB) = 10 \cdot \text{Log}_{10} \frac{P_{out}}{P_{in}}. \quad (1.1.1)$$

Where, P_{in} is the signal power at the transmitting end (source) of a communication circuit and P_{out} is the signal power at the receiving end (destination).

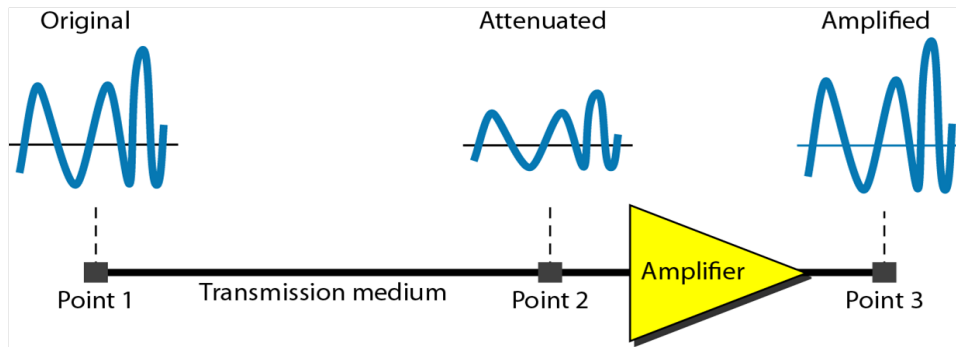


Figure 1.2: Attenuation of signal [1].

1.1.2 Distortion

Another manifestation of distortion is the change in the shape of the signal. This type of distortion is observed for the composite signals made by different frequencies. Each signal component has its own propagation speed through a medium, and therefore its own delay for arriving to the final destination. Thus, various frequency components of a signal will arrive at the receiver at different times. This effect is referred to delay distortion, as the received signal is distorted due to variable delay in its components, as shown in Figure 1.3. In other words, signal components at the receiver side have different phases from what they had at the transmitter side. The shape of the composite signal is therefore not the same [11].

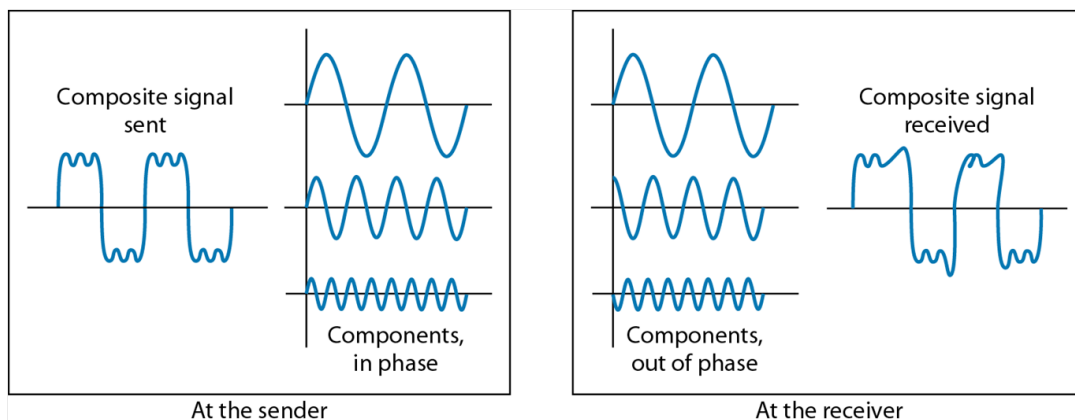


Figure 1.3: Distortion of signal [1].

1.1.3 Noise

Noise refers to any unwanted signal. For any data transmission process, the received wave will contain the transmitted signal, adjusted by the several distortions forced by the transmission system, plus additional undesirable signals that are inserted somewhere between the sender and the receiver as shown in Figure 1.4. There are several types of noise, such as thermal noise, induced noise, cross-talk, and impulse noise, which may corrupt the signal. Thermal noise is the random movement of electrons in a wire which produces an additional signal not originally sent by the transmitter. Induced noise is the noise created in a circuit by a varying magnetic or electrostatic field made by another circuit. Cross-talk is a disturbance produced by the electric or magnetic fields of one telecommunication signal affecting a signal in an adjacent circuit. In a telephone circuit, cross-talk can result in your hearing part of a voice conversation from another circuit. The phenomenon that causes cross-talk is called electromagnetic interference (EMI). It can occur in microcircuits inside computers and audio equipment as well as network circuits. The cross-talk term is also applied to optical signals that interfere with each other [11]. Impulse noise is a signal with high energy in a very short time that comes from power lines, lightning, and so on.

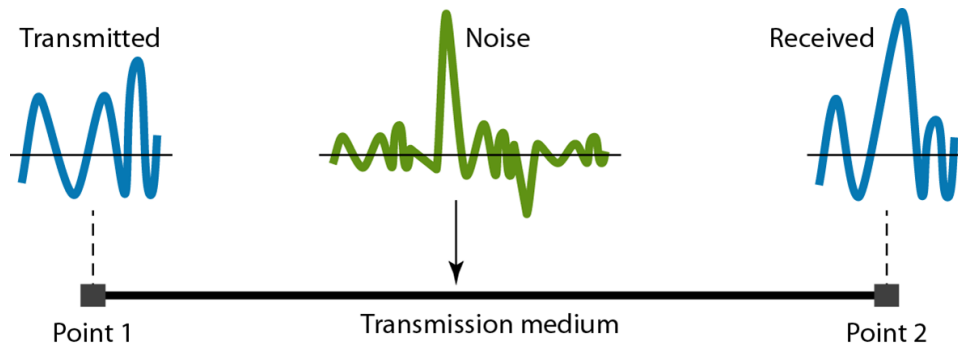


Figure 1.4: Noise effect on the signal [1].

1.2 Signal to Noise Ratio (SNR)

A signal-to-noise ratio compares the level of signal power to the level of noise power. It is most often expressed as a measurement in decibels (dB). Higher numbers generally mean a better specification, since there is more useful information (the signal) than unwanted data (the noise). The ratio between the signal power and the noise power is the Signal-Noise Ratio (SNR). Mathematically, SNR can be calculated as [11]:

$$SNR = \frac{P_{signal}}{P_{noise}}. \quad (1.2.1)$$

Where, P_{signal} is the power of the signal and P_{noise} is the power of the noise.

SNR is usually represented in decibels (dB) as follows:

$$SNR(dB) = 10 \cdot \text{Log}_{10} \left(\frac{P_{signal}}{P_{noise}} \right). \quad (1.2.2)$$

Or if working with the amplitudes of signal and noise, it can be represented as follows:

$$SNR(dB) = 20 \text{Log}_{10} \left(\frac{A_{signal}}{A_{noise}} \right). \quad (1.2.3)$$

Where, A_{signal} is the amplitude of the signal and A_{noise} is the amplitude of the noise.

1.3 Multi-path transmission

Most broadband systems are subject to multi-path transmission. In wireless communication systems, the transmission mediums between senders and receivers are not perfect. Consequently, the signal may be reflected by many objects such as buildings, mountains, cars, trees, etc. Therefore, at the receiver side, multiple signals will arrive at different time and various intensities. The received signal is the sum of several versions of transmitted signal with varying delay and attenuation as shown in Figure 1.5. Multi-path transmission leads to inter-symbol interference [13].

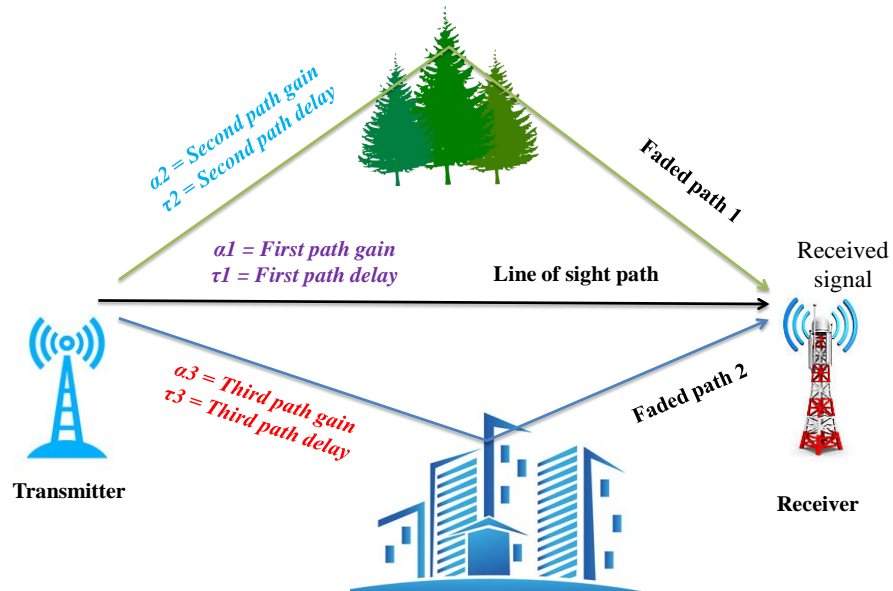


Figure 1.5: A wireless channel with multipath propagation [2].

1.4 Inter-symbol interference (ISI)

One of the causes of inter-symbol interference is multi-path transmission, where in a wireless communication system the signal arrives at the receiver via several paths. The several paths between transmitter and receiver cause different versions of the received signal at different time and power intensities. This delay means that part or all of a given symbol will be spread into the next symbols. The ISI appears significantly in high data rate systems, because the symbol period is less than the delay spread in high data rate systems. The presence of ISI in the system produces errors at the receiver output. Therefore, in the design of the transmitting and receiving filters, the goal is to reduce the impacts of ISI, and thereby to transport the information to its destination with minimum error rate possible [13].

1.5 Single-carrier and multi-carrier modulation

Single-carrier and multi-carrier modulation are two modulation techniques that are used in modern communication systems.

1.5.1 Single-carrier modulation

Single carrier is also called serial transmission. In this modulation, the data is modulated onto only one carrier, as shown in Figure 1.6. In any digital system, the data is in bits or in collection of bits (symbol). The symbol duration of a single-carrier modulation is the inverse of bandwidth ($T_s = 1/B$). When information rates increase, that means the duration of symbol (T_s) becomes smaller [14]. In the case of a channel delay spread τ is larger than the symbol duration T_s , inter-symbol interference (ISI) will arise significantly and errors will increase too. Several conditions (such as frequency selective fading due to multi-path transmission, impulse noise and interference from other sources) make the system more likely to lose information.

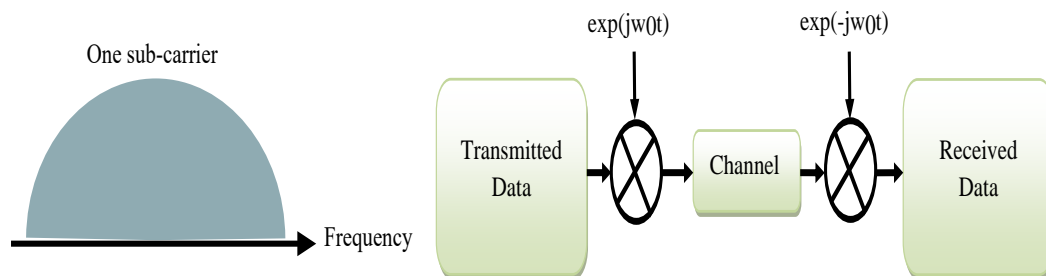


Figure 1.6: Basic structure of a single carrier system [3].

1.5.2 Multi-carrier Modulation

Multi-carrier modulation (MCM) is a technique that transmits information by dividing it into many streams of bits, each stream is sent by a separate carrier. In other words, this technique divides the bandwidth into sub-bandwidths (narrow bandwidths). However, the composite signal still has broad bandwidth. Frequency division multiplexing (FDM) is an example of the multi-carrier modulation. In FDM systems, the transmitting information (data) is split into N lower rate streams. Each stream is modulated over separate sub-carrier simultaneously, as shown in Figure 1.7. If the data rate is R_s , then the data rate for each stream is R_s/N . Therefore, the symbol duration is NT_s for each parallel stream. This means that the symbol duration of a multi-carrier system is N times longer than the symbol duration of a single carrier; and also much greater than the channel delay spread τ . So the MCM has immunity to multi path fading and inter-symbol interference [15].

To avoid one sub-carrier's spectrum from interfering with another, and to guarantee accurate individual demodulation of sub-carriers using filters, FDM systems need guard bands between the modulated sub-carriers. However, using these guard bands leads to poor bandwidth efficiency, as shown in Figure 1.7. Orthogonal frequency division multiplexing (OFDM) is used to overcome the problem of bandwidth loss. Chapter 2 will explain in details the Principle of OFDM modulation and how it can overcome the problem of poor spectral efficiency.

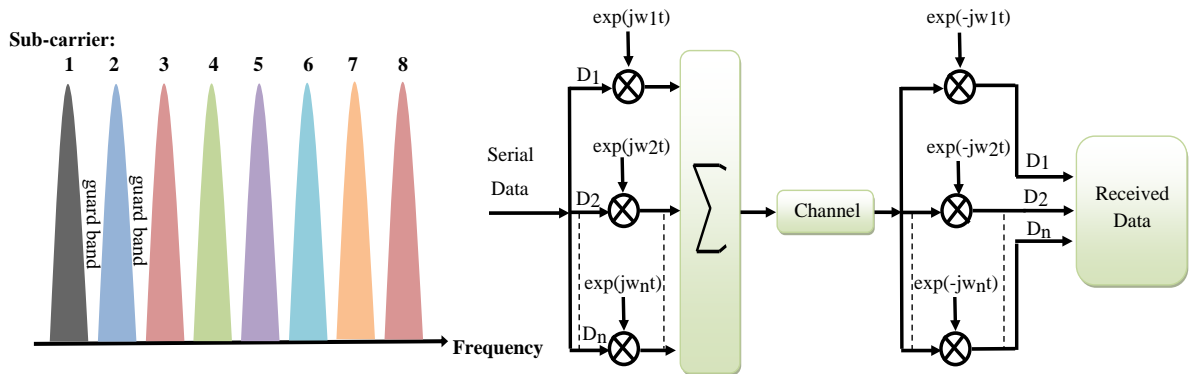


Figure 1.7: Basic structure of a multi-carrier system [3].

Basic principles of OFDM system

2.1 Introduction

Orthogonal frequency division multiplexing (OFDM) [16] [17] [18] is a multi-carrier technique, which is effective and active in 4G communication systems. OFDM divides the available bandwidth into many sub-bandwidths. In OFDM, the data is divided into several streams of low rates, and the parallel data are modulated simultaneously, using multiple carriers. Due to this parallel transmission, the symbol duration increases, thus decrease the prorated amount of dispersion in time resulting from the multi-path delay spread. OFDM has several advantages that make it widely used for many communication systems such as Worldwide Interoperability for Microwave Access (WiMAX), Terrestrial Digital Video Broadcasting (DVB-T), Digital Audio Broadcasting (DAB), IEEE 802.11a standard for Wireless Local Area Networks (WLAN) and IEEE 802.16a standard for Wireless Metropolitan Area Networks (WMAN) [19–21]. OFDM is also used for wire-line applications, such as power line communication (PLC) [22] and digital subscriber lines (DSL) [23]. OFDM has the ability to minimize the multi-path propagation effects and the impulse noise, because it effectively transforms the frequency selective fading channel into a flat fading channel. In addition, OFDM eliminates the need for equalizers and uses modern digital signals processing techniques, such as the fast Fourier transform (FFT) technique. Unfortunately, some major drawbacks are still associated with the OFDM transmission technique. One of these drawbacks is the high peak-to-average-power-ratio (PAPR) of transmitted OFDM signals [24].

For an OFDM signal, consisting of N individual and independent data symbols, when the N signals add up to the same phase, a substantial increase in the PAPR is observed. The value of the observed instantaneous PAPR might reach as high as N times of the average OFDM symbol amplitude [21]. In this case, the high power amplifier (HPA) and the digital to analog converter (DAC) need large dynamic ranges to avoid the clipping of the observed large amplitude of the OFDM symbol. On the other hand, adapting the dynamic range of the HPA and the DAC to the high PAPR values increases the power consumption as well as the implementation complexity of the transceiver design. Therefore, the PAPR of OFDM signals should be reduced as long as an efficient and economic operation of the entire OFDM signal processing circuitry is desired.

2.2 Orthogonal Frequency Division Multiplexing

Inter-symbol Interference (ISI) is one of the most challenging issues in communication systems. To avoid this problem, the delay spread τ should be smaller than the symbol duration [20]. A multi-carrier system such as frequency division multiplexing (FDM) splits the total bandwidth into non overlapping sub-bands. Each sub-band is used to send a separate signal in parallel [20]. In order to get high data rate, the sub-carriers should be placed closely in the spectrum. Because of the lack of spacing between neighboring sub-carriers, the inter-carrier interference (ICI) will happen. To solve this problem, guard bands are needed between neighboring sub-carriers, as shown in Figure 2.1(a). However, this solution leads to decrease in the data rate transmission and then decreases the bandwidth efficiency.

Orthogonal frequency division multiplexing (OFDM) is a multi-carrier digital communication technique. The OFDM signal can be described as a set of closely spaced FDM sub-carriers [20, 21, 25]. In OFDM, in addition to split the available bandwidth into several sub-bandwidths, it also combines large number of overlap sub-carriers to get the high data rate communication system, as shown in Figure 2.1(b). The low data rate of each sub-carrier leads to long symbol duration, which greatly minimizes the inter-symbol interference (ISI). Orthogonality is used in this technique to prevent interference between overlapping carriers. Consequently, the OFDM system solves both problems: Inter-carrier interference (ICI) and inefficiency of bandwidth [26, 27].

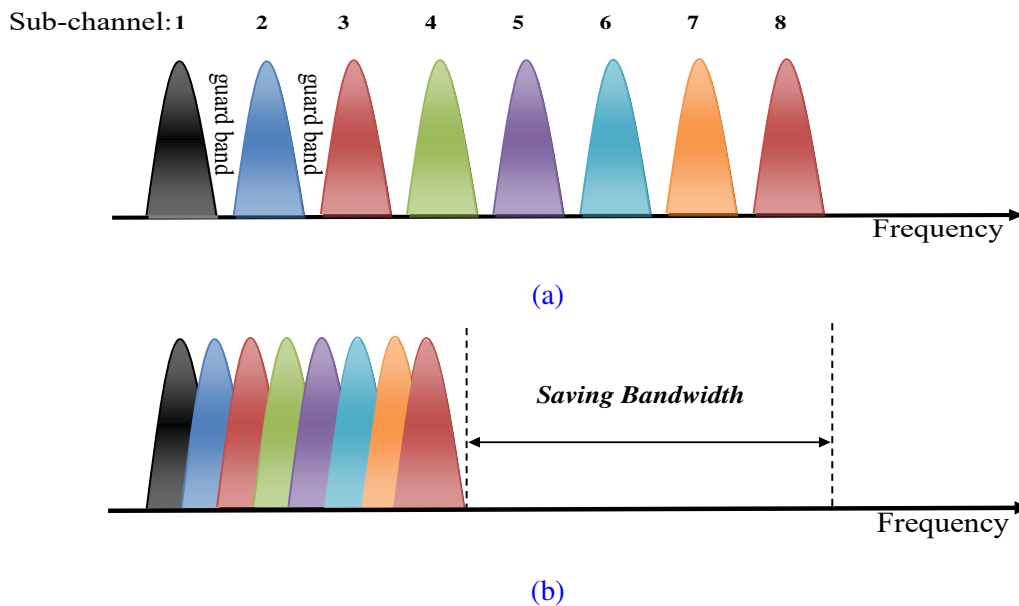


Figure 2.1: Representation of OFDM: (a) Conventional multi-carrier technique (FDM), (b) Orthogonal multi-carrier modulation technique (OFDM) [4].

2.3 The Concept of Orthogonality

The main idea of OFDM technique is the orthogonality. Orthogonality permits several signals to be carried and detected over a common channel, without any interference [28]. There are two conditions to achieve the orthogonality between sub-carriers [29]. The first condition in the frequency domain is that, the orthogonality can be achieved by doing the peak of each sub-carrier synchronizes with the null of adjacent sub-carriers, as shown in Figure 2.2. This leads to a completely aligned and spaced sub-carrier signal [30]. Figure 2.2 shows three sub-carriers (red, green and blue). At sub-carrier 1 (red sub-carrier), only sub-carrier 1 has non zero value and all other sub-carriers have zero value, which means that other sub-carriers don't influence on the first sub-carrier. At sub-carrier 2 (green sub-carrier), only sub-carrier 2 has non zero value and all other sub-carriers have zero value, which means that other sub-carriers don't influence on the second sub-carrier. Same thing for the third sub-carrier, as it is clear in Figure 2.2. Black curve in Figure 2.2 displays the sum of all sub-carriers (red, green and blue). Second condition is in the time domain, duration of the OFDM symbol (T); each sub-carrier has an integer number of cycles. Between two neighboring sub-carriers; the difference between the number of cycles equal to one as shown in Figure 2.3.

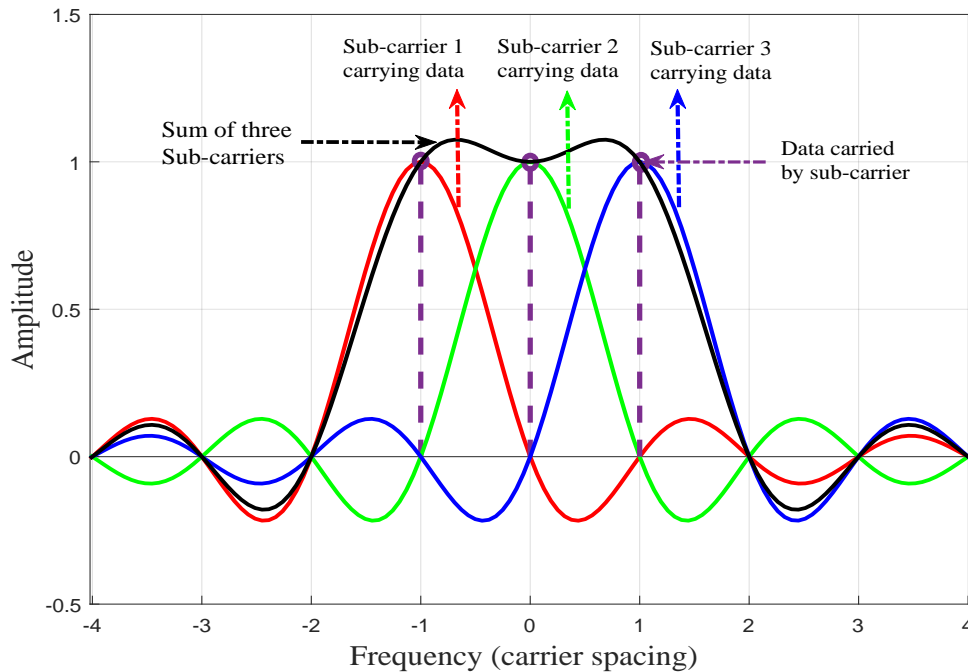


Figure 2.2: Frequency response of 3 sub-carriers of OFDM signal.

Two signals are said to be orthogonal if they are mutually independent of each other. In other words, to achieve orthogonality, the product of two signals must equal to zero [31]. Mathematically, it can be expressed as follows:

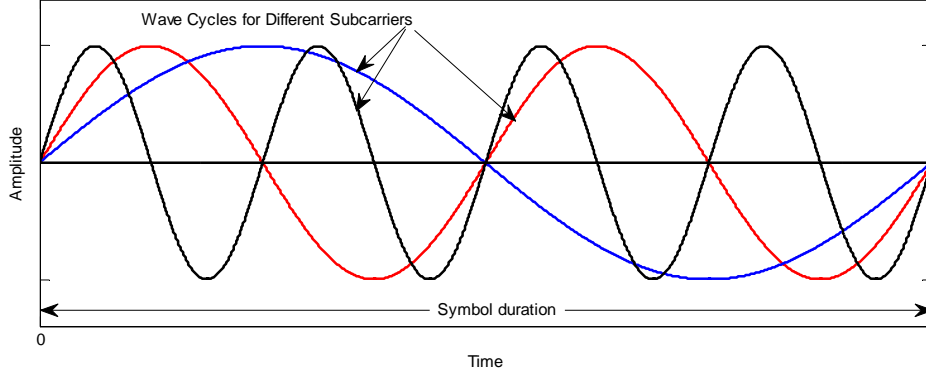


Figure 2.3: Orthogonality among the sub-carriers in time domain [5].

$$\begin{aligned}
 \frac{1}{T_s} \int_0^{T_s} \varphi_k(t) \varphi_l^*(t) dt &= \frac{1}{T_s} \int_0^{T_s} e^{j2\pi f_k t} e^{-j2\pi f_l t} dt \\
 &= \frac{1}{T_s} \int_0^{T_s} e^{j2\pi (f_k - f_l) t} dt \\
 &= \delta[k - l]
 \end{aligned} \tag{2.3.1}$$

Where $\delta[k - l]$ is the delta function defined as:

$$\delta[k - l] = \begin{cases} 1 & \text{if } k = l \\ 0 & \text{otherwise} \end{cases}$$

In general the product of any two functions equal one if they are orthogonal and equal to zero if they are not orthogonal.

$$\frac{1}{T_s} \int_{t_1}^{t_1+T_s} \varphi_k(t) \varphi_l^*(t) dt = \begin{cases} 0 & \text{if } k \neq l \\ 1 & \text{if } k = l \end{cases} \tag{2.3.2}$$

Where, $\varphi_k(t)$ and $\varphi_l(t)$ are two functions (signals) over time interval $[t_1, t_1 + T_s]$ and T_s is the period of the signals [31]

2.4 The advantages of OFDM systems

OFDM has been used in many high data rate wireless systems, because of the several advantages it provides. Some of the advantages include [32]:

- **Immunity to selective fading:** One of the major merits of OFDM is the ability to resist the frequency selective fading more than the single carrier system, because it splits the bandwidth into several narrow-band channels. Each narrow-band channel suffers individually from flat fading and this leads to a robust system.
- **Flexibility to interference:** In a single carrier system, if the interference appears, all data will suffer from the interference. Unlike the OFDM system, not all data will suffer from the interference. If the interference happens on some sub-channels that have limited sub-bandwidth, only these sub-channels will suffer from the interference.
- **Spectrum efficiency:** The OFDM system is more bandwidth efficient in comparison to frequency division multiplexing (FDM), because the sub-carriers overlap each other due to orthogonality feature. Due to overlapping of sub-carriers, the usage of bandwidth is reduced drastically and consequently it makes efficient use of the available spectrum. Figure 2.1 shows how the OFDM saves the bandwidth compared to the FDM system.
- **Protection against Inter-symbol Interference (ISI):** Due to the extension of symbol time, the OFDM system is more protected against inter-symbol interference (ISI) than the single carrier system. In the OFDM systems, the bandwidth is split into several sub-bandwidths and hence creating a long symbol time. Every sub-bandwidth has long symbol time (*i.e.* every sub-bandwidth carries a low data rate) and this makes the signal less sensitive to the effect of multi-path transmission which introduces Inter Symbol Interference (ISI).
- **Easy to implement modulation and demodulation:** In a multi-carrier modulation (MCM) system, a bank of modulators is needed on the transmitter side and a bank of demodulators is needed at the receiver side. This produces a high complexity. However, in OFDM system, IFFT at the transmitter and FFT at the receiver are used instead of the bank of modulators and demodulators.

2.5 Major problems of OFDM system

Despite of several advantages, the OFDM systems also have some major problems [4]:

- **High sensitivity to carrier frequency offsets and phase noise:** Carrier frequency offset happens when the local oscillator in the receiver is not synchronized with the carrier signal contained in the received signal. When the carrier frequency offset occurs, the received signal will not be sampled at the peak and the orthogonality among the sub-carriers brakes and this causes inter-carrier interference (ICI) [4]. Figure 2.4 shows the effect of carrier frequency offset.

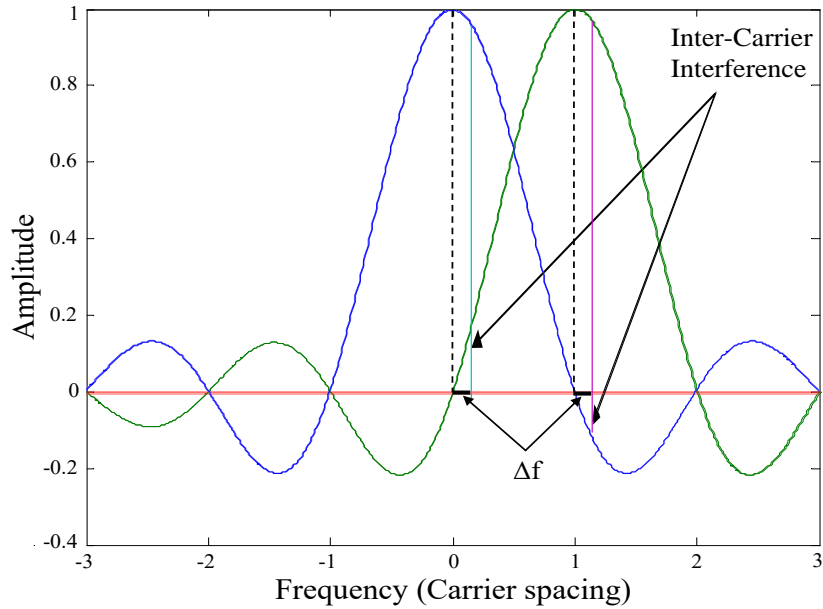


Figure 2.4: Effects of carrier frequency offset [6].

- High peak to average power ratio (PAPR):** High PAPR of transmitting signals is one of the major issues of the OFDM systems. For an OFDM signal, consisting of N individual and independent data symbols, when the N signals add up to the same phase, a substantial increase in the PAPR is observed. The value of the observed instantaneous PAPR might reach as high values as N times of the average OFDM symbol amplitude [21]. Figure 2.5 shows an OFDM signal with high PAPR.

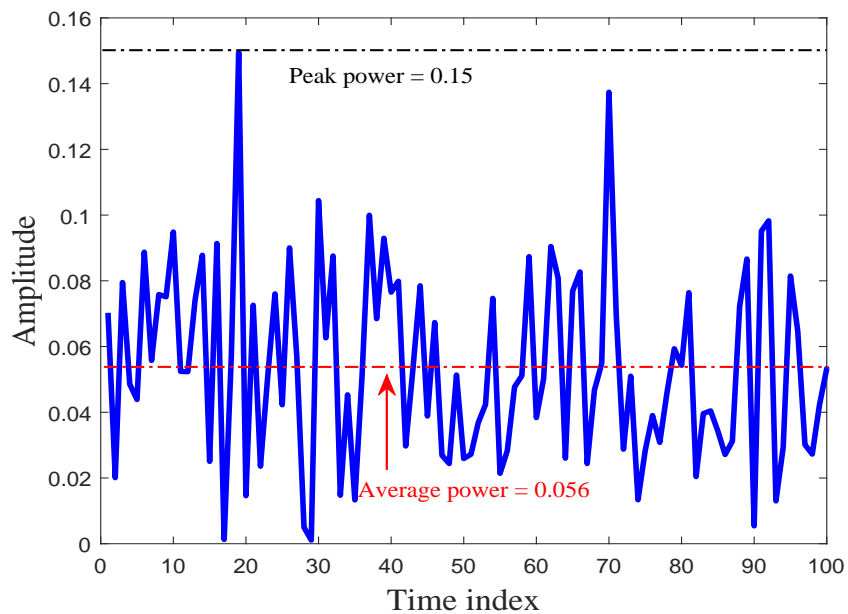


Figure 2.5: One OFDM symbol in time domain.

2.6 Basic Concept of the OFDM

OFDM [20, 21, 25] is a multi-carrier transmission system (also is called parallel transmission technique). In the OFDM systems, the channel is divided into sub-channels (sub-channel is sometimes called sub-carrier or tone). Every sub-channel carries a data stream with a low rate and transmits this data in parallel over a number of closely spaced orthogonal sub-carriers. Unlike the single carrier transmission, the symbol period of sub-carriers will increase and this results in decreasing the effect of multi-path propagation [33].

The concept of the OFDM system is very similar to the concept of the conventional multi-carrier system (FDM) with a few differences. In conventional multi-carrier system (FDM), the bandwidth is split into non-overlapping sub-carriers. Each sub-carrier carries a separate data stream in parallel. This technique seems appropriate to avoid the overlapping between sub-carriers and hence it is able to minimize the inter-carrier interference (ICI). However, this results in inefficient use of the bandwidth, and as a consequence the efficiency of bandwidth is reduced [34]. To improve the bandwidth efficiency, OFDM uses N overlapping sub-carriers, where orthogonality removes the inter-channel interference.

Figure 2.1 illustrates the difference between a conventional non overlapping multi-carrier technique such as FDM and an overlapping multi-carrier modulation technique such as OFDM. By using the overlapping multi-carrier modulation technique, almost 50 % of the bandwidth can be saved [21]. To realize this technique, the orthogonality between the different sub-carriers must be achieved. Figures 2.2 and 2.3 illustrate orthogonality among the sub-carriers in frequency domain and time domain, respectively. The name ‘OFDM’ is an abbreviation for orthogonal frequency division multiplexing, which reflects the fact that the digital data is sent using several sub-carriers; each having a different frequency, and these sub-carriers are orthogonal to each other.

2.7 Block Diagram of OFDM System

Figure 2.6 shows a typical block diagram of an OFDM transceiver chain. Firstly, the input data are mapped by using various mapping schemes, such as the M-ary phase shift keying (PSK) and the quadrature amplitude modulation (QAM). Then, they are converted from serial to parallel (S/P). After that the mapped data X_k is processed by an inverse discrete Fourier transform (IDFT). A parallel-to-serial (P/S) converter is applied to the resulting time domain symbols $x(n)$. A cyclic prefix of suitable length is added to combat the effect of multi-path propagation such as inter-symbol interference (ISI). Then, the signals with cyclic prefix are passed through the digital-to-analog (D/A) converter to obtain the continuous-time OFDM signal $x(t)$. Finally, the signal is amplified using power amplifier to the desired power level and transmitted over the communication channel. At the receiver side, the transmitter processing is functionally reversed in the reverse order to obtain an estimated form of the binary information sequence.

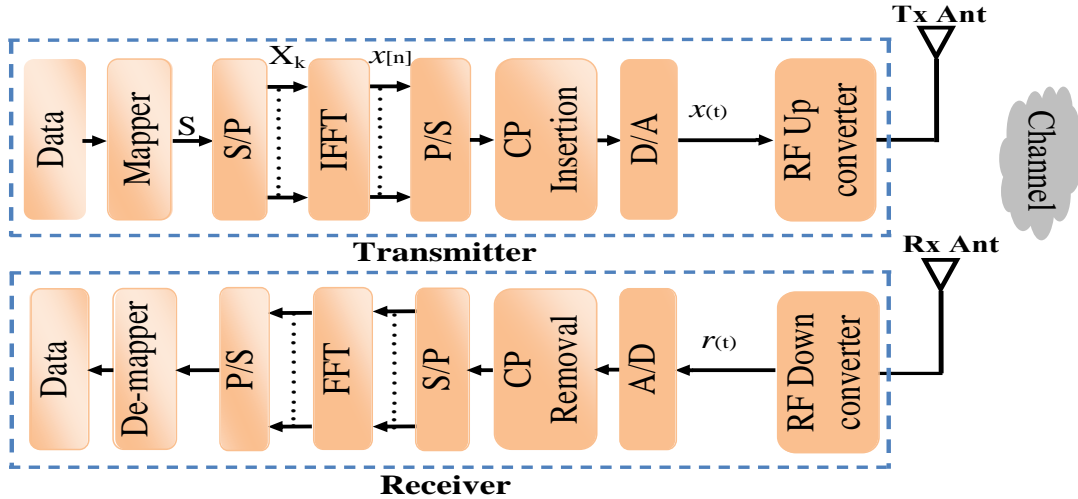


Figure 2.6: Block Diagram of OFDM System [4].

2.7.1 Modulation

A modulation scheme is a mapping of data words to a real (In phase) and imaginary (In quadrature) constellation, known as an IQ constellation. For example, quadrature amplitude modulation (QAM), 16-QAM has 16 IQ points in the constellation, 4 columns in the real axis and 4 rows in the imaginary axis. Using a single symbol, the number of bits that can be carried corresponds to $m = \log_2(M)$, where M is the number of points in the constellation. Figure 2.7 shows 64-QAM, 16-QAM and quadrature phase shift keying (QPSK) constellation.

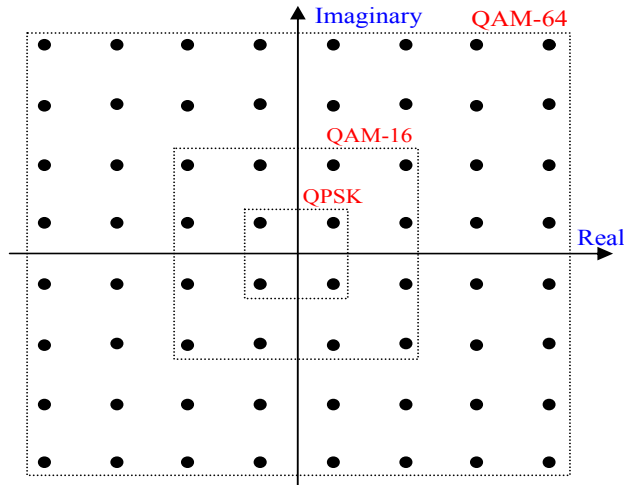


Figure 2.7: QPSK, 16-QAM, and 64-QAM constellation [4].

In the constellation, if the number of points increases, the bandwidth will not change. Accordingly, the larger the number of constellations point is, the better efficiency can be expected. The number of bits transmitted per second for each hertz (bps/Hz) is the measure of the spectral efficiency of any channel. Binary PSK (BPSK) has a spectral efficiency of 1 (bps/Hz),

QPSK has 2 (bps/Hz), 8PSK has 3 (bps/Hz), 16-QAM has 4 (bps/Hz), 32-QAM has 5 (bps/Hz) and 64-QAM has 6 (bps/Hz). However, if the number of constellation points is large, the locations of IQ will be placed close together. In other words, the greater the number of points in the modulation constellation, the harder they are to resolve at the receiver. In this case, a small amount of noise will lead to errors in the transmission. This results in a direct trade-off between noise tolerance and the bandwidth efficiency of the modulation scheme. [4].

2.7.2 Serial to Parallel Conversion (S/P)

The mapping data S should be converted from serial to parallel depending on the type of modulation and the number of sub-carriers. Figure 2.8 illustrates the conversion of data from serial to parallel. At the receiver, the reverse process takes place, with the data from the sub-carriers being converted back to the original serial data stream.

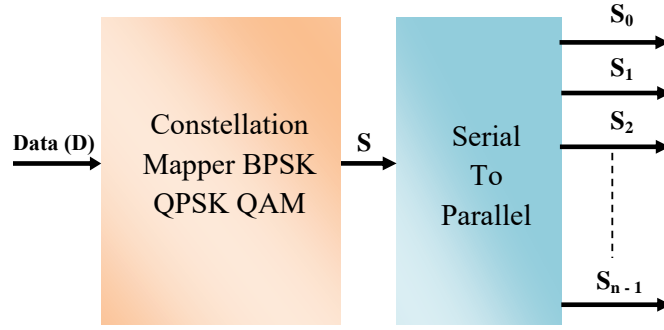


Figure 2.8: Serial to Parallel Conversion [7].

2.7.3 OFDM Modulation

OFDM transmitter maps the bits of data into a sequence of digital modulation such as QAM or QPSK, which will be later converted into N parallel streams. When serial-to-parallel (S/P) conversion is applied, the N symbols that are indexed from 0 to $N - 1$ will carry over N different sub-carriers [13]. Suppose that $S_k, \{k = 0, 1, \dots, N - 1\}$, are the complex symbols, these complex symbols will be transferred through IFFT block to get the OFDM signal; as shown in Figure 2.9. The OFDM modulated signal can be expressed as follows:

$$s(t) = \frac{1}{\sqrt{N}} \sum_{k=0}^{N-1} S_k \cdot e^{j2\pi f_k t} \quad \text{for } 0 \leq t \leq T_s \quad (2.7.1)$$

$$f_k = k\Delta f$$

$$T_s = NT$$

Where T_s denotes to the symbol duration and Δf denotes to the sub-channel spacing of OFDM. T is the original symbol period and N is the number of sub-carriers. The symbol du-

ration should be long enough such that $T_s \Delta f = 1$ (which is also called the condition of orthogonality), in order to correctly demodulate the OFDM signal and get the desired information [8].

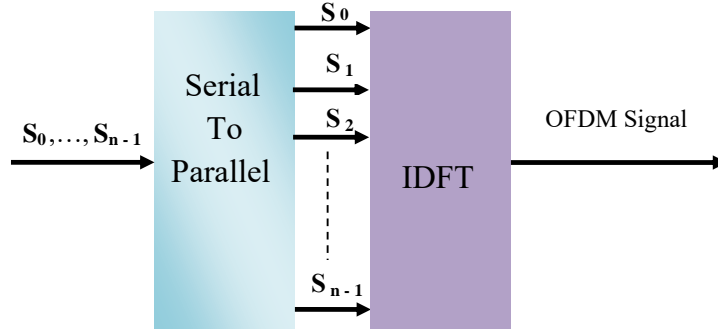


Figure 2.9: OFDM Modulator [7].

2.7.4 Implementation of FFT

This section explains the relationship between discrete Fourier transform (DFT) and OFDM. DFT can be executed by fast Fourier transform (FFT) with low complexity. Equation (2.7.1) can be considered an IFFT process. The Fourier transform (FT) decomposes a waveform (a signal or function) into different frequencies by multiplying this waveform with a series of sinusoids [7]. The Fourier transform converts the waveform from time domain to frequency domain, while the IFFT is a conversion process that converts a signal from frequency domain to time domain. An OFDM signal can be expressed as follows:

$$s(t) = \frac{1}{\sqrt{N}} \sum_{k=0}^{N-1} S_k \cdot e^{j2\pi f_k t}.$$

Where S_k are the data symbols, $\exp(j2\pi f_k t)$ represents the sub-carriers, and $f_k = k/T$ is the center frequency of the k_{th} sub-carrier. Assume that OFDM waveform $s(t)$ is sampled at $(\frac{nT_s}{N})$, then:

$$s_n = s\left(\frac{nT_s}{N}\right) = \frac{1}{\sqrt{N}} \sum_{k=0}^{N-1} S_k \cdot e^{j2\pi f_k \frac{nT_s}{N}}. \quad (2.7.2)$$

With $f_k T_s = k$ the equation (2.7.2) becomes:

$$s_n = \frac{1}{\sqrt{N}} \sum_{k=0}^{N-1} S_k \cdot e^{j\frac{2\pi kn}{N}} = IDFT\{S_k\} \quad (2.7.3)$$

OFDM modulator transmits a large number of narrow-band carriers, closely spaced in the frequency domain. In order to avoid a large number of modulators at the transmitter and large number of de-modulators at the receiver, it is desirable to be able to use modern digital signal processing techniques, such as fast Fourier transform (FFT). The FFT algorithm introduces an effective way to perform the DFT and the IDFT. It minimizes the number of complex multiplications from N^2 to $\frac{N}{2} \log_2 N$ and reduces the number of complex additions from $N(N - 1)$ to $N \cdot \log_2(N)$ for an N-point DFT or IDFT.

2.7.5 Cyclic Prefix Extension

In any wireless system, the design of the system should be robust enough to overcome the difficulties that exist in the wireless channel. Multi-path transmission causes the ISI problem. ISI depends on the maximum transmission delay, τ_{max} , of the channel and symbol duration, T_s . To show this, assume the maximum transmission delay $\tau_{max} = 5\mu s$ and the symbol duration $T_s = 0.5\mu s$, this leads to a span over of the ISI $\tau_{max}/T_s = 10$ symbols [4]. In order to get reliable communication, ISI should be treated at the receiver. Time domain equalizers are used to combat the ISI. However, this method is not practical, because of its high complexity, where the complexity increases with the length of ISI [4]. Figure 2.10 shows the inter-symbol interference.

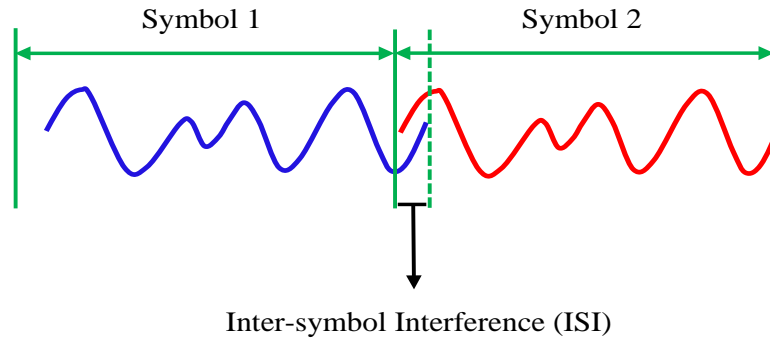


Figure 2.10: The ISI due to multi-path propagation [4].

This section shows how the OFDM system copes with the multi-path transmission problems such as ISI. The bandwidth in any OFDM system is divided into N sub-carriers. This means that the symbol rate for each sub-channel will be low compared to the symbol rate in single carrier system. The symbol rate in a single carrier system is N times greater than the symbol rate in OFDM system. In other words, the symbol duration in an OFDM system is N times longer than the symbol duration in a single carrier system.

$$T = NT_s. \quad (2.7.4)$$

Where, T is the OFDM symbol time, T_s is the original symbol time and N is the number of sub-carriers. Consequently, this makes the OFDM system robust enough to the effect of the ISI.

A cyclic prefix (CP) refers to a small part of the transmitted symbol, where this small part is taken from the end of the symbol and fixed in the beginning of the transmitted symbol [25], as shown in Figure 2.11. As long as the delay of multi-path signals is shorter than the guard time, no ISI will happen [4].

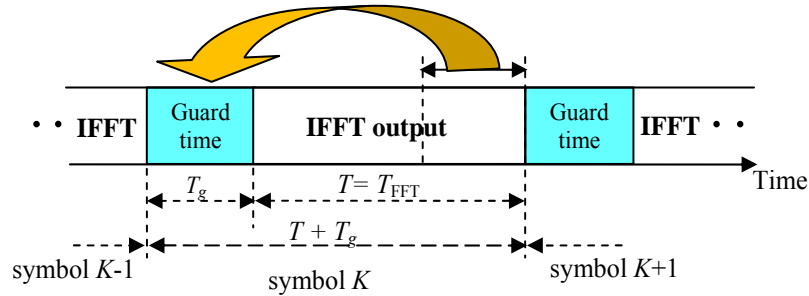


Figure 2.11: OFDM symbol with cyclic extension [4].

A CP can be used for each OFDM symbol to remove the ISI problem, as shown in Figure 2.12. To avoid the interference between symbols, the length of the cyclic prefix should be longer than the expected delay spread. The addition of cyclic prefix expands the duration time of OFDM symbols as follows:

$$T_{sym} = T + T_g \quad (2.7.5)$$

Where T_{sym} is OFDM symbol with cyclic prefix, T is OFDM symbol and T_g is guard time. The major disadvantage of cyclic prefix (CP) is a small loss of efficient transmitted power, where the transmitted symbol is longer than the original OFDM symbol due to the CP. This minimizes the bandwidth efficiency by the factor $(T/T + T_g)$ [14, 15]. Commonly, the CP is chosen to have a length of one-tenth to one quarter of the symbol time [4, 21].

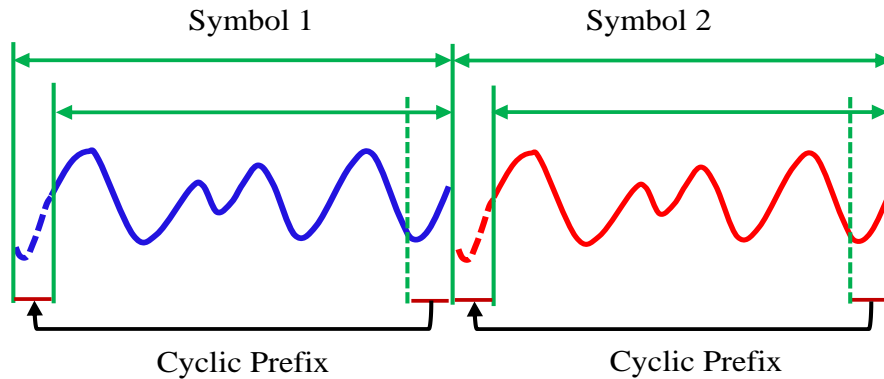


Figure 2.12: OFDM symbol with cyclic prefix (CP) [4].

2.8 Base-band and Pass-band signals

This section describes the difference between base-band and pass-band signals. Base-band refers to the original data signal. In base-band transmission, the signals are transferred without frequency shifting. In other words, they are transferred without modulation. Base-band has a low frequency, included in the bandwidth from 0 Hz to a higher cut off frequency. However, pass-band transmission shifts the signal to a higher frequency to be transmitted, where at the receiver the signal is shifted back to its original frequency [8].

The OFDM signals are complex base-band signals. However, in wireless communication systems, complex base-band signals must be converted into real pass-band signals. The base-band signal, $s(t)$, is generally a complex function of time. Thus, it can be expressed into a rectangular form as follows:

$$s(t) = s_I(t) + js_Q(t) \quad (2.8.1)$$

Where

- $s_I(t)$: is the real part and it is called in-phase component of the base-band signal
- $s_Q(t)$: is the imaginary part and it is called quadrature component.

For the base-band OFDM signal in equation 2.7.1:

$$\begin{aligned}
 s(t) &= \sum_{k=0}^{N-1} S_k \cdot e^{j2\pi f_k t} \\
 &= \sum_{k=0}^{N-1} [R(S_k) + jIm(S_k)] \cdot e^{j2\pi f_k t} \\
 &= \sum_{k=0}^{N-1} [R(S_k) + jIm(S_k)] \cdot [\cos(j2\pi f_k t) + jsin(j2\pi f_k t)] \\
 &= \sum_{k=0}^{N-1} \left(R\{S_k\} \cdot \cos(2\pi f_k t) - Im\{S_k\} \cdot \sin(2\pi f_k t) \right) \\
 &\quad + j \sum_{k=0}^{N-1} \left(Im\{S_k\} \cdot \cos(2\pi f_k t) + R\{S_k\} \cdot \sin(2\pi f_k t) \right) \quad (2.8.2)
 \end{aligned}$$

and therefore,

$$s_I(t) = \sum_{k=0}^{N-1} \left(R\{S_k\} \cdot \cos(2\pi f_k t) - \text{Im}\{S_k\} \cdot \sin(2\pi f_k t) \right),$$

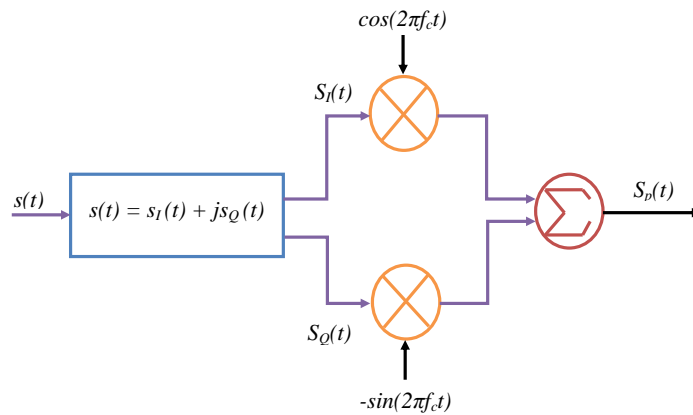
and

$$s_Q(t) = \sum_{k=0}^{N-1} \left(\text{Im}\{S_k\} \cdot \cos(2\pi f_k t) + R\{S_k\} \cdot \sin(2\pi f_k t) \right)$$

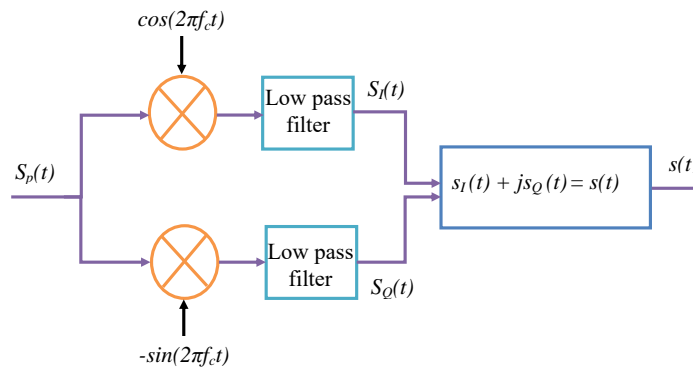
where

- $R\{s_k\}$: is the real part of the complex symbol S_k
- $\text{Im}\{s_k\}$: is the imaginary part of the complex symbol S_k

Figure 2.13 explains how to convert from base-band signal to pass-band signal and vice versa.



(a)



(b)

Figure 2.13: Base-band versus pass-band: (a) base-band to pass-band conversion, and (b) pass-band to base-band conversion [8].

From Figure 2.13(a), the pass-band signal can be further simplified as follows:

$$\begin{aligned}
s_p(t) &= R\{s(t).e^{j2\pi f_c t}\} \\
&= R\left\{ [s_I(t) + jS_Q(t)].[\cos(j2\pi f_c t) + jsin(j2\pi f_c t)] \right\} \\
&= s_I(t).\cos(2\pi f_c t) - s_Q(t).\sin(2\pi f_c t) \\
&= \sum_{k=0}^{N-1} \left\{ R\{S_k\}.\cos[2\pi(f_c + f_k)t] - Im\{S_k\}.\sin[2\pi(f_c + f_k)t] \right\}
\end{aligned}$$

Assume that the magnitude of complex symbol, S_k , is A_k and the phase of complex symbol, S_k , is θ_k . This means, $S_k = A_k.e^{j\theta_k}$, then:

$$s_p(t) = \sum_{k=0}^{N-1} A_k.\cos\left(2\pi(f_c + f_k)t + \theta_k\right) \quad (2.8.3)$$

At the receiver side, the pass-band signal can be converted to the base-band by making the reverse steps that were done in the transmitter, as shown in Figure 2.13(b).

2.9 Modeling of the channel

In wireless communication systems, in order to send data from a transmitter to a receiver, the data should pass through a medium, which is called the channel. The received signal is not the same as the transmitted signal, because of several phenomena, such as diffraction, reflection, refraction, attenuation and noise. Consequently, it is important to model the channel between the transmitter and the receiver; however, it is very complicated to model real environments. Various environments were studied to find a way to model them [7]. In order to generate a noise in an OFDM system, a few random data should be added to the symbol of OFDM. For the multi-path environment, it can be done by adding delayed copies and attenuated copies of the OFDM signal [31]. The impulse response of L paths for wireless channel is expressed as follows [35]:

$$h(\tau, t) = \sum_{l=0}^{L-1} h_l(t)\delta(t - \tau_l) \quad (2.9.1)$$

Where, τ_l is a transmission delay (propagation delay) and $h_l(t)$ is a tap coefficient of the l^{th} path.

2.10 Modeling of the receiver

The inverse steps of transmission are done at the receiver side. Firstly, the received OFDM signal is converted from serial to parallel form. Then, the CP is removed from the OFDM symbol; the unguarded symbol passes through the FFT block, where the FFT block converts the signal from the time domain to the frequency domain. After that, the data in the frequency domain crosses through a channel equalization block. The de-mapping process is applied on the equalized data to recover information symbol. Finally, the information symbol is converted from a parallel to a serial form to get the originally transmitted signal.

The received signal $r(t)$ after crossing through a multi-path fading channel can be expressed as follows [35]:

$$r_i(t) = \sum_{l=0}^{L-1} h_l(\tau).x_i(t - \tau_l) + w_i(t) \quad (2.10.1)$$

Where

- $r_i(t)$: The i^{th} received signal
- $h_l(t)$: The multi-path fading channel
- $w(t)$: Represents the Additive White Gaussian Noise (AWGN)
- $x_i(t - \tau_l)$: The i^{th} transmitted signal

The transmission of a cyclic prefix during the guard time makes the linear convolution given in equation (2.10.1) equivalent to a circular convolution [4]. The equivalent circular convolution in frequency domain can be written as:

$$R_i(k) = H(k)X_i(k) + W_i(k) \quad for \quad 0 \leq k \leq N - 1 \quad (2.10.2)$$

Where,

- $W(k)$: Is the AWGN component in frequency domain
- $H(k)$: Is the frequency response of the multi-path fading channel at the k^{th} sub-channel

The response of channel in the frequency domain is expressed as follows:

$$H(k) = \sum_{l=0}^{N-1} h_l(\tau).e^{\frac{-j2\pi kl}{N}} \quad (2.10.3)$$

OFDM does not eliminate the equalization process associated with conventional single carrier systems; rather, it converts the problem to frequency-domain equalization. From the equation (2.10.2), in order to recover the complex data symbol $X_i(k)$ correctly, the equation (2.10.2) should be multiplied by a factor $G(k)$, where $G(k)$ is the gain of a single tap equalizer in the frequency domain. It is expressed as follows [35]:

$$G(k) = \frac{1}{H(k)} \quad (2.10.4)$$

Eventually, the data symbols that are recovered will be demodulated by using a digital modulation technique such as M-QAM or Q-PSK. Then, they are converted from a parallel to a serial form to get the original data.

Peak to average power ratio (PAPR)

3.1 Introduction

The high peak to average power ratio (PAPR) is one of the main disadvantages of the OFDM systems. The PAPR occurs when the sub-carriers are combined via an IFFT block, which can produce a high PAPR. At the transmitter side, the OFDM signals are amplified to the required power level by using the high power amplifiers (HPA's). In order to deal with the large fluctuations in the envelope of OFDM signal, HPA's should have a large linear range. However, the HPA's with a large range are costly, bulky and difficult to design [36]. Consequently, in the practical communication systems, power amplifier (PA) with limited linear range is used to amplify the OFDM signal, as shown in Figure 3.1. When a PA works in the saturation region (non-linear region), an unwanted distortion such as in-band distortion and out-of-band radiation (OOB) is appeared. The OOB causes inadmissible adjacent channel interference (ACI) and the in-band distortion maximizes the bit error rate (BER) [4, 24]. Also, the converters, either from the analog to digital (ADC) or, vice versa, the digital to analog (DAC), are required to have a large dynamic range in order to adapt the large fluctuations of the OFDM signals. However, this means extra cost and more complicated system [36]. Consequently, it is very important to use the PAPR reduction techniques to deal with the high PAPR problem, because without using any PAPR reduction technique the received signals will be clipped and this means the receiver will be susceptible to errors.

3.2 Definition of the PAPR

The PAPR of an OFDM signal $x(t)$ is the ratio between the maximum peak power and the average power of the OFDM signal [37]. Mathematically, it can be expressed as follows:

$$PAPR_x(t) = \frac{P_{peak}}{P_{avg}} = \frac{\max_{0 \leq t \leq T_s} \{|x(t)|^2\}}{E[|x(t)|^2]} \quad (3.2.1)$$

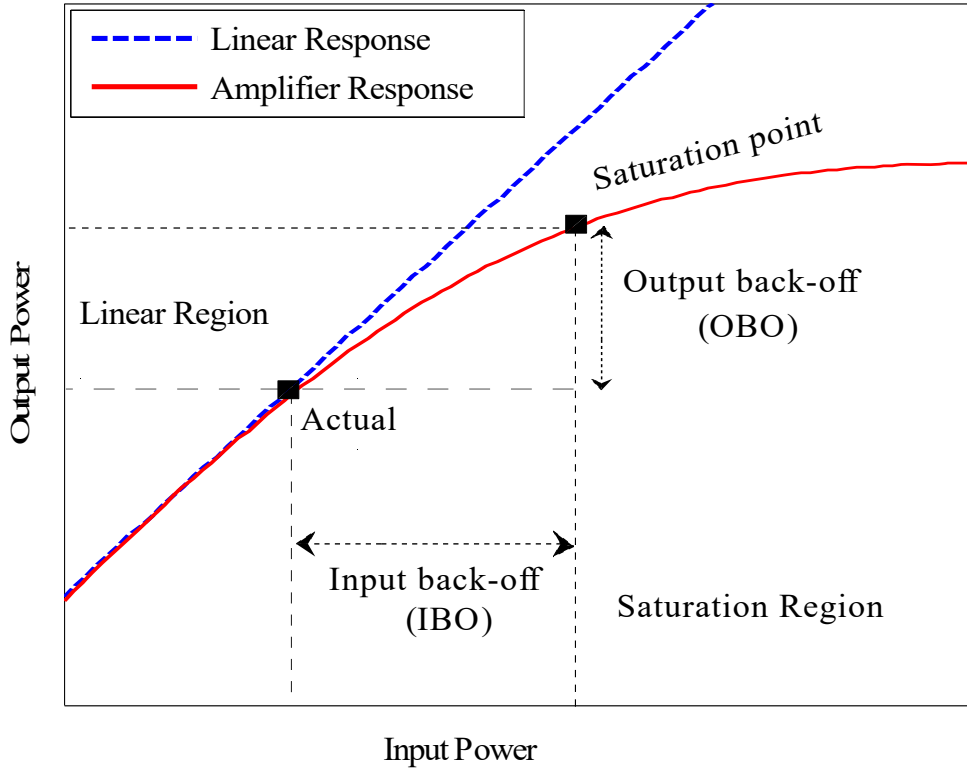


Figure 3.1: Power amplifier transfer function.

Where,

- $E[\cdot]$: is the expected value.
- P_{peak} : is the maximum peak power.
- P_{avg} : is the mean average output power.

With,

$$P_{avg} = E[|x(t)|^2] = \frac{1}{T} \int_0^T |x(t)|^2 dt \quad (3.2.2)$$

For a discrete OFDM signal $x(n)$, the PAPR can be defined as follows [36]:

$$PAPR\{x(n)\} = \frac{P_{peak}}{P_{avg}} = \frac{\max_{0 \leq n \leq N} \{|x(n)|^2\}}{E[|x(n)|^2]} \quad (3.2.3)$$

Where,

$$P_{avg} = E[|x(n)|^2] = \frac{1}{N} \sum_{n=0}^{N-1} |x(n)|^2, \quad (3.2.4)$$

$$x(n) = \frac{1}{\sqrt{N}} \sum_{k=0}^{N-1} X_k \cdot e^{j\frac{2\pi kn}{N}} \quad 0 \leq n \leq N - 1$$

An OFDM signal is a sum of several individual signals modulated over a group of orthogonal sub-carriers with equal bandwidths. Therefore, If the data on the sub-carriers add up in a constructive manner at the transmitter, the resulting signal could exhibit large PAPR. As a result, the composite transmit signal could be severely clipped by the power amplifier for its limited dynamic range as shown in Figure 3.2. In this case, the reconstructed output can possess a significant amount of distortion [9].

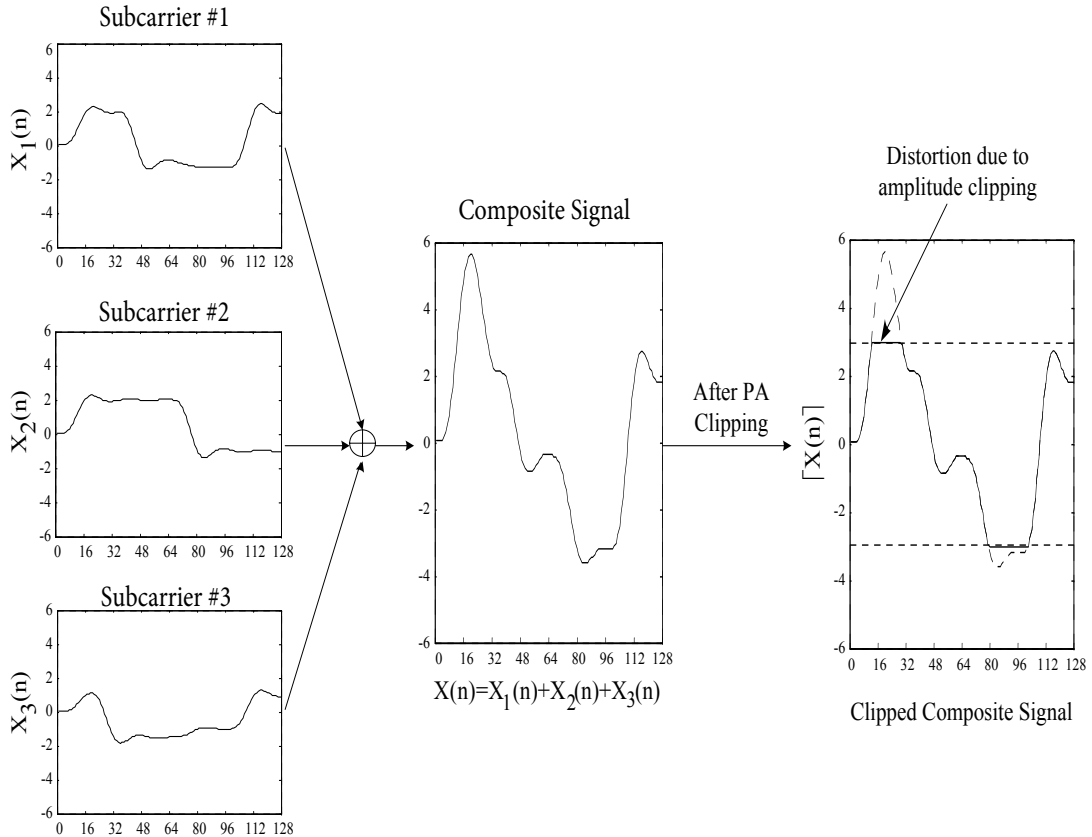


Figure 3.2: An example illustrating effects of clipping [9].

3.3 Complementary cumulative distribution function

One of the most popular measurements for the reduction techniques of PAPR is the cumulative distribution function (CDF). In this thesis, complementary cumulative distribution function (CCDF) is used in place of CDF. The CCDF of the PAPR indicates the probability that the PAPR of a data overrides a given threshold [38]. In other words, the CCDF curve shows the amount of time a signal spends above the average power level of the measured signal, or equivalently, the probability that the signal power will be above the average power level. For an OFDM signal, the CDF of the amplitude z is expressed as follows [4]:

$$F(z) = 1 - e^{-z} \quad (3.3.1)$$

Assuming that the signal samples are statistically independent and identically distributed (*i.i.d*); accordingly, the imaginary and real parts of $s[n]$ are orthogonal and uncorrelated. From the central limit theorem and for large number of sub-carriers N , the real and imaginary parts are independent and identically distributed (*i.i.d*). Therefore, they follow Gaussian distribution with zero mean and variance ($\sigma^2 = E[|x(n)|^2]/2$). For large number of sub-carriers N , the CDF of PAPR for an OFDM signal is given by [21]:

$$\begin{aligned} CDF(z) &= Pr(PAPR(s[n]) \leq z) \\ &= (1 - e^{-z})^N \end{aligned} \quad (3.3.2)$$

Where, z is pre-set level of PAPR. Therefore, the CCDF of PAPR will be as follows [21]:

$$\begin{aligned} CCDF(z) &= Pr(PAPR(s[n]) > z) \\ &= 1 - (1 - e^{-z})^N \end{aligned} \quad (3.3.3)$$

Figure 3.3 displays the CCDF of PAPR for $N = 64, 256, 1024$ and 4096 sub-carriers. The QPSK modulation scheme is considered in this simulation. At $Prob(PAPR > PAPR_0) = 10^{-2}$, the corresponding peak-to-average ratio for 64 sub-carriers is 9 dB, for 256 sub-carriers is 10 dB, for 1024 sub-carriers is 10.6 dB and for 4096 sub-carriers is 11.2 dB. This means the signal power exceeds the average by at least 9 dB for 1 percent of the time for 64 sub-carriers. It can be easily noted from the Figure 3.3 that the PAPR of the OFDM signal increases by increasing the number of sub-carriers.

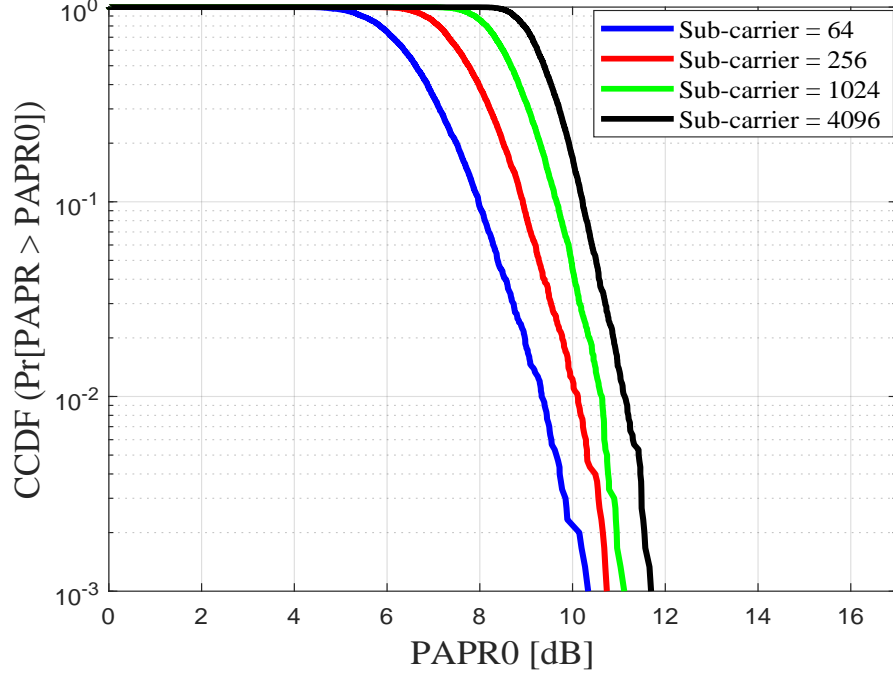


Figure 3.3: CCDF of PAPR for N=64, 256, 1024 and 4096 sub-carriers.

3.4 Non-linear Power Amplifier effects

In order to show the effect of the high PAPR on OFDM system performance, non-linear power amplifier should be defined. The high PAPR of OFDM requires system components with a large linear range capable of accommodating the signal. Otherwise, the nonlinear distortion occurs, which results in a loss of sub-carrier orthogonality, and degrades the performance. Figure 3.4 shows the effects of non-linear PA on signal spectrum (a), signal constellation (b), linear response (c) and bit error rate (d). In reality, the PA has a limited linear region, beyond which it saturates to a maximum output level as shown in Figure 3.4(c).

The solid-state power amplifier (SSPA) model is used in this thesis. The amplitude and phase characteristics of this amplifier are given by [39, 40]:

$$A_{SSPA}(|s(t)|) = \frac{G_0 |s(t)|}{\left(1 + \left(\frac{|s(t)|}{A_{sat}}\right)^{2p}\right)^{\frac{1}{2p}}} \quad (3.4.1)$$

$$\phi_{SSPA}(|s(t)|) = 0. \quad (3.4.2)$$

Where G_0 is the amplifier gain, A_{sat} is the input saturation level, P controls the sharpness of the saturation region.

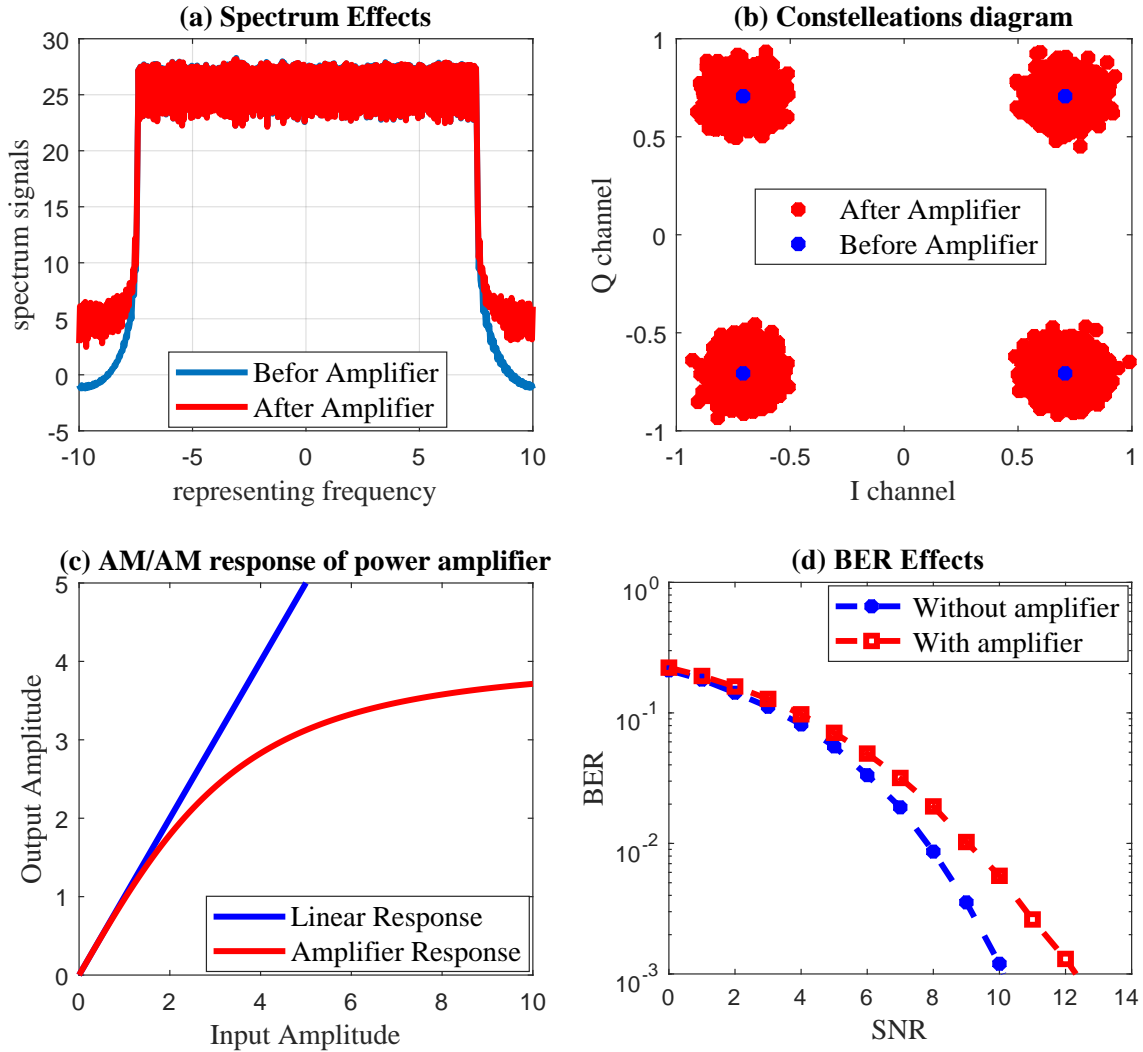


Figure 3.4: Effects of non-linear power amplifier on: (a) signal spectrum, (b) signal constellation, (c) amplifier response and (d) bit error rate.

3.5 PAPR reduction schemes

Many PAPR reduction methods are proposed in the literature [41–61]. The PAPR reduction schemes are majorly divided into three categories:

- Distortion based techniques [41, 51]
- Non-distortion techniques [52, 55]
- Hybrid techniques [56–61]

3.5.1 Distortion based techniques

Distortion based techniques are the simplest PAPR reduction schemes. These schemes distort the spectrum and the distortion of spectrum can be corrected to a certain extent by using filter-

ing operation [36]. They reduce the PAPR by distorting the OFDM signal. Methods such as clipping, peak windowing, and non-linear companding are the examples of these techniques. The distortion based techniques are applied after the generation of OFDM signal, which they attempt to decrease PAPR by the manipulation of the signal before the amplification [62]. Clipping of signal prior to the amplification is the simplest method, but it causes increasing in both out-of-band (OOB) as well as in-band interference, thus compromises upon performance of the system. A technique that is used to decrease high PAPR should have high spectral efficiency, compatibility with the existing modulation schemes and has low computational complexity.

3.5.2 Non-distortion techniques

This type of PAPR reduction techniques doesn't distort the shape of the OFDM signal, and therefore no spectral distortion takes place [63]. The main idea of this type is generating multiple permutation of the OFDM signal and transmitting the one with minimum PAPR. Scrambling techniques, selective level mapping (SLM) and partial transmit sequences (PTS) are examples of non-distortion techniques. This type of PAPR reduction techniques can reduce the high PAPR problem efficiently. However, this type has high computational complexity. To recover the transmitted signal correctly at the receiver side, this type needs side information to be sent with the original data, which causes reducing bandwidth efficiency [64, 65].

3.5.3 Hybrid techniques

In addition to the different PAPR reduction schemes, some hybrid techniques are also available in the literature [56–61]. These methods reduce high PAPR by combining two techniques or more such as clipping with coding, SLM with coding, pre-coding with clipping, interleaving with companding, selective mapping with binary cyclic codes, combining Hadamard transform and Hann peak windowing, etc. The hybrid methods are considered as a good choice for PAPR reduction because it possesses the advantages of both techniques used in the hybridization with slight increases in the complexity.

3.6 Criteria for Selection of PAPR Reduction Techniques

Every technique has its own advantages and disadvantages. Consequently, techniques or hybrid techniques can be chosen according to practical demand, and the following factors should be considered before choosing the proper techniques [66].

- **High capability of PAPR reduction:** Obviously, this is the primary and most important factor to be considered in selecting the PAPR reduction techniques. The level of PAPR reduction should be as large as possible when other factors are not greatly affected.
- **Low average power:** Increasing the average power can reduce PAPR, but it requires a larger linear operation region in HPA, which results in higher distortions and BER performance degradation. Increasing the average power eventually leads to distort the constellation points and making the small points close to the large ones. And therefore, the BER increases as the constellation points get closer.

- **Low computational complexity:** Generally, the more complex the technique is, the more PAPR reduction capability it will get. However, complex techniques need more time, complex hardware and more power that should be as minimal as possible in overall systems.
- **Less bandwidth expansion:** The bandwidth expansion occurs when side information is needed to be transmitted with the original data in some PAPR reduction techniques such as PTS and interleaving. Considering the bandwidth is a rare resource in communication systems, it is desirable to reduce PAPR without bandwidth expansion. Moreover, if the side information is received in error at the receiver, this result in a whole erroneous data frame and thus the BER performance is reduced.
- **Less BER performance degradation:** The goal of PAPR reduction is to get better system performance including BER than that of the original OFDM system. Therefore, all the techniques, which have an increase in BER at the receiver side, should be paid more attention in practice.

Companding techniques

One of the most attractive schemes to reduce high PAPR is nonlinear companding transform, due to its good system performance including PAPR reduction and BER, low implementation complexity and no bandwidth expansion. The first nonlinear companding transform is the μ -law companding, which is based on the speech processing algorithm μ -law, and it has shown better performance, than the clipping method [45]. The μ -law companding technique fundamentally focuses on increasing small amplitudes of the signals, with maintaining the peak of signals unchanged, and thus it increases the average power of the transmitted signals and possibly results in exceeding the saturation region of HPA to make system performance worse. Actually, the companding technique is also a special clipping technique. The differences between the companding technique and clipping can be summarized as follows [24]:

- Companding transforms compand original OFDM signals by using the strict monotone increasing function. Therefore, the companded signals at the transmitter side can be recovered correctly through the corresponding inversion of the nonlinear transform function at the receiver side. However, in clipping methods, the large amplitudes will be clipped when they exceed a predefined level (threshold). And therefore, the clipped signals cannot be recovered at the receiver side.
- Companding transforms increase the small amplitudes and decrease large amplitudes. And therefore, this leads to increase the resistance of small amplitudes from noise. Whereas clipping techniques only clip large amplitudes, and maintain small amplitudes unchanged. Consequently, clipping methods suffer from three major problems: spectral distortion, out-of-band radiation and in-band distortion. However, companding techniques can work well with good BER performance while maintaining good PAPR reduction.

Figure 4.1 shows a typical block diagram of an OFDM transceiver chain that incorporates a compandor and de-compandor to reduce the PAPR. Firstly, the input data is mapped by using various mapping schemes, such as the M-ary phase shift keying (PSK) and the quadrature amplitude modulation (QAM). The mapping data (S) should be converted from serial to parallel, depending on the type of modulation and the number of sub-carriers. The mapped data X_k is processed by an inverse discrete Fourier transform (IDFT). A parallel-to-serial (P/S) converter is applied to the resulting time domain symbols $x(n)$. A cyclic prefix (CP) of a suitable length

is added to combat the effect of multi-path propagation, such as inter-symbol interference (ISI). The cyclic prefixed signal is passed through the digital-to-analog (D/A) converter to obtain the continuous-time OFDM signal $x(t)$. To avoid the clipping-induced non-linearities introduced by the HPA, a companding operator, denoted by $f(x)$, is applied to the amplitude of the signal $|x(t)|$ to keep the phases of the output signals unchanged. The companded signal can be expressed as follows:

$$x_{compd} = f(|x(t)|) \quad (4.0.1)$$

Then the companded signal is multiplied by the phase of the signal ($e^{j\varphi(x)}$) as follows:

$$\tilde{x}(t) = f(|x(t)|).e^{j\varphi(x)} \quad (4.0.2)$$

Finally, the signal is amplified using power amplifier to the desired power level and is transmitted over the communications channel. As shown in Figure 4.1, at the receiver side, the transmitter processing is functionally reversed in the receiver side to obtain an estimated form of the binary information sequence.

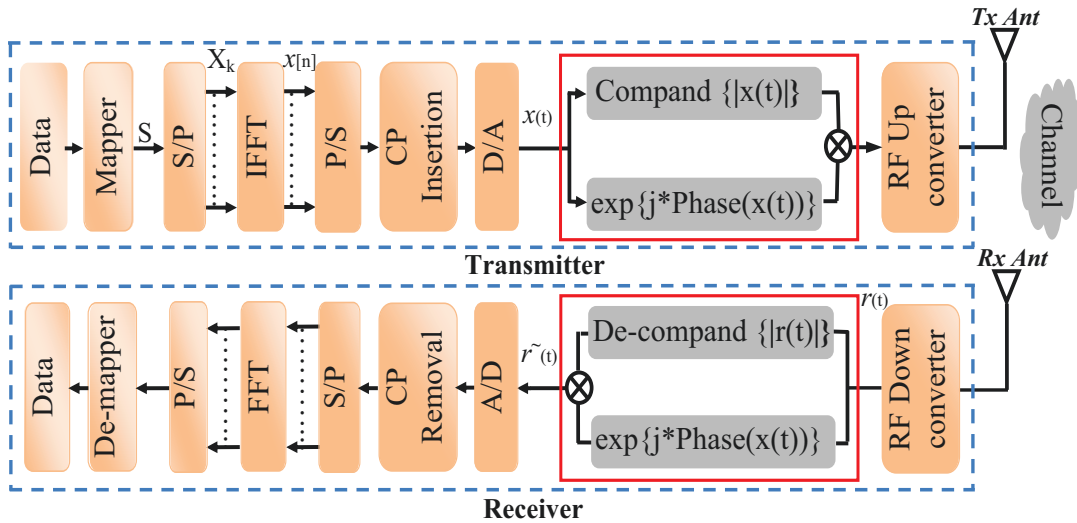


Figure 4.1: Bloc diagram of companding technique for an OFDM system

4.1 A-law companding technique

In A-law companding technique, uniform quantization is achieved at $A = 1$, where the characteristic curve is linear and no compression is conducted. For A is greater than one ($A > 1$), the characteristic of the curve becomes non-linear. The practically used value of A is 87.6 as defined by the Consultative Committee for International Telephony and Telegraphy (CCITT). As the parameter A increases, the curve becomes more concave, as shown in Figure 4.2. Mathematically the companding and de-companding of A-law function can be defined as [67]:

$$f(x) = \begin{cases} \frac{A|x|}{1 + \ln A} \operatorname{sgn}(x), & 0 < |x| \leq \frac{V}{A} \\ V \frac{1 + \ln \left[A \frac{|x|}{V} \right]}{1 + \ln A} \operatorname{sgn}(x). & \frac{V}{A} < |x| \leq V \end{cases} \quad (4.1.1)$$

$$f^{-1}(x) = \begin{cases} \frac{|x|(1 + \ln A)}{A} \operatorname{sgn}(x), & 0 < |x| \leq \frac{V}{1 + \ln A} \\ \frac{V \cdot e^{\frac{x(1 + \ln A)}{V}}}{A} \operatorname{sgn}(x), & \frac{V}{1 + \ln A} < |x| \leq V \end{cases} \quad (4.1.2)$$

Where, A is the A-law parameter of the compandor, $\operatorname{sgn}(x)$ is the sign function and V is the peak signal magnitude for the signal x .

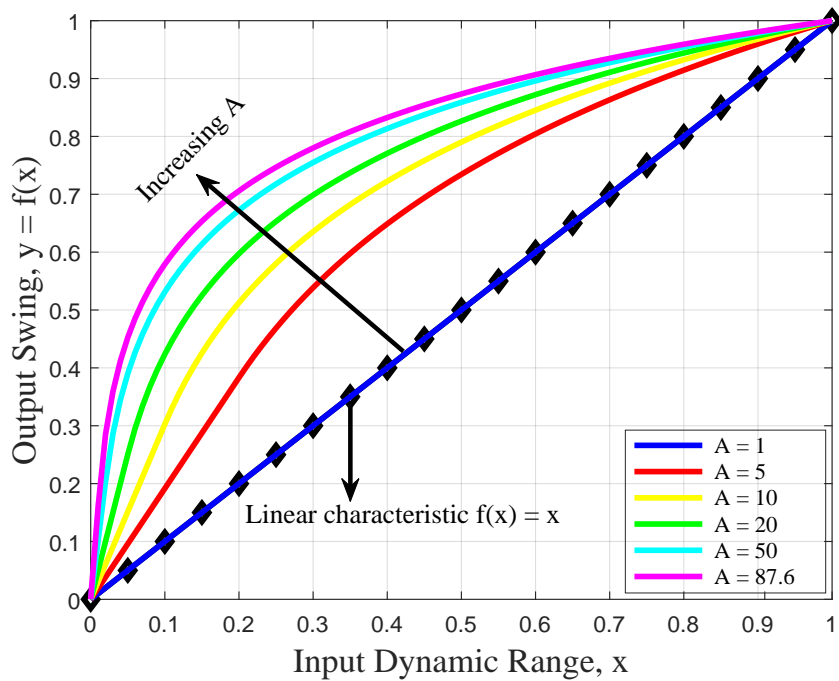


Figure 4.2: Transfer function of A-law companding technique

4.2 μ -law companding

In μ -law companding, uniform quantization is achieved at $\mu = 0$, where the characteristic curve is linear and no compression is done. For μ is greater than zero ($\mu > 0$), the characteristic curve becomes non-linear. The practically used value of $\mu = 255$ as defined by the CCITT. As the parameter μ increases, the curve becomes more concave, as shown in Figure 4.3. Mathematically the companding and de-companding of μ -law companding technique can be defined as [68]:

$$f(x) = V \frac{\ln(1 + \mu \frac{|x|}{V})}{\ln(1 + \mu)} \text{sgn}(x) \quad (4.2.1)$$

$$f^{-1}(x) = \frac{V}{\mu} \left(e^{\frac{|x| \ln(1 + \mu)}{V}} - 1 \right) \text{sgn}(x) \quad (4.2.2)$$

Where, μ is the μ -law parameter of the compandor, $\text{sgn}(x)$ is the sign function and V is the peak signal magnitude for the signal x .

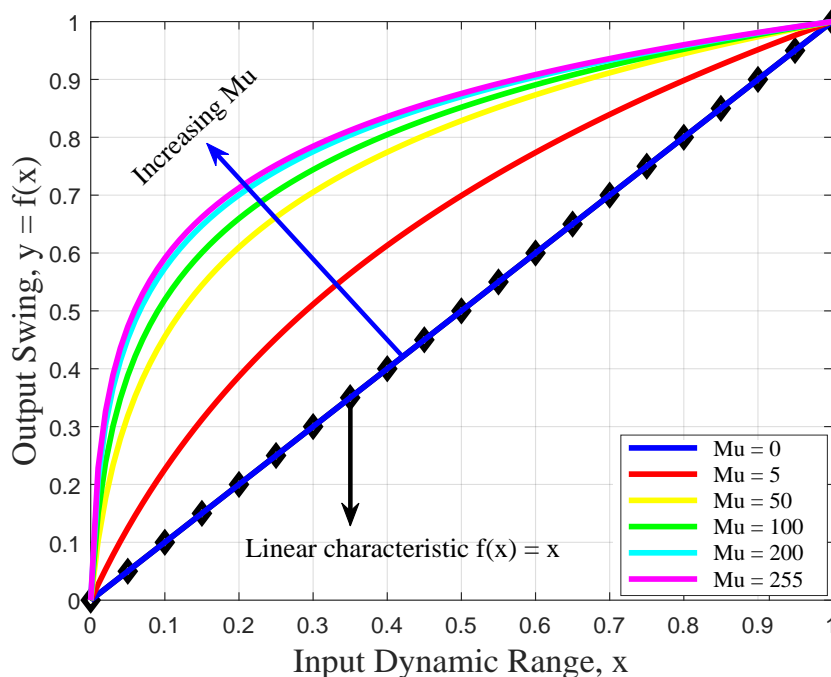


Figure 4.3: Transfer function of μ -law companding technique

A-law and μ -law are currently in use in different areas of the world. μ -law is currently being used by companies in North America and in Japan, while A-law is being used in Europe. Other areas use a mixture of the two, depending on the country.

4.3 Absolute exponential (AEXP) companding technique

Absolute exponential (AEXP) companding technique is developed to decrease the high PAPR of OFDM signals. It reduces the high PAPR by enlarging the small signals and compressing the peak of the signals simultaneously, which leads to maintain the average power before and after companding unchanged. Figure 4.4 shows the transfer function of the AEXP companding technique, where increasing the parameter d leads to enlarge small signals and compressing large signals simultaneously. As seen in Figure 4.4, the differences between absolute exponential (AEXP) companding functions are ignorable when $d \geq 8$. The equation of AEXP is derived from Trapezoidal power companding and exponential companding [47]. The AEXP companding and de-companding function can be defined as follows:

$$f(x) = \text{sgn}(x) \left(\alpha \left(1 - \exp \left(-\frac{|x|^2}{\sigma^2} \right) \right) \right)^{1/d} \quad (4.3.1)$$

$$f^{-1}(x) = \text{sgn}(x) \sqrt{-\sigma^2 * \log_e \left(1 - \frac{|x|^d}{\alpha} \right)} \quad (4.3.2)$$

Where d is the degree of companding scheme, σ^2 is the variance of input signal applied for companding and α is a positive constant that defines the average power of the output signals. To maintain the same average power level for input and output signals, α should be set as follows:

$$\alpha = \left(\frac{\mathbf{E}\{|x|^2\}}{\mathbf{E}\left\{\left(1 - \exp\left(-\frac{|x|^2}{\sigma^2}\right)\right)^{2/d}\right\}} \right)^{d/2} \quad (4.3.3)$$

It should be noted that, in the AEXP companding technique, the non-linear function $f(x)$ operates on the magnitude of the base-band signal x . The phase of x is intentionally discarded to avoid further distortions impressed to the OFDM signal when including the phase to the companding operation.

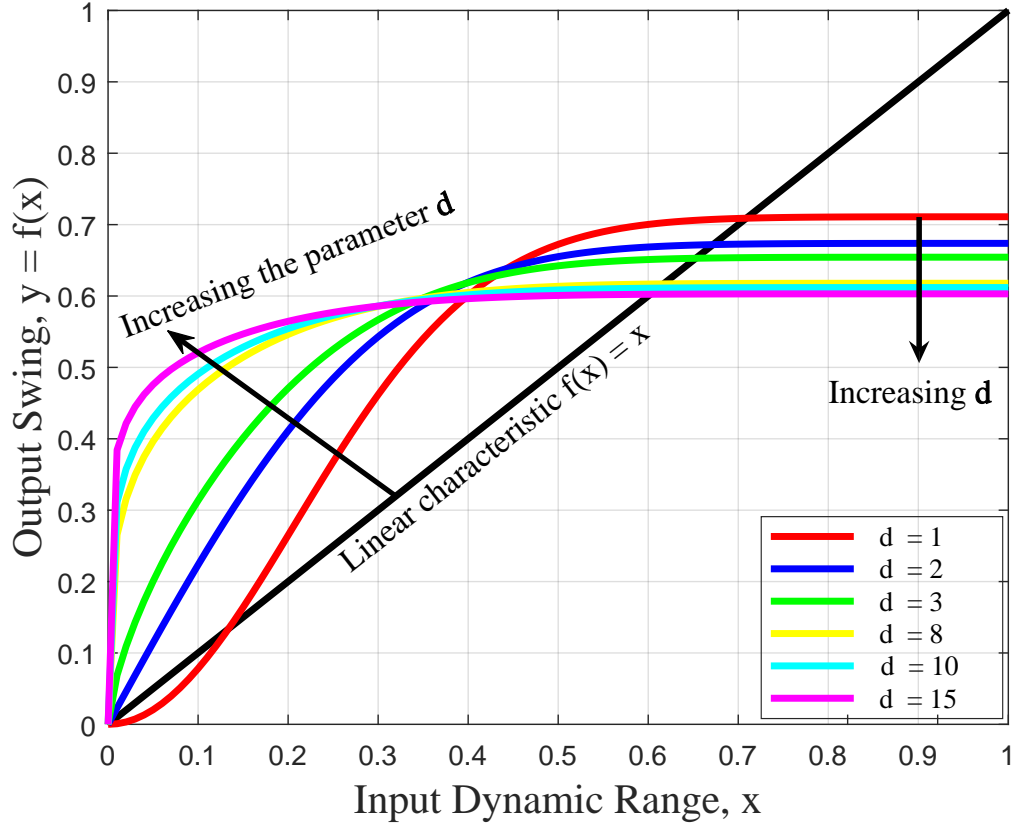


Figure 4.4: Plots of AEXP transfer function

4.4 Non-linear error function (NERF) companding technique

Non-linear error function companding (NERF) technique is suggested to minimize the high PAPR. This technique is based on the error function (erf). It changes both large and small signals, by enlarging small signals and compressing large signals. Figure 4.5 shows the transfer function of the NERF companding technique. The NERF function at the transmitter is [46]:

$$f(x) = k_1 \cdot \text{erf}\left(\frac{|x|}{\sqrt{2}\sigma}\right) \cdot \text{sgn}(x) \quad (4.4.1)$$

Where, x is the input signal before companding, $f(x)$ is the output signal after companding, k_1 is a positive constant that defines the average power of the output signals, σ is the standard deviation of input signal x , $\text{erf}(\cdot)$ is the error function and $\text{sgn}(\cdot)$ is the signum function. To maintain the same level of average power for the input and output signal (*i.e* the average power of the transmitted signal before companding should be equal to the average power of the transmitted signal after companding), the value of k_1 should be set to $\sqrt{3} * \sigma$.

At the receiver side, the NERF de-companding equation is defined by:

$$f^{-1}(x) = \sqrt{2}\sigma.erf^{-1}\left(\frac{|x|}{\sqrt{3}\sigma}\right)sgn(x) \quad (4.4.2)$$

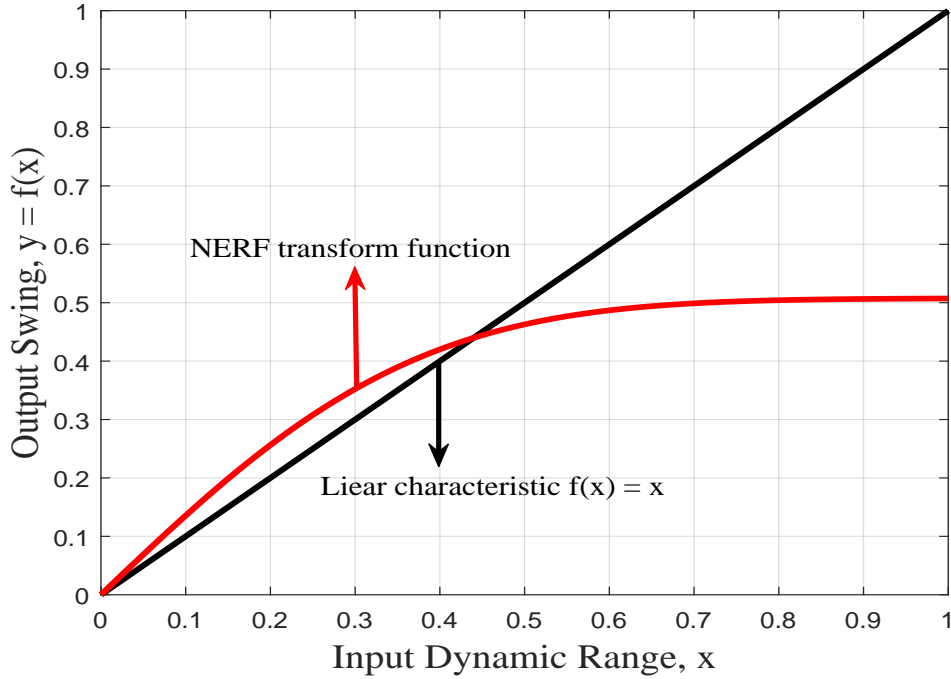


Figure 4.5: Plots of NERF transfer function

4.5 Proposed companding technique (IMADJS)

Image adjustment function (IMADJS) is used in image processing to do enhancement for pictures [69], it is also called intensity transformation function. This function maps the intensity values in signal f to new values in another signal g , such that values between low-input and high-input map to values between low-output and high-output. Values under low-input and over high-input are clipped; that is, values under low-input map to low-output, and those over high-input map to high-output [70], as seen in Figure 4.6. This function is applied on an OFDM signal to reduce the high PAPR problem. Then, the results of the new technique will be compared with the well-known companding methods. This function can change small signals and large signals simultaneously, as shown in Figure 4.7. The IMADJS technique also has the benefit of keeping a constant average power level (*i.e* average power before companding is nearly the same after companding). The IMADJS companding and de-companding function can be defined as follows:

$$f(x) = \begin{cases} c & , x \leq a \\ \left(\left(\frac{x-a}{b-a} \right)^\gamma (d-c) + c \right) & , a < x < b \\ d & , x \geq b \end{cases} \quad (4.5.1)$$

$$f^{-1}(x) = \begin{cases} a & , x \leq c \\ \left(\left(\frac{x-c}{d-c} \right)^{\frac{1}{\gamma}} (b-a) + a \right) & , c < x < d \\ b & , x \geq d \end{cases} \quad (4.5.2)$$

Where, a is low input of the signal x , b is high input of the signal x , c is low output of the signal x , d is high output of the signal x and γ is a positive number uses as a degree of companding.

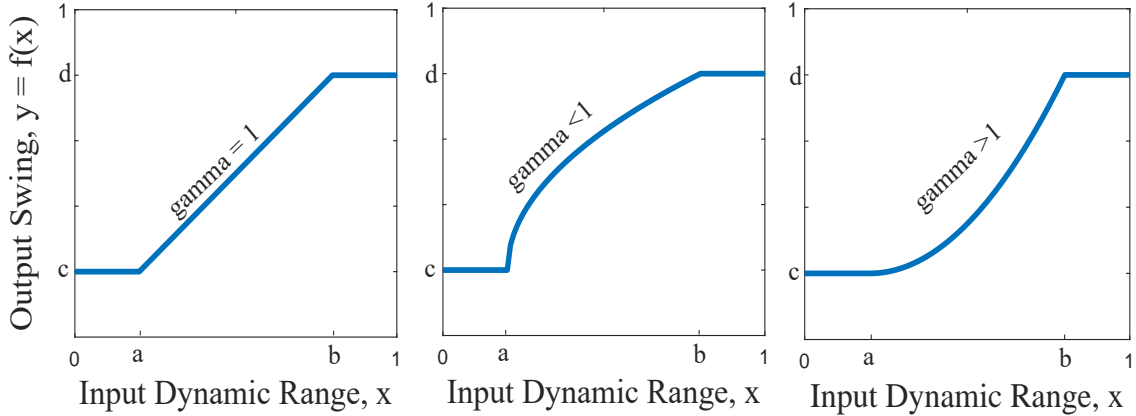


Figure 4.6: The IMADJS function with $\gamma=1$, $\gamma < 1$ and $\gamma > 1$.

Figure 4.7 displays the transfer function of the IMADJS companding technique. If the parameter γ is equal to 1, a linear mapping is used. However, the values less than one produce a function which is concave downward. Decreasing *high-in* parameter compresses large signals, while the *high-out* parameter adjusts small signals. In this thesis, the value of *low-input* and *low-output* are fixed to zero, because the minimum degradation in BER is achieved at these values (*low-in* = 0 and *low-out* = 0), as it will be explained in details in chapter 5.

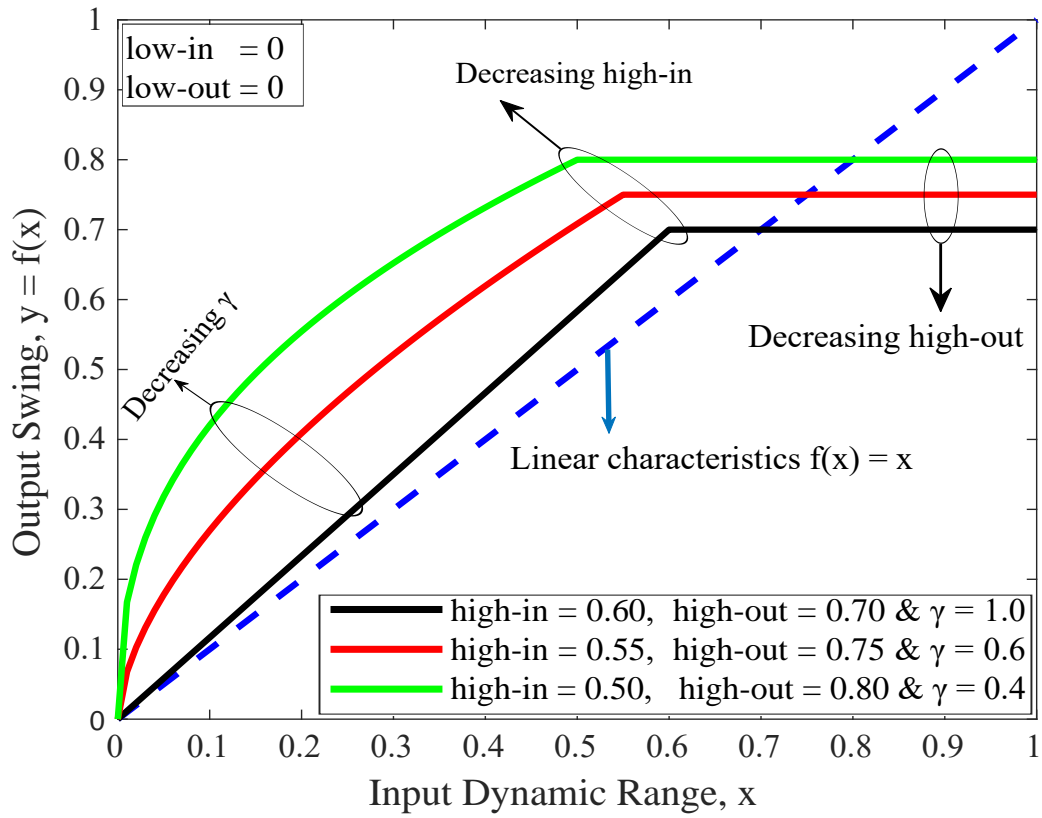


Figure 4.7: Plots of IMADJS transfer function

Simulation Results and Analysis

This chapter presents the numerical simulation results for the OFDM system using the companding techniques. The improvement in PAPR, degradation in BER, average power (Avg-pw) and power spectral density (PSD) are used as the performance metrics of interest. The improvement in PAPR is the difference between the PAPR of original signal and the PAPR of companded signal (*i.e.* Improvement in PAPR = PAPR of original signal - PAPR of companded signal). Similarly, the degradation in BER is the difference between the BER of original signal and the BER of companded signal. Table (5.1) lists the used simulation parameters of the system.

Table 5.1: Simulation Parameters

Parameter	Value and Unit
Spacing frequency (sub-carrier spacing), Δf	15 kHz
Sampling frequency (sampling rate), f_s	3.84 MHz
Number of symbols	1000 symbols
FFT size, N	256
CP length, N_{CP}	64 samples
Modulation type	M-QAM
Channel model	Additive white Gaussian noise (AWGN)
Power amplifier model (PA)	Solid-state power amplifier (SSPA)

5.1 Simulation results of companding techniques

This section presents the simulation results of different companding techniques including: A-law companding technique, μ -law companding technique, NERF companding technique and AEXP companding technique.

5.1.1 Simulation results for A-law companding technique

Figure 5.1(a) shows the PAPR reduction performance of A-law companding technique. Increasing the parameter A leads to decreasing the PAPR, which means increasing the improvement in PAPR. Less PAPR is achieved when the parameter A is 87.6, where the improvement in PAPR is around 8.1 dB (10.9 dB - 2.8 dB). Figure 5.1(b) displays the performance of BER versus Signal-to-Noise Ratio (SNR) under the A-law companding technique for five values of the parameter A . Specifically, to achieve a BER of 10^{-3} , the minimum required SNR of original OFDM signal is around 10 dB. When the parameter A is 87.6, the required SNR to achieve a BER of 10^{-3} is around 19.5 dB. Consequently, increasing the parameter A leads to increase the degradation in BER.

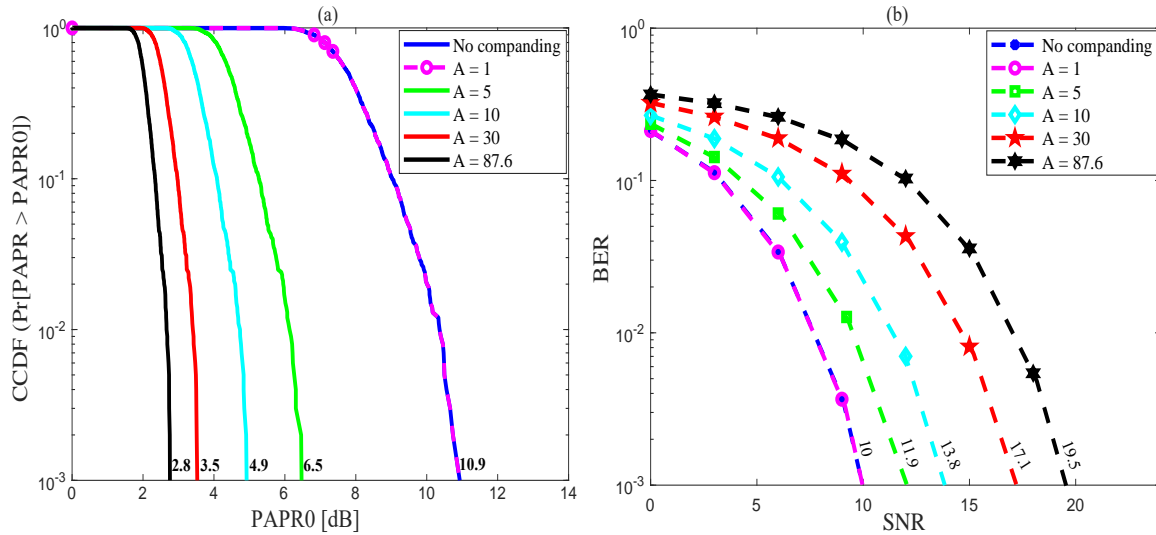


Figure 5.1: The effect of changing the parameter A on: (a) PAPR and (b) BER.

Table 5.2 shows the improvement in PAPR and the degradation in BER of A-law companding technique for five values of A . When the parameter A increases, the PAPR decreases. However, the improvement in PAPR is at the expense of the degradation in BER. When the parameter A is 1, there is neither improvement in PAPR nor degradation in BER, because the uniform quantization is achieved at $A = 1$. From the Table 5.2, it is clear that there is a trade-off between the improvement in PAPR and the degradation in BER.

Table 5.2: Performance comparison for different values of parameter A

A-law Companding Technique						
Parameter	Original signal	A=1	A=5	A=10	A=30	A=87.6
PAPR(dB) at 10^{-3}	10.9	10.9	6.5	4.9	3.5	2.8
SNR(dB) at BER 10^{-3}	10	10	11.9	13.8	17.1	19.5
Improvement in PAPR(dB)	-----	0	4.4	6	7.4	8.1
Degradation in BER (dB)	-----	0	1.9	3.8	7.1	9.5

Figure 5.2 displays the effect of increasing the parameter A on the average power of signals after companding and the constellation diagram of received signals. When the parameter A is one ($A = 1$), the input signals are equal to the output signals (characteristic curve is linear and no compression is done), which leads to maintain the average power before and after companding unchanged, as shown in Figure 5.2 (a). Consequently, the received constellation points are very close to the original ones, as seen in Figure 5.2 (b). At the parameter $A = 87.6$, the average power of the companded signal increases significantly, where the average power of the companded signal is 0.122, as portrayed in Figure 5.2 (c). This large increase in the average power leads to distortion in the received constellation points, as declared in Figure 5.2 (d). Based on the above, the more the average power is, the higher the distortion in receiving constellation points. Therefore, increasing the average power eventually leads to distort the constellation points and making the small points close to the large ones. And therefore, the BER increases as the constellation points get closer.

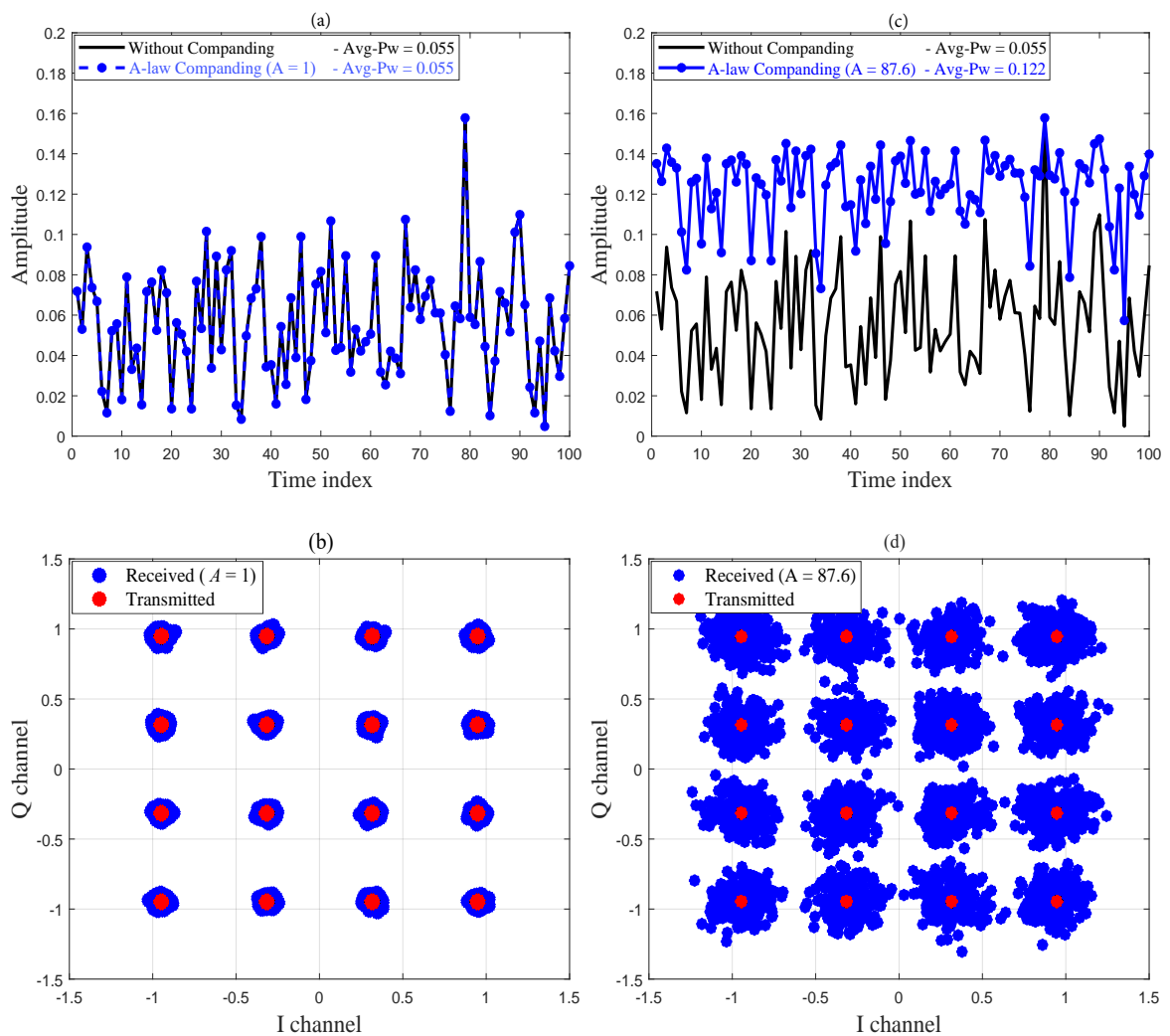


Figure 5.2: The effect of changing the parameter A on the average power and constellation points

5.1.2 Simulation results for μ -law companding technique

Figure 5.3(a) shows the complementary cumulative distribution functions (CCDF) of the PAPR for original OFDM signal and μ -law companded signal. Obviously, increasing the parameter μ leads to decreasing the PAPR, this means increasing the improvement in PAPR. The less PAPR is achieved when the parameter μ is 255, where the improvement in PAPR is around 7.9 dB (10.5 dB - 2.6 dB). Figure 5.3(b) shows the performance of BER versus Signal-to-Noise Ratio (SNR) under the μ -law companding technique for five values of the parameter μ . Specifically, to achieve a BER of 10^{-3} , the minimum required SNR of original OFDM signal is around 10 dB. When the parameter μ is 255, the required SNR to achieve a BER of 10^{-3} is around 19.7 dB. Consequently, increasing the parameter μ leads to increase the degradation in BER.

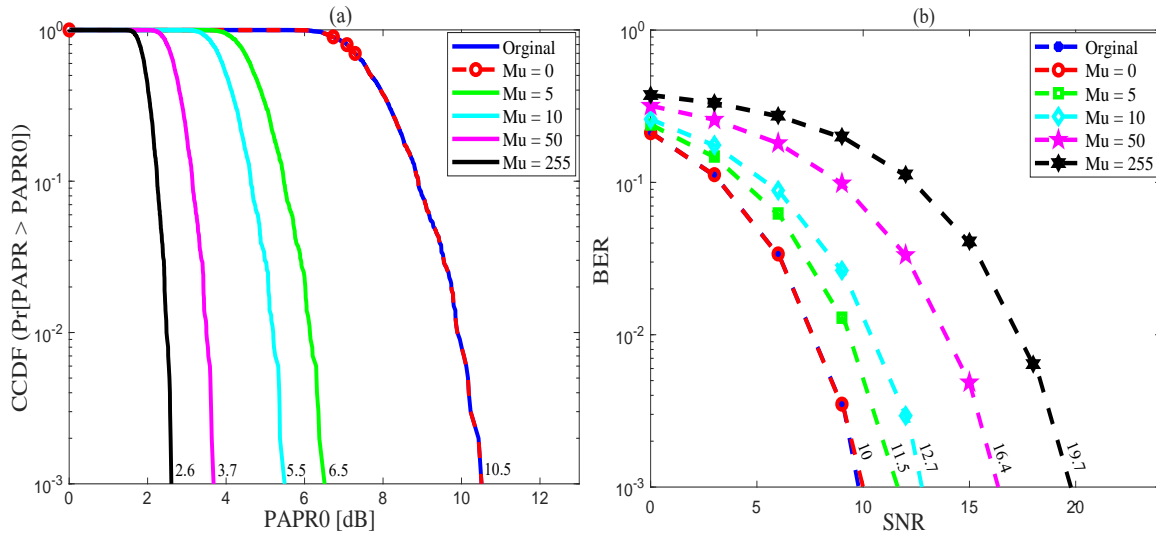


Figure 5.3: The effect of changing the parameter μ on: (a) PAPR and (b) BER.

Table 5.3 summarizes the improvement in PAPR and the degradation in BER of μ -law companding technique. When the parameter μ increases, the PAPR decreases. However, the improvement in PAPR is at the expense of the degradation in BER. When the parameter μ is 0, there is neither improvement in PAPR nor degradation in BER, because the uniform quantization is achieved at $\mu = 0$. It is clear from the table 5.3, that there is a trade-off between the improvement in PAPR and the degradation in BER.

Table 5.3: Performance comparison for different values of parameter μ

μ -law Companding Technique						
Parameter	Original signal	$\mu=0$	$\mu=5$	$\mu=10$	$\mu=50$	$\mu=255$
PAPR(dB) at 10^{-3}	10.5	10.5	6.5	5.5	3.7	2.6
SNR(dB) at BER 10^{-3}	10	10	11.5	12.7	16.4	19.7
Improvement in PAPR(dB)	-----	0	4	5	6.8	7.9
Degradation in BER (dB)	-----	0	1.5	2.7	6.4	9.7

5.1.3 Simulation results for AEXP companding technique

Figure 5.4(a) shows respectively the complementary cumulative distribution functions (CCDF) of PAPR for original OFDM signals and absolute exponential (AEXP) companded signals with degrees $d = 1$, $d = 2$, $d = 4$, $d = 8$ and $d = 10$. As seen, increasing the degree of companding d leads to decrease the PAPR. Figure 5.4 (b) displays the effect of increasing the parameter d on the degradation in BER. As seen, the degradation in BER increases with increasing the parameter d . From Figure 5.4 (a) and Figure 5.4 (b), there is a trade-off between the improvement in PAPR and the degradation in BER. When the parameter d increases, the PAPR decreases. However, this improvement is at the expense of the degradation in BER.

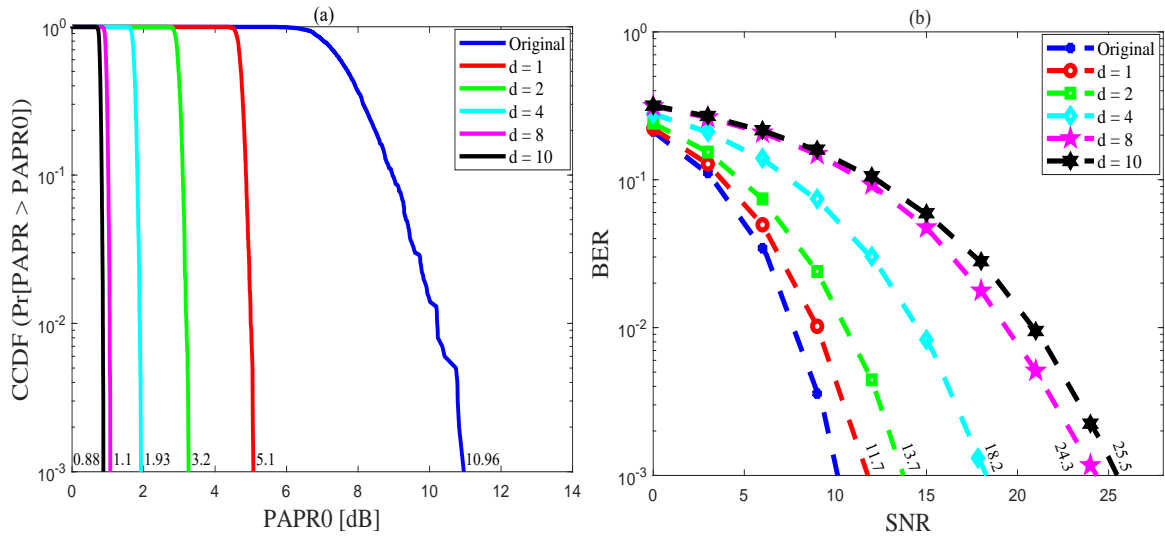


Figure 5.4: The effect of changing the parameter d on: (a) PAPR and (b) BER.

Table 5.4 summarizes the improvement in PAPR and the degradation in BER with different values for the degree of companding d . When the degree of companding d increases, the PAPR decreases. However, this improvement in PAPR leads to increase the degradation in BER. Consequently, there is a trade-off between the improvement in PAPR and the degradation in BER.

Table 5.4: Performance comparison for different values of parameter d

AEXP Companding Technique						
Parameter	Original signal	d=1	d=2	d=4	d=8	d=10
PAPR(dB) at 10 ⁻³	10.96	5.1	3.2	1.93	1.1	0.88
SNR(dB) at BER 10 ⁻³	10	11.7	13.7	18.2	24.3	25.5
Improvement in PAPR(dB)	-----	5.86	7.76	9.03	9.86	10.08
Degradation in BER (dB)	-----	1.7	3.7	8.2	14.3	15.5

5.1.4 Simulation results for NERF companding technique

Figure 5.5(a) shows the complementary cumulative distribution function (CCDF) versus the PAPR for the NERF companding technique, whereas Figure 5.5(b) plots the BER performance versus the signal to noise ratio (SNR) for the same techniques in Figure 5.5(a). It is clear from 5.5(a), a reduction of about 6.2 dB (from 10.56 dB to 4.34 dB) in the PAPR of the OFDM signal is observed at a CCDF value of 10^{-3} . However, this improvement is accompanied by a deterioration in the BER performance, as seen in Figure 5.5(b). Furthermore, a power penalty of 1.3 dB is required for a companded OFDM system to achieve the same forward error correction (FEC) BER limit of 10^{-3} that is achieved by its un-companded counterpart.

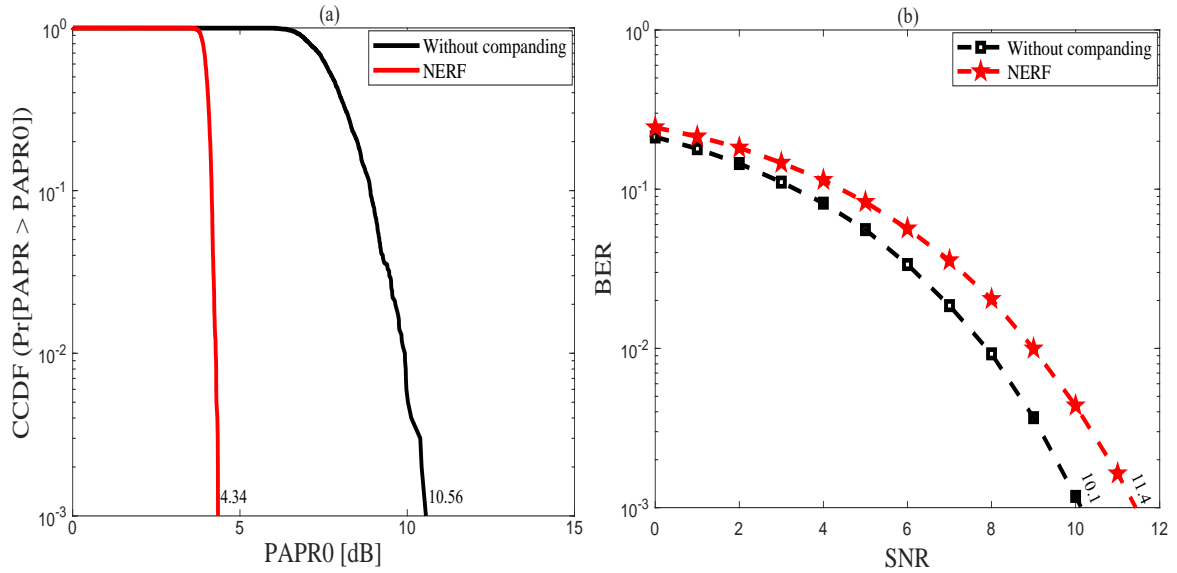


Figure 5.5: Plots of PAPR & BER for NERF companding technique: (a) PAPR and (b) BER

5.2 Simulation results for the new companding technique

The IMADJS technique has five parameters (*low-in*, *high-in*, *low-out*, *high-out* and γ). Each parameter will be studied separately to show its effect on the PAPR reduction and BER performance.

To study the effect of IMADJS parameters on the PAPR and BER, these parameters should be set to get the same PAPR and BER of the original OFDM signal. Consequently, the IMADJS parameters should be set as follows: *low-in* = 0, *low-out* = 0, *high-in* = 0.15, *high-out* = 0.15 and $\gamma = 1$. It is clear from Figure 5.6 that, the OFDM signal before companding is equal to the OFDM signal after companding. Figure 5.7 (a) shows the complementary cumulative distribution function (CCDF) versus the PAPR for the considered OFDM signal in Figure 5.6, whereas Figure 5.7 (b) plots the BER performance versus the signal to noise ratio (SNR) for the same considered OFDM signal. It is clear from Figure 5.7 (a) and Figure 5.7 (b) that, there is no improvement in PAPR and no degradation in BER when the IMADJS parameters are set as displayed in the Figures 5.7 (a) and 5.7 (b).

Firstly, Figure 5.7 (a) and Figure 5.7 (b) are used as a reference to study the effect of IMADJS parameters on the improvement in PAPR and the degradation in BER. Then, each parameter changes separately with fixing the other parameters to show the effect of changing this parameter on the PAPR reduction and BER performance. Finally, the PAPR and BER of the companded signal under IMADJS technique are compared with the PAPR and BER of the original OFDM signal in Fig. 5.7 (a) and Fig. 5.7 (b). The SNR, PAPR and BER are set to 10 dB, 10.6 dB and 10^{-3} , respectively, as references.

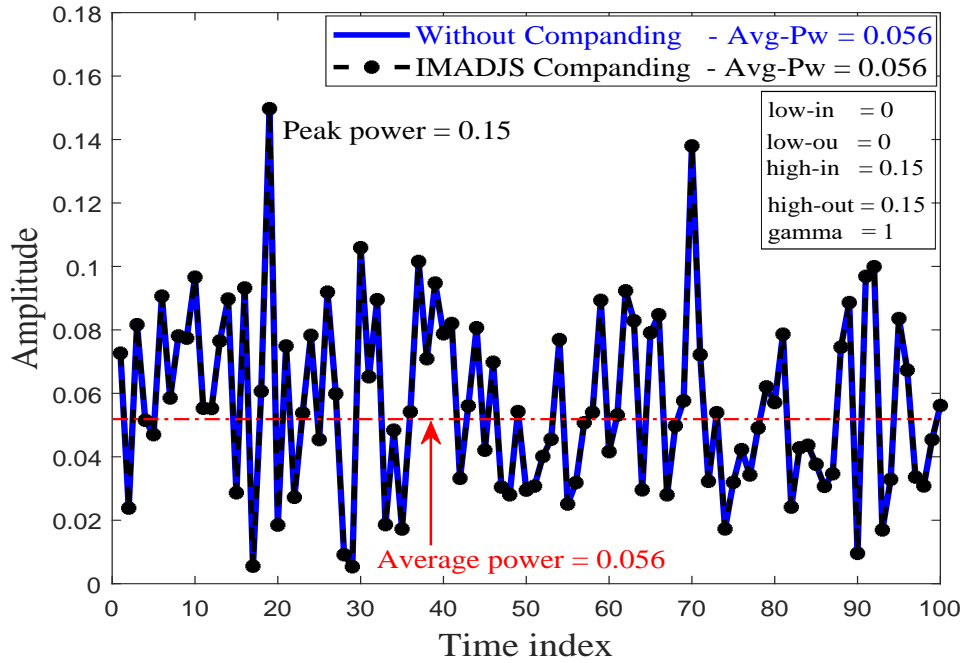


Figure 5.6: An OFDM signal with high PAPR.

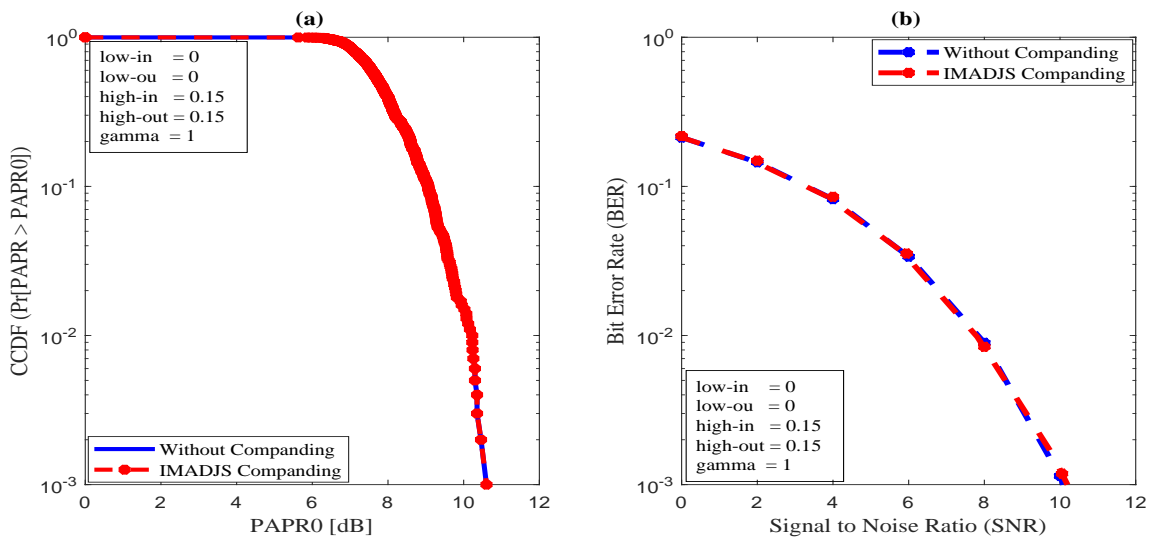


Figure 5.7: Plot of PAPR & BER for the OFDM signal: (a) PAPR and (b) BER.

5.2.1 The effect of changing the *low-in* parameter on PAPR and BER

To study the effect of *low-in* parameter on the PAPR and BER, the *low-in* parameter increases by small value ($low-in = 0:0.0015:0.15$) to show the effect of increasing this parameter on the PAPR reduction and BER performance. It is clear from Figure 5.8(a) and Figure 5.8(b) that, increasing *low-in* parameter leads to increase the PAPR and the degradation in BER. From Figure 5.8(a) and Figure 5.8(b), the best value for *low-in* parameter is zero, where the less PAPR and less degradation in BER is achieved at this value ($low-in = 0$).

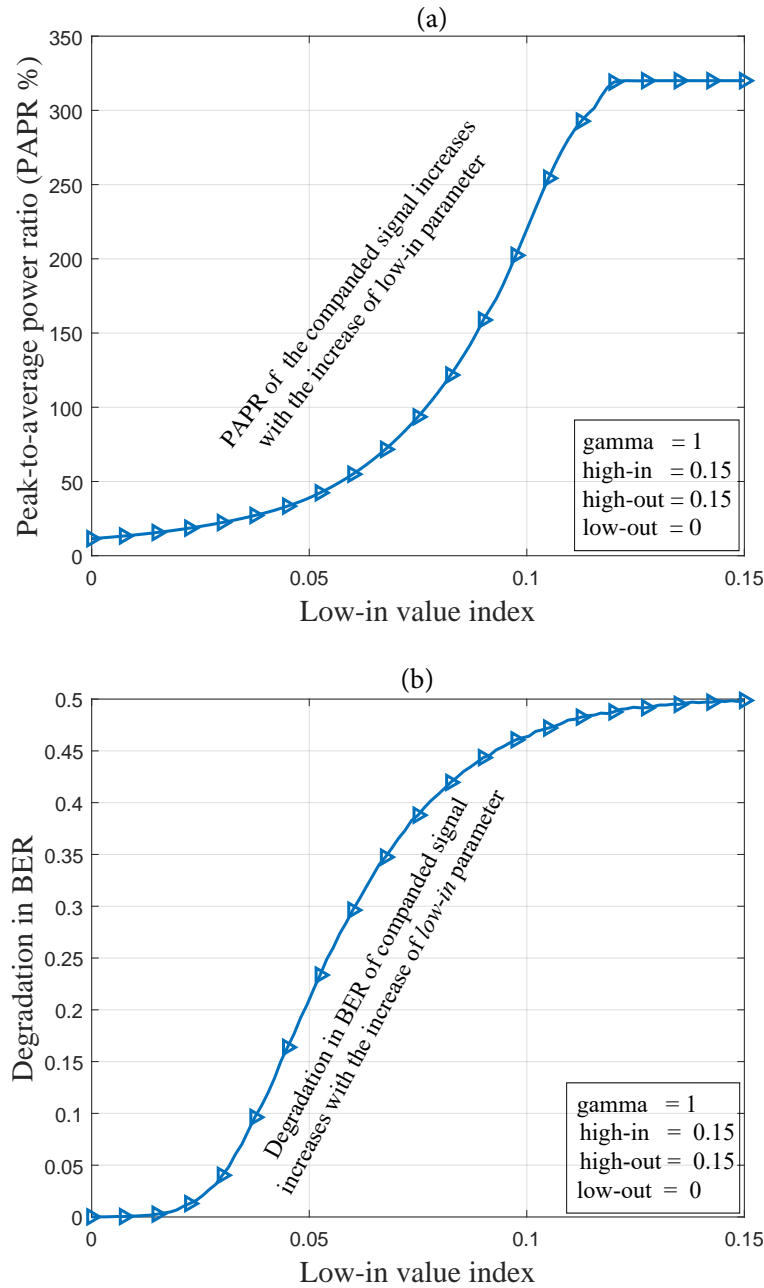


Figure 5.8: The effect of changing the *low-in* parameter on: (a) PAPR and (b) BER

Figure 5.9 shows the transfer function of IMADJS technique with increasing the *low-in* parameter. Three values for *low-in* parameter ($low-in = 0; 0.02; 0.04$) are considered and the rest parameters are fixed ($low-out = 0, high-in = 0.15, high-out = 0.15$ and $\gamma = 1$), as shown in Figure 5.9. When the *low-in* parameter is zero ($low-in = 0$), the curve of IMADJS technique (black curve) is identical to the curve of linear characteristic function {blue cure, $f(x) = x$ }. Thus, there is neither an improvement in PAPR nor degradation in BER, because the input signal is equal to the output signal. Increasing the *low-in* parameter leads to compress the small signals and keeps the peak of the signal unchanged, as it is seen with the two curves (red and green) in Figure 5.9. Decreasing small signals leads to decrease the average power of the signal. Consequently, increasing the PAPR and the degradation in BER, as shown in Figures 5.8(a) and 5.8(b). Based on the above, the optimum value of *low-in* parameter is zero.

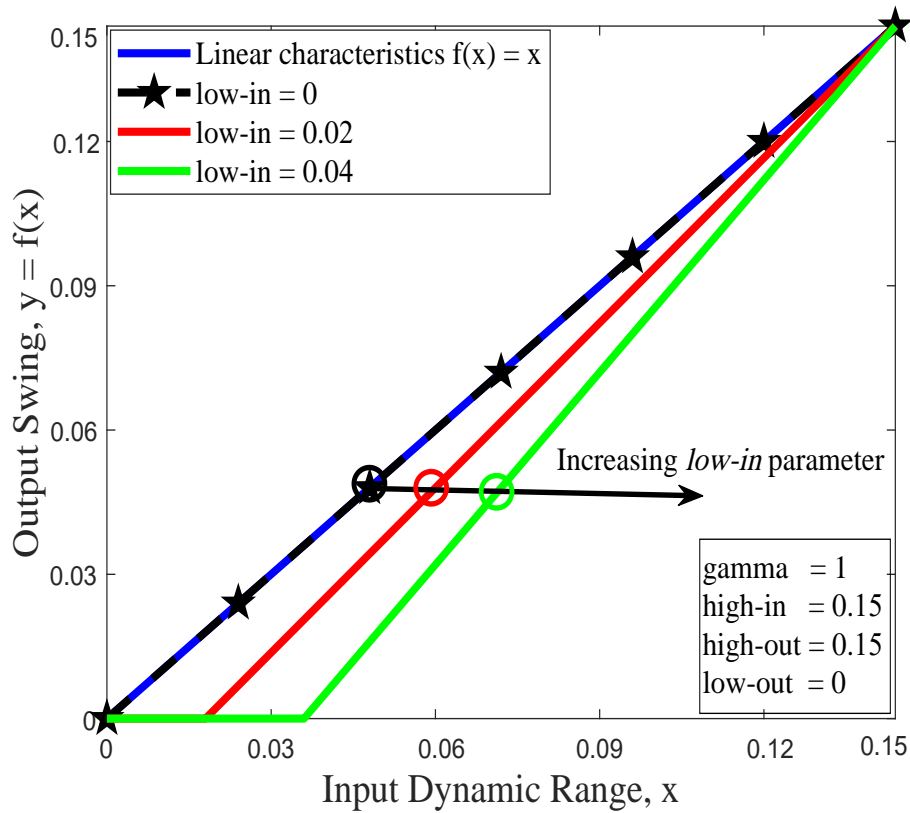


Figure 5.9: Transfer function of IMADJS companding technique with the change of *low-in* parameter.

Figure 5.10(a) displays the PAPR of IMADJS technique with three values of *low-in* parameter. When the *low-in* parameter is zero ($low-in = 0$), there is no improvement in PAPR (*i.e.* PAPR of original OFDM signal = The PAPR of companded signal = 10.6 dB). Also, the BER before companding (blue curve) is equal the BER after companding (red curve), which means there is no degradation in BER, as shown in Figure 5.10(b). Increasing *low-in* parameter leads to decrease the average power of the signal, which leads to increase the PAPR and the degradation in BER, as it is clear in the two curves (green and black) in Figure 5.10(a) and Figure 5.10(b). This confirms again that the optimum value for *low-in* parameter is zero.

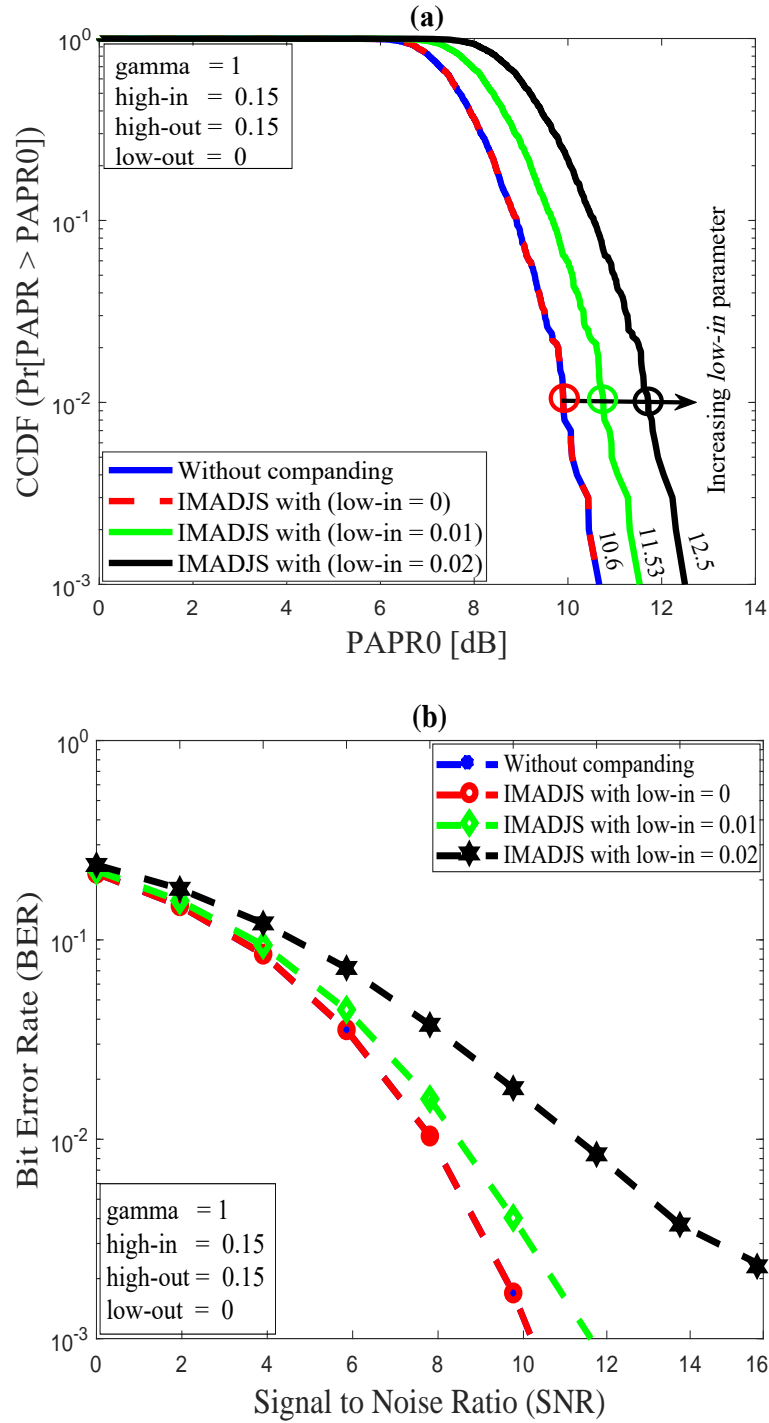


Figure 5.10: IMADJS technique with the change of $low-in$ parameter: (a) PAPR and (b) BER

5.2.2 The effect of changing the $low-out$ parameter on PAPR and BER

To present the effect of $low-out$ parameter on the PAPR and BER, the $low-out$ parameter increases by small value ($low-out = 0:0.0015:0.15$) to show the effect of increasing this parameter on the PAPR

reduction and BER performance. Figure 5.11(a) shows that the improvement in PAPR increases by increasing the *low-out* parameter. However, this improvement in PAPR is at the expense of the degradation in BER, where increasing the *low-out* parameter leads to increase the degradation in BER, as seen in Figure 5.11(b).

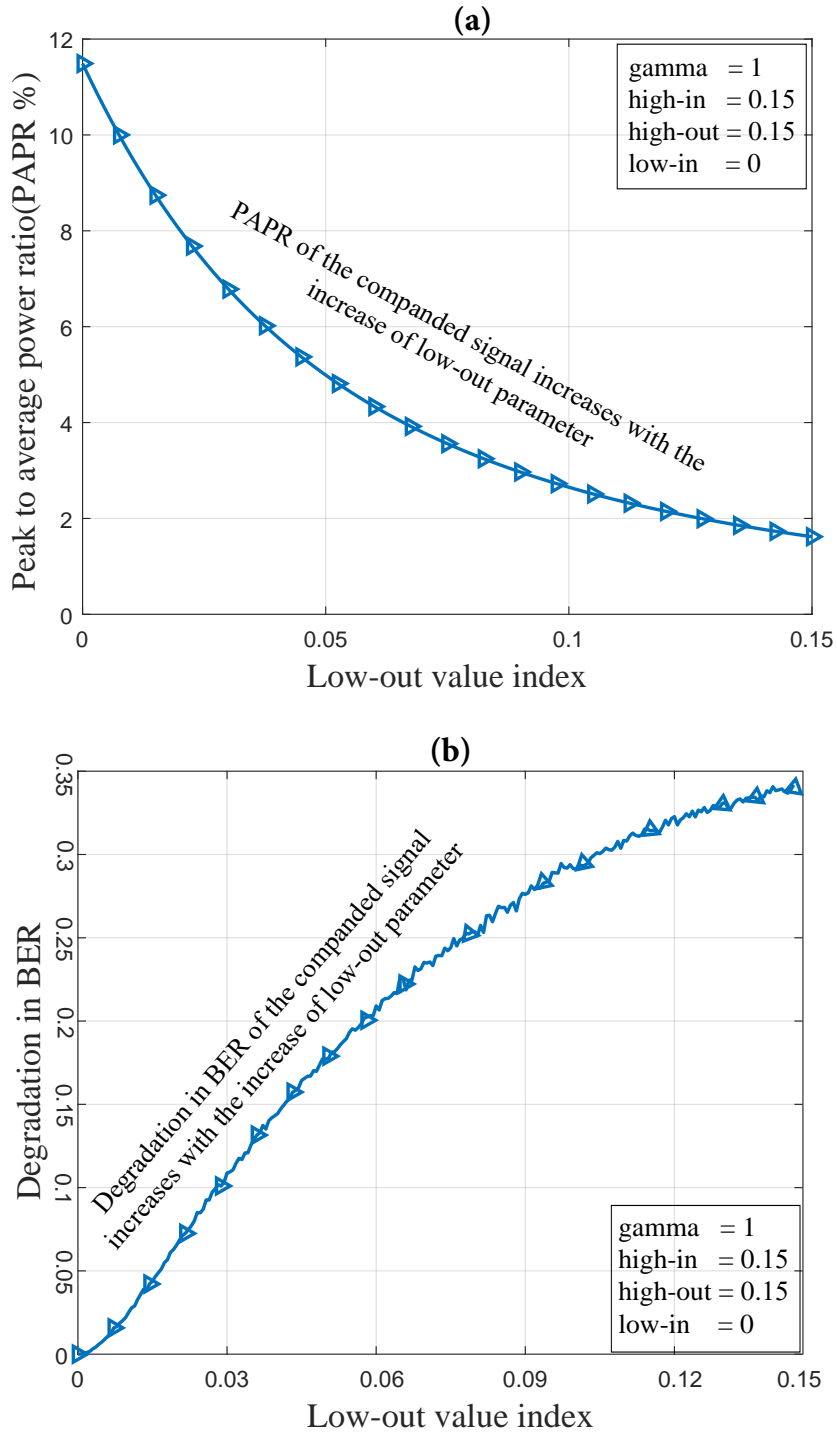


Figure 5.11: The effect of changing the *low-out* parameter on: (a) PAPR and (b) BER

Figure 5.12 shows the transfer function of IMADJS technique when the *low-out* parameter increases. Three values for *low-out* parameter ($low-out = 0; 0.025; 0.050$) are considered and the rest parameters are fixed ($low-in = 0, high-in = 0.15, high-out = 0.15$ and $\gamma = 1$), as shown in Figure 5.12. When the *low-out* parameter is zero ($low-out = 0$), the curve of IMADJS technique (red curve) is identical to the curve of linear characteristic function {blue curve, $f(x) = x$ }. Thus, there is neither an improvement in PAPR nor degradation in BER, because the input signal is equal to the output signal. Increasing *low-out* parameter leads to enlarge small signals and keeps the peak of the signal unchanged, as it is seen with the two curves (green and black) in Figure 5.12. Increasing the *low-out* parameter leads to increase the average power of the signal, which leads to increase the improvement in PAPR and the degradation in BER, as shown in Figures 5.11(a) and 5.11(b).

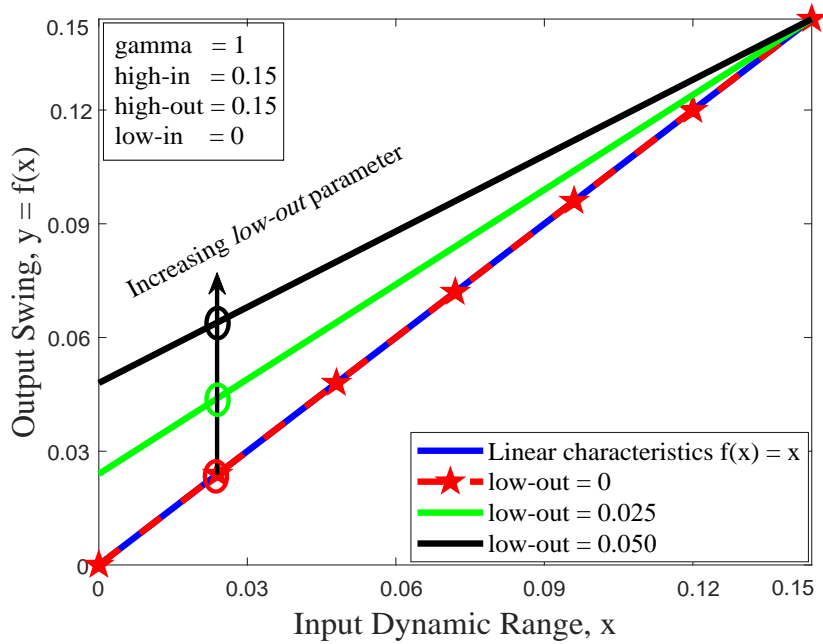


Figure 5.12: Transfer function of IMADJS companding technique with the change of *low-out* parameter.

Figure 5.13 shows the improvement in PAPR and degradation in BER for three values of *low-out* parameter in IMADJS technique. Figure 5.13(a) displays the improvement in PAPR with four fix parameters ($low-in = 0, high-in = 0.15, high-out = 0.15$ and $\gamma = 1$) and three values for the *low-out* parameter. At $low-out = 0$, there is no companding (the signal before and after companding is the same). Increasing the *low-out* parameter leads to increase the small signals, which cause to increase the average power; therefore, decreasing the PAPR. Increasing the *low-out* parameter by a small value (0.001 and 0.002) leads to negligible improvement in PAPR (0.32 dB, 0.60 dB), as seen in Figure 5.13(a). However, this improvement is accompanied by deterioration in the BER performance, as shown in Figure 5.13(b). In order to achieve the same BER (10^{-3}) of the original OFDM signal (without companding), the required SNRs are about 10.5 dB at $low-out = 0.001$ and 11 dB at $low-out = 0.002$. Accordingly, the degradation in BER is large compared to the improvement in PAPR. Based on the above, the best choice for *low-out* parameter is zero. Where at $low-out = 0$, the improvement in PAPR is zero and the degradation in BER is zero as well.

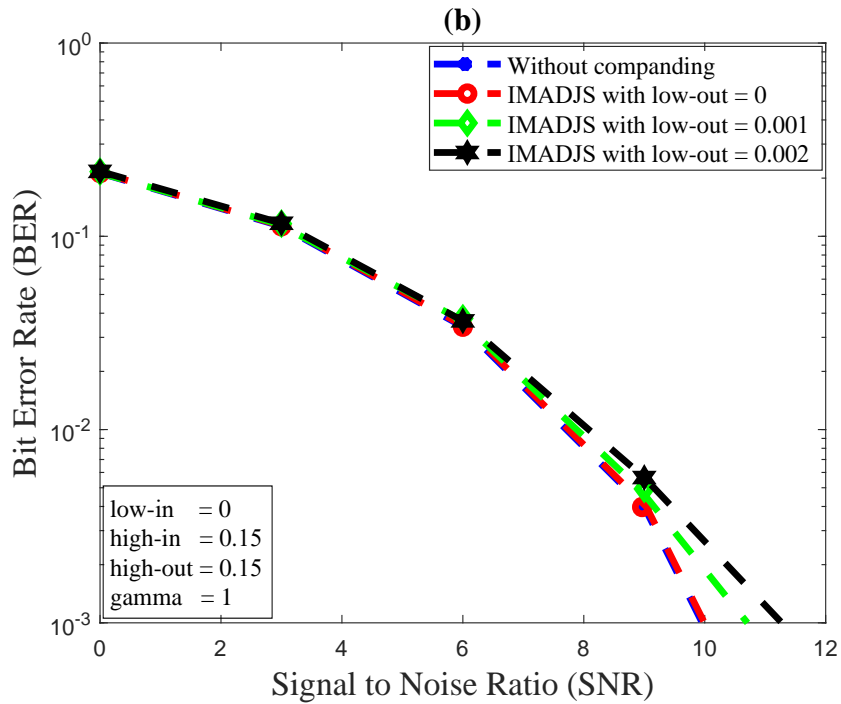
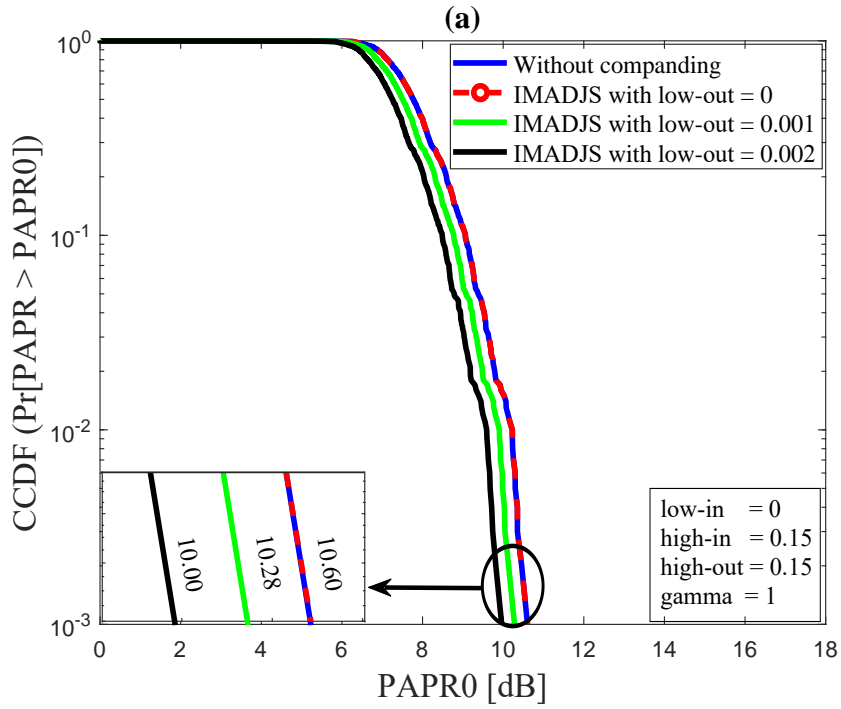


Figure 5.13: IMADJS technique with the change of *low-out* parameter: (a) PAPR and (b) BER

5.2.3 The effect of changing the *high-out* parameter on PAPR and BER

To show the effect of changing the *high-out* parameter on the PAPR and the BER, the *high-out* parameter changes by small value ($high-out = 0.0015:0.0015:0.15$) to see the effect of alteration of this

parameter on the PAPR and BER. Figure 5.14(a) shows that the PAPR is fixed (the PAPR after companding = the PAPR before companding) with the increase of *high-out* parameter and the BER is fixed as well, as seen in Figure 5.14(b).

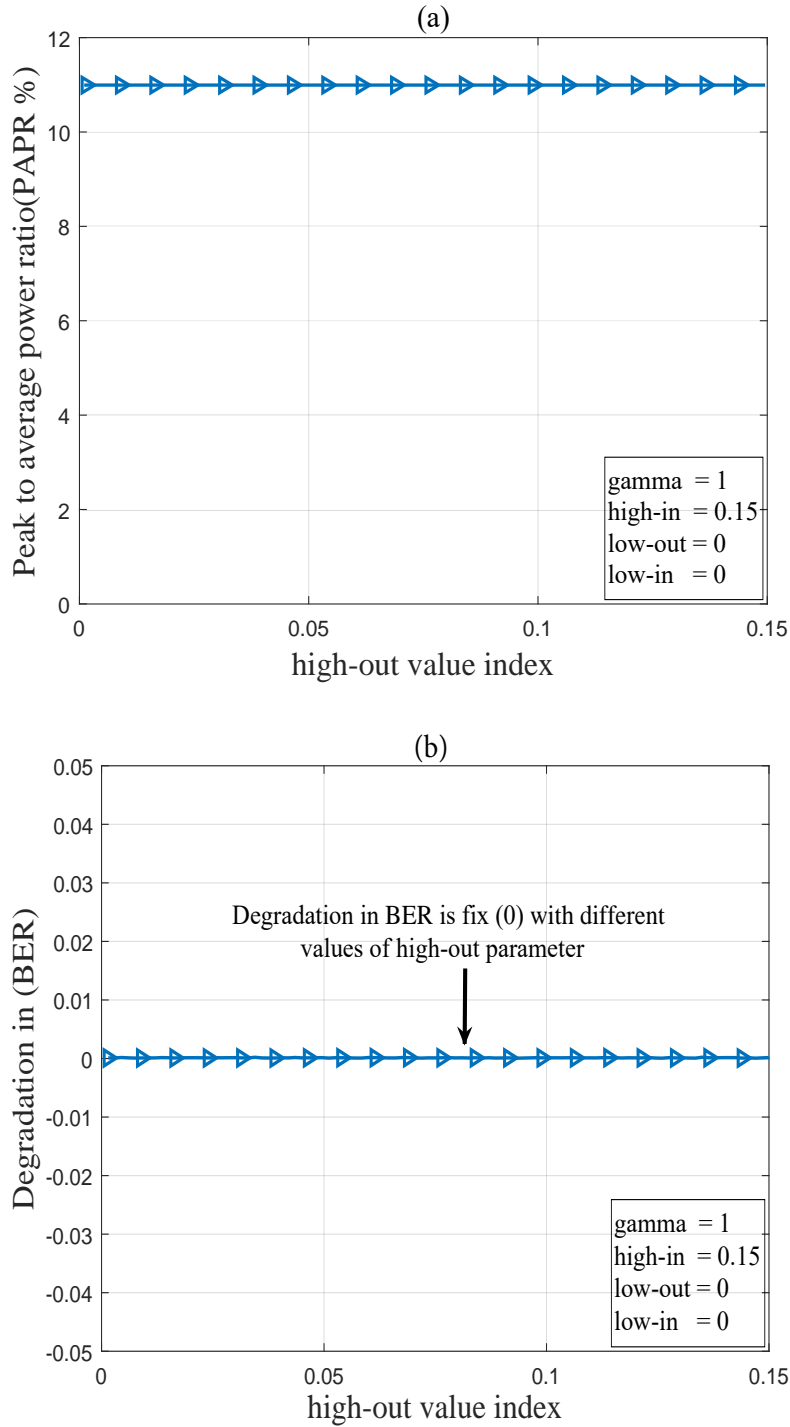


Figure 5.14: The effect of changing the *high-out* parameter on: (a) PAPR and (b) BER

Figure 5.15 shows the transfer function of IMADJS technique when the *high-out* parameter decreases. Three values for *high-out* parameter ($high-out = 0; 0.025; 0.050$) are considered and the rest parameters are fixed as follows: $low-in = 0$, $high-in = 0.15$, $low-out = 0$ and $\gamma = 1$, as shown in Figure 5.15. At $high-out = 0.15$, the curve after companding (red curve) is identical to the curve before companding (blue curve) and this means there is no companding. Decreasing the *high-out* parameter leads to do scaling for the input signal (compress all the signal by the same level), as it is clear in the two curves green and black in Figure 5.15. Consequently, this is the reason that the PAPR and BER are unchanged in Figures 5.14(a) and 5.14(b), although the *high-out* parameter decreases.

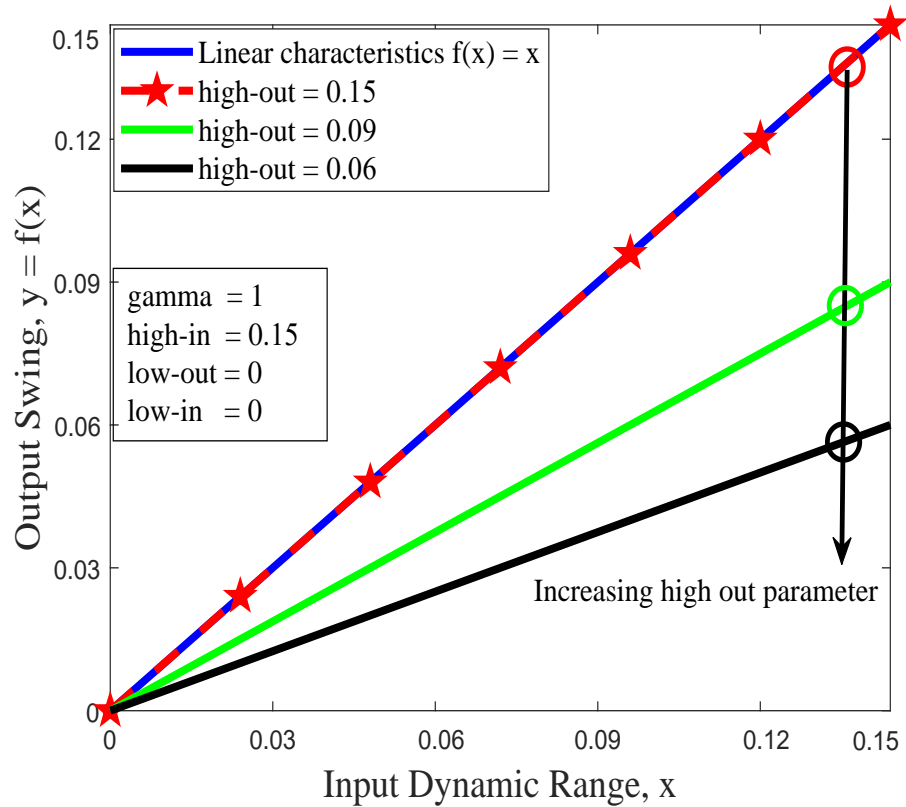


Figure 5.15: Transfer function of IMADJS companding technique with the change of *high-out* parameter.

Figure 5.16(a) displays the complementary cumulative distribution function (CCDF) versus the PAPR for the considered companding technique, whereas Figure 5.16(b) plots the BER performance versus the signal to noise ratio (SNR) for the same techniques in Figure 5.16(a). It is clear from Figure 5.16(a) that, decreasing the *high-out* parameter leads to do scaling for the input signal (compress all the signal by the same level) and hence keeping the PAPR and BER unchanged.

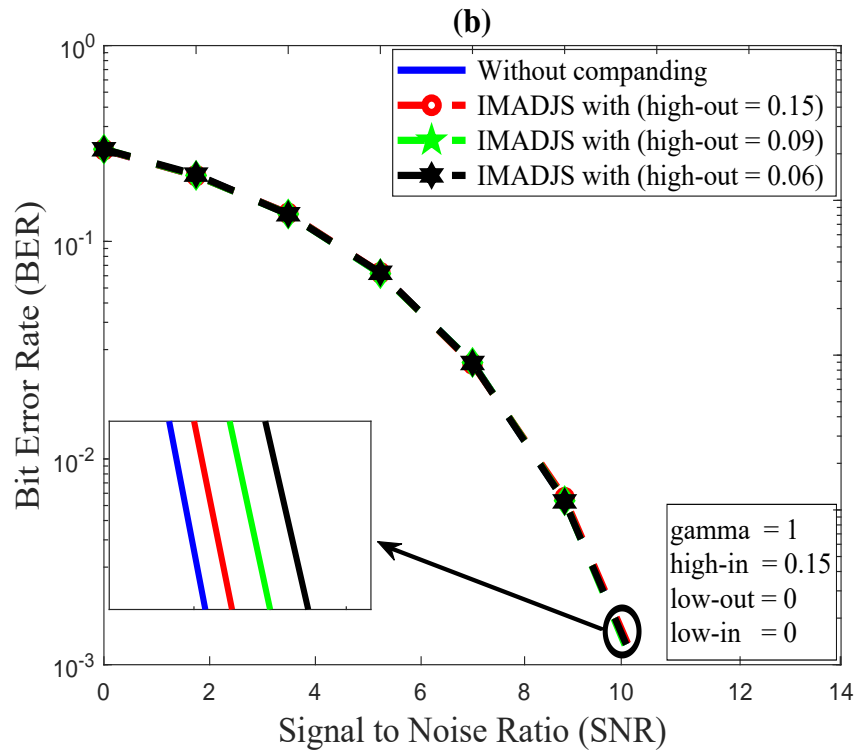
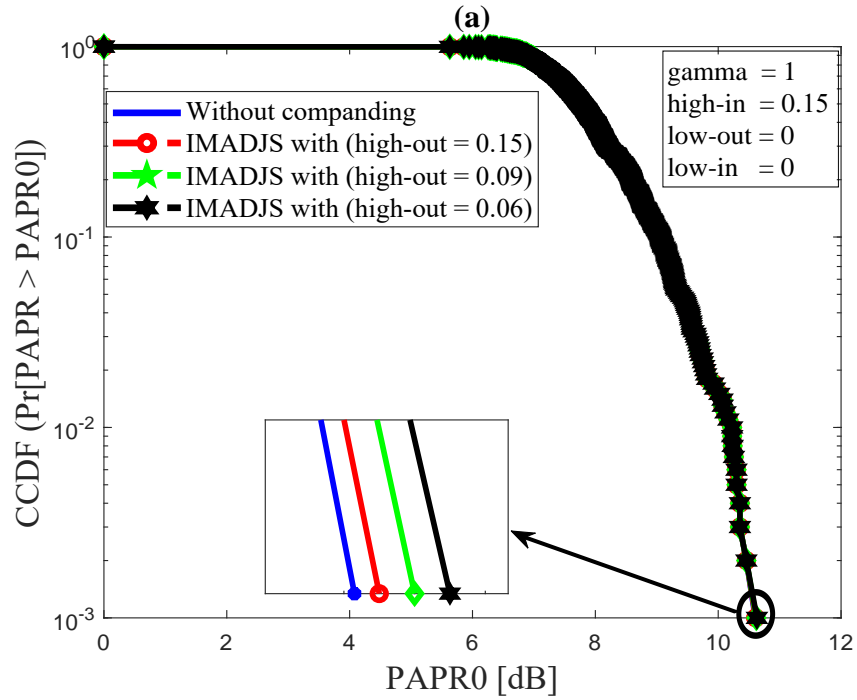


Figure 5.16: IMADJS technique with the change of *high-out* parameter: (a) PAPR and (b) BER

5.2.4 The effect of changing the *high-in* parameter on PAPR and BER

To study the effect of *high-in* parameter on the PAPR and BER, the *high-in* parameter changes by small value ($high-in = 0.0015:0.0015:0.15$) to show the effect of decreasing this parameter on the PAPR reduction and BER performance. Decreasing the *high-in* parameter leads to decrease the PAPR and hence increasing the improvement in PAPR, as seen in Figure 5.17(a). For the BER, Figure 5.17(b) shows that the degradation in BER increases with the decrease of *high-in* parameter.

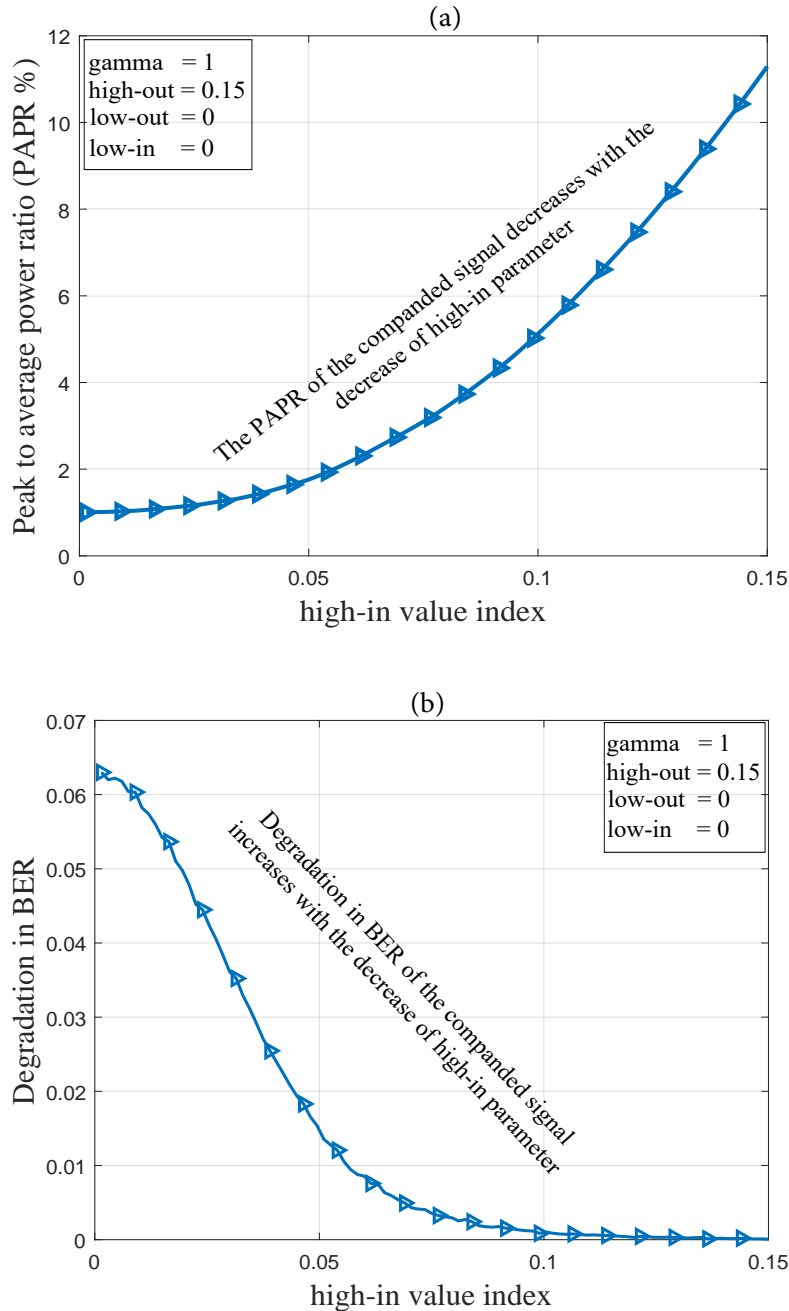


Figure 5.17: The effect of changing the *high-in* parameter on: (a) PAPR and (b) BER

Figure 5.18 displays the transfer function of IMADJS technique with four fix parameters and three values for *high-in* parameter. At *high-in* = 0.15, the curve after companding (green curve) is identical to the curve before companding (blue curve) and this means there is no companding. Decreasing the *high-in* parameter leads to map the values that are over *high-in* parameter to *high-out* parameter, as it is clear in the two curves red and black in Figure 5.18. This in turn would cause to decrease the PAPR and increase the improvement in PAPR. However, this improvement is at the expense of the degradation in BER.

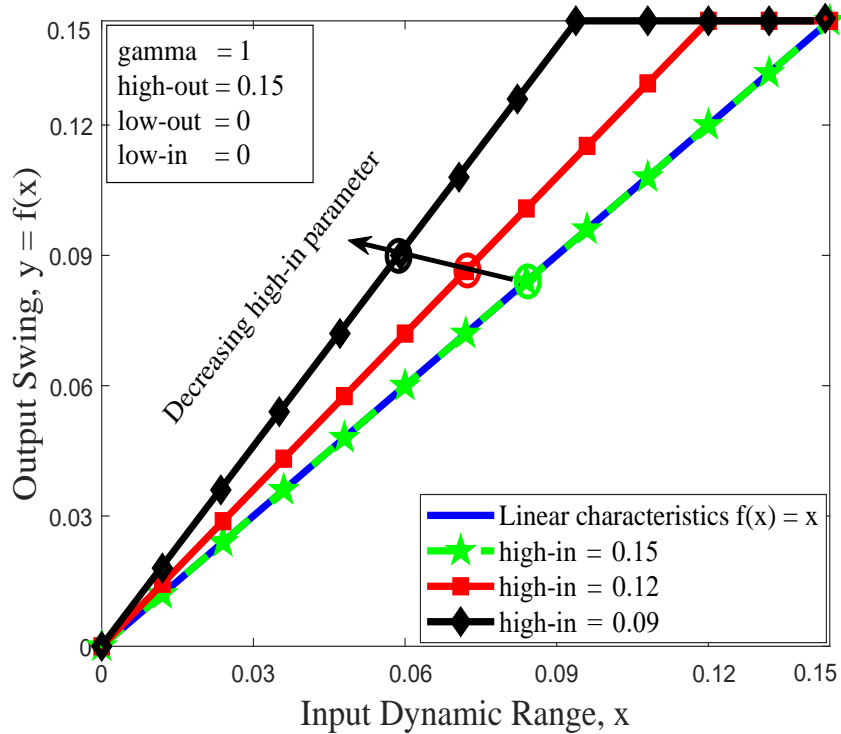


Figure 5.18: Transfer function of IMADJS companding technique with the changing of *high-in* parameter.

Figure 5.19(a) shows the PAPR of IMADJS technique for three values of *high-in* parameter (*high-in* = 0.15; 0.12; 0.09). At *high-in* = 0.15, the PAPR of companded signal (red curve) is equal to the PAPR of original OFDM signal (blue curve) = 10.60 dB. Therefore, the improvement in PAPR is zero, as shown in Figure 5.19(a). Similarly, the degradation in BER is zero, as shown in Figure 5.19(b). At *high-in* = 0.12, the PAPR of companded signal (green curve) is 6.07 dB. Therefore, the improvement in PAPR is 4.53 dB, and the SNR at BER 10^{-3} degradation is 1.1 dB. At *high-in* = 0.09, the PAPR of companded signal (black curve) is 4.13 dB. Accordingly, the improvement in PAPR is 6.47 dB, and the SNR at BER 10^{-3} degradation is 2 dB. Consequently, decreasing the *high-in* parameter leads to decrease the PAPR, this in turn leads to increase the improvement in PAPR, as shown in Figure 5.19(a). However, this improvement in PAPR is at the expense of the degradation in BER, where decreasing the *high-in* parameter leads to increase the degradation in BER, as seen in Figure 5.19(b). It is clear from Figure 5.19(a) and Figure 5.19(b) that there is a trade-off between the improvement in PAPR and the degradation in BER.

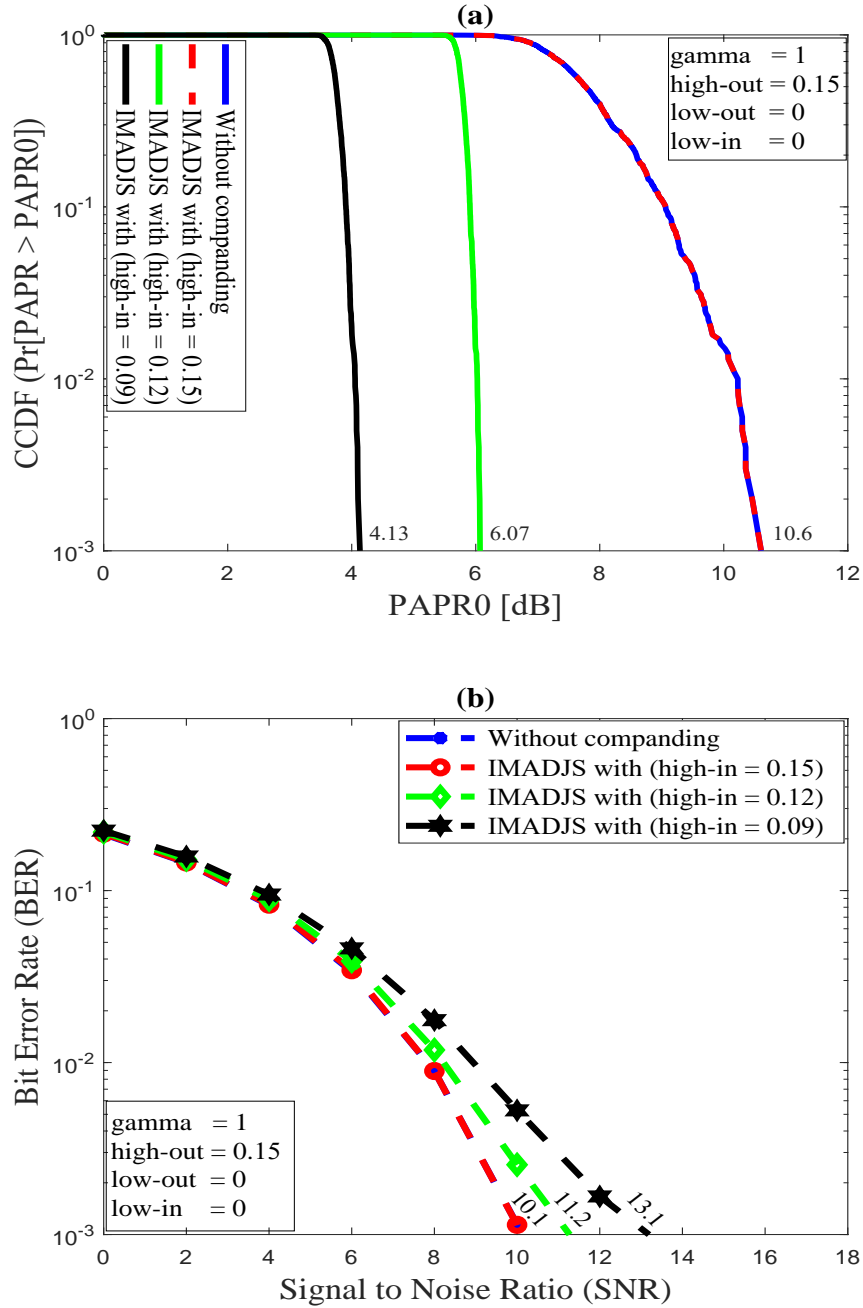


Figure 5.19: IMADJS technique with the change of $high-in$ parameter: (a) PAPR and (b) BER

5.2.5 The effect of changing the degree of companding (γ) on PAPR and BER in IMADJS technique

To show the effect of changing the degree of companding (γ) on the PAPR and BER in IMADJS technique, the parameter γ changes by small value ($\gamma = 0:0.02:2$). The PAPR of the original signal (before companding) is 11.49 (10.6 dB) and the PAPR of companded signal with $\gamma = 1$ is 11.49 as well.

The PAPR decreases when the parameter γ less than 1, because the small signals are enlarged with γ less than 1. However, PAPR increases when the parameter γ greater than 1, because the small signals are compressed with γ greater than 1, as seen in Figure 5.20(a). The BER increases when the parameter γ less than 1 or greater than 1, as shown in Figure 5.20(b).

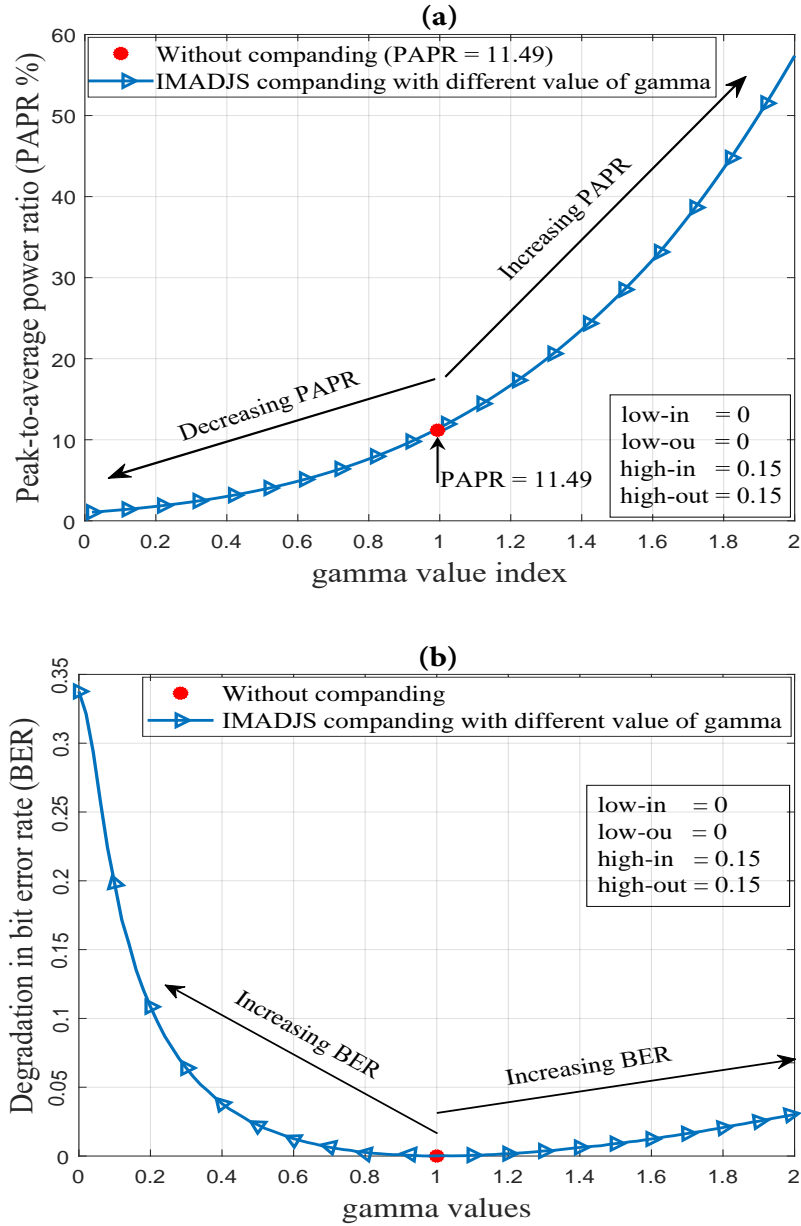


Figure 5.20: Effect of decreasing the γ value on the IMADJS technique with (a): PAPR and (b): BER.

In order to get the optimum point for the parameter γ , the two curves in Figure 5.20 (the curve of the PAPR and the curve of the BER) are multiplied. The optimum value for γ is 1, as it is clear in Figure 5.21.

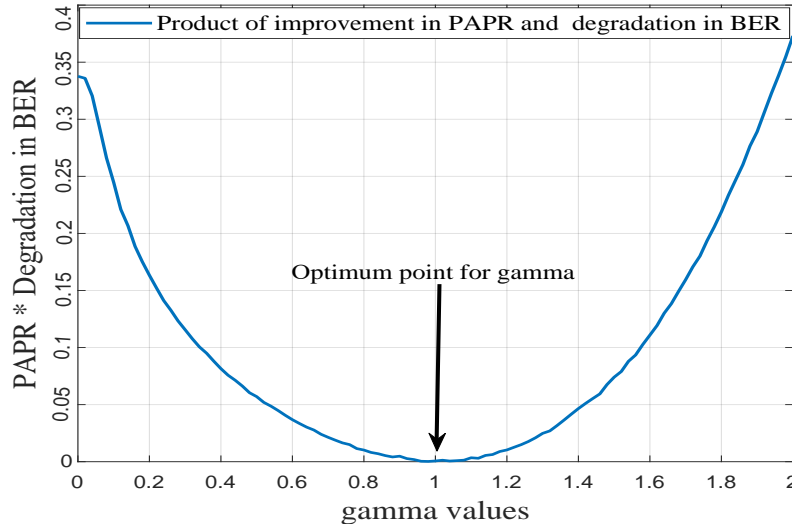


Figure 5.21: Product of the PAPR curve and the BER curve

Figure 5.22 shows the transfer function of IMADJS technique for different values of γ ($\gamma = 0.5$, $\gamma = 0.8$, $\gamma = 1.0$, $\gamma = 1.5$ and $\gamma = 2.0$) and four fix parameters ($low-in = low-out = 0$ and $high-in = high-out = 0.15$). For $\gamma = 1.0$, the signal after companding is equal to the signal before companding. Decreasing γ ($\gamma < 1$) leads to enlarge small signals and keep the peak of the signal unchanged, as shown in Figure 5.22. Consequently, the improvement in PAPR increases, as shown in Figure 5.20(a). Increasing γ ($\gamma > 1$) leads to compress small signals and keep the peak of the signal unchanged, as seen in Figure 5.22. Therefore, this leads to increase the PAPR, as shown in Figure 5.20(a). Distorting signal (increasing or decreasing γ) leads to increase the degradation in BER, as shown in Figure 5.20(b).

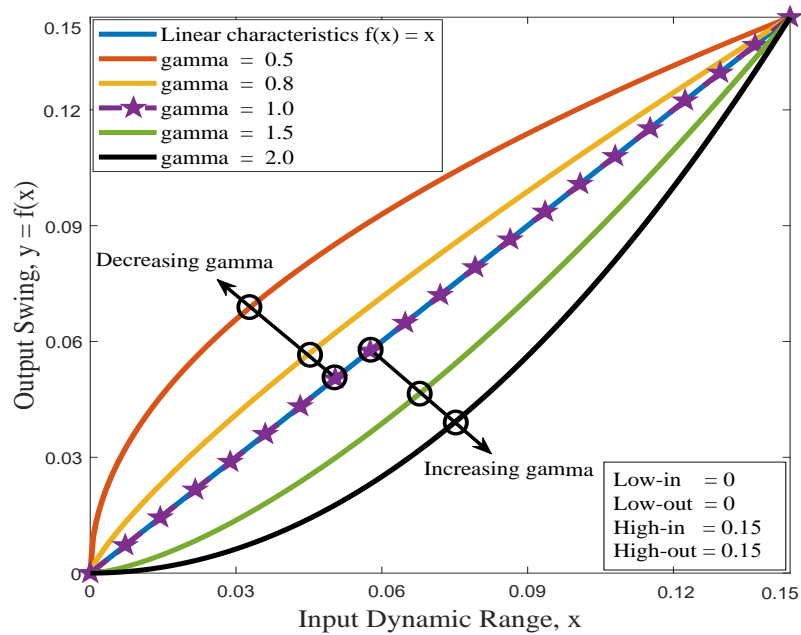


Figure 5.22: Transfer function of IMADJS technique with the change of γ parameter.

5.3 Performance comparison of companding-based PAPR suppression techniques using multi-path channel.

In this section, the different companding techniques are compared by using a multi-path channel. Rural Urban channel (COST207) with 6 paths is used as a multi-path channel. Table 5.5 shows the channel power and delay according to COST207. NERF companding technique is used as a reference for a PAPR reduction and BER performance. Unlike the other companding techniques, NERF companding technique produces one value for PAPR and one value for BER. Consequently, in order to obtain fair comparison between all techniques, the parameters of all techniques are set to get the same PAPR with NERF companding technique (4.3 dB), as shown in Figure 5.23 (a). Then, the BER performance will be compared for different companding techniques, as seen in Figure 5.23 (b).

Table 5.5: Channel Power-Delay profile [10].

Rural Urban channel (COST207)						
Tap number	1	2	3	4	5	6
Power (dB)	0	-4	-8	-12	-16	-20
Delay (μ s)	0	0.1	0.2	0.3	0.4	0.5

5.3.1 Comparing IMADJS technique with the existing companding techniques based on the PAPR and BER.

In this section, the new technique (IMADJS) is compared with μ -law, AEXP and NERF companding techniques, based on the PAPR and BER. In order to get a fair comparison, the parameters for all techniques are changed carefully to obtain the same PAPR of NERF companding technique "4.3 dB", as seen in Figure 5.23(a). The NERF companding technique gives one value for PAPR (The PAPR for NERF = 4.3 dB). Accordingly, it is used as a reference. In order to get the same PAPR of the NERF companding technique (4.3 dB), the degree of companding for AEXP technique is 1.3 ($d = 1.3$) and the μ -law parameter is 28 ($\mu = 28$). For the IMADJS technique, it has two cases: first case is IMADJS technique with $\gamma = 1$ and the second case is IMADJS technique with γ is less than 1 ($\gamma < 1$). For the first case, in order to get the same PAPR of the NERF technique, the IMADJS technique parameters are set as follows: $low-in = 0$, $low-out = 0$, $high-in = 0.094$, $high-out = 0.10$ and $\gamma = 1$. For the second case, to get the same PAPR of the NERF technique, the parameters of IMADJS technique are set as follows: $low-in = 0$, $low-out = 0$, $high-in = 0.104$, $high-out = 0.11$ and $\gamma = 0.8$.

At the same improvement in PAPR for all techniques, as seen in Figure 5.23(a), the less degradation in BER is achieved by using the new technique (IMADJS) with $\gamma = 1$, as shown in Figure 5.23(b). Accordingly, the new technique (IMADJS) is a good choice to reduce high PAPR in a noisy channel (multi-path channel). The μ -law companding technique has the worst degradation in BER, as shown in Figure 5.23(b). The μ -law companding technique enlarges the small signals and keeps the peak of the signal unchanged. Accordingly, the resulting companded signals possess high average power levels. However, the increase in the average power of the companded OFDM signals is accompanied by degradation in the BER performance.

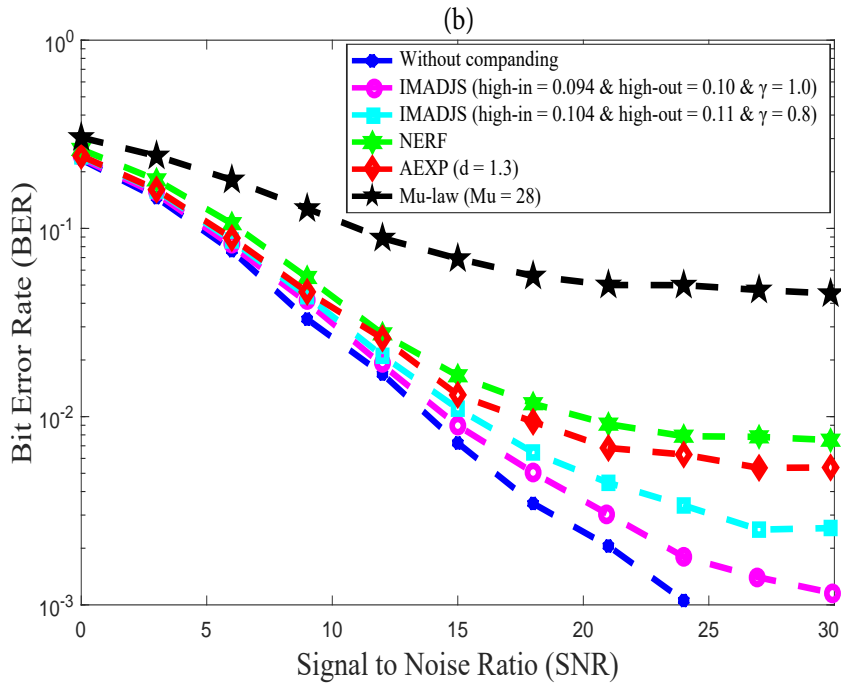
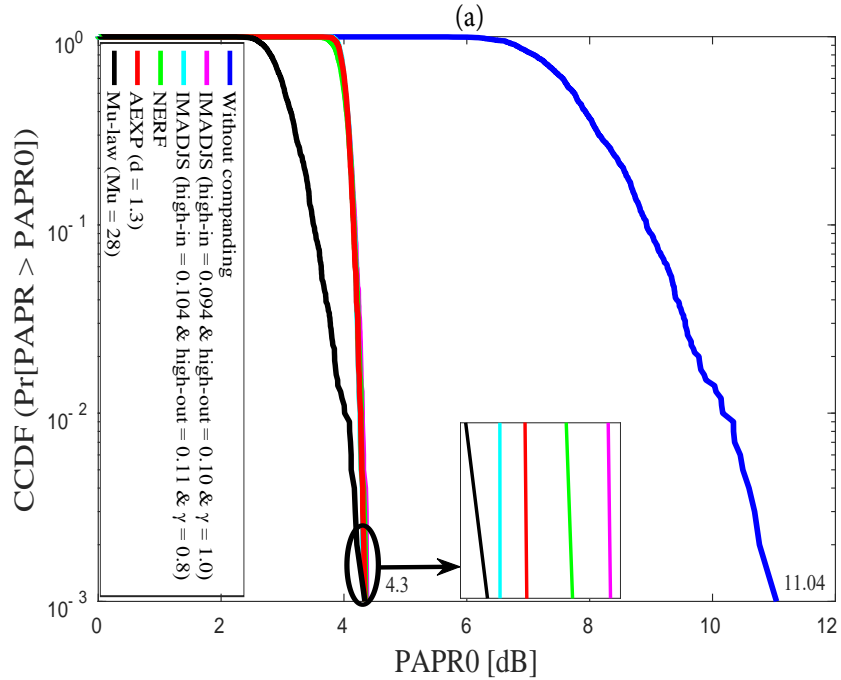


Figure 5.23: Comparing the different companding techniques based on BER when they have same PAPR: (a) same PAPR and (b) BER.

Figure 5.24 shows the BER and PAPR for four different companding techniques, which compares companded with un-companded signal. The parameters for all techniques are changed carefully to obtain the same BER of NERF companding technique, as seen in Figure 5.24(a). To get same degradation

in BER for all techniques, the degree of companding for AEXP is 1.42 ($d = 1.42$) and the parameter of μ -law technique is 4.2 ($\mu = 4.2$). The parameters of IMADJS technique are set as follows: $\gamma = 1$, $low-in = 0$, $low-out = 0$, $high-in = 0.054$ and $high-out = 0.06$. At the same degradation in BER for all techniques, as displayed in Figure 5.24(a), the less PAPR is achieved with IMADJS technique (PAPR = 1.81 dB). The PAPR of companded signal by using AEXP technique is 4.08 dB, while the PAPR by using the NERF companding technique is 4.30 dB. The highest PAPR is achieved with the μ -law companding technique (PAPR = 6.87 dB). Consequently, at the same degradation in BER, the best improvement in PAPR (8.89 dB) is achieved by using IMADJS technique, as displayed in Figure 5.24(b).

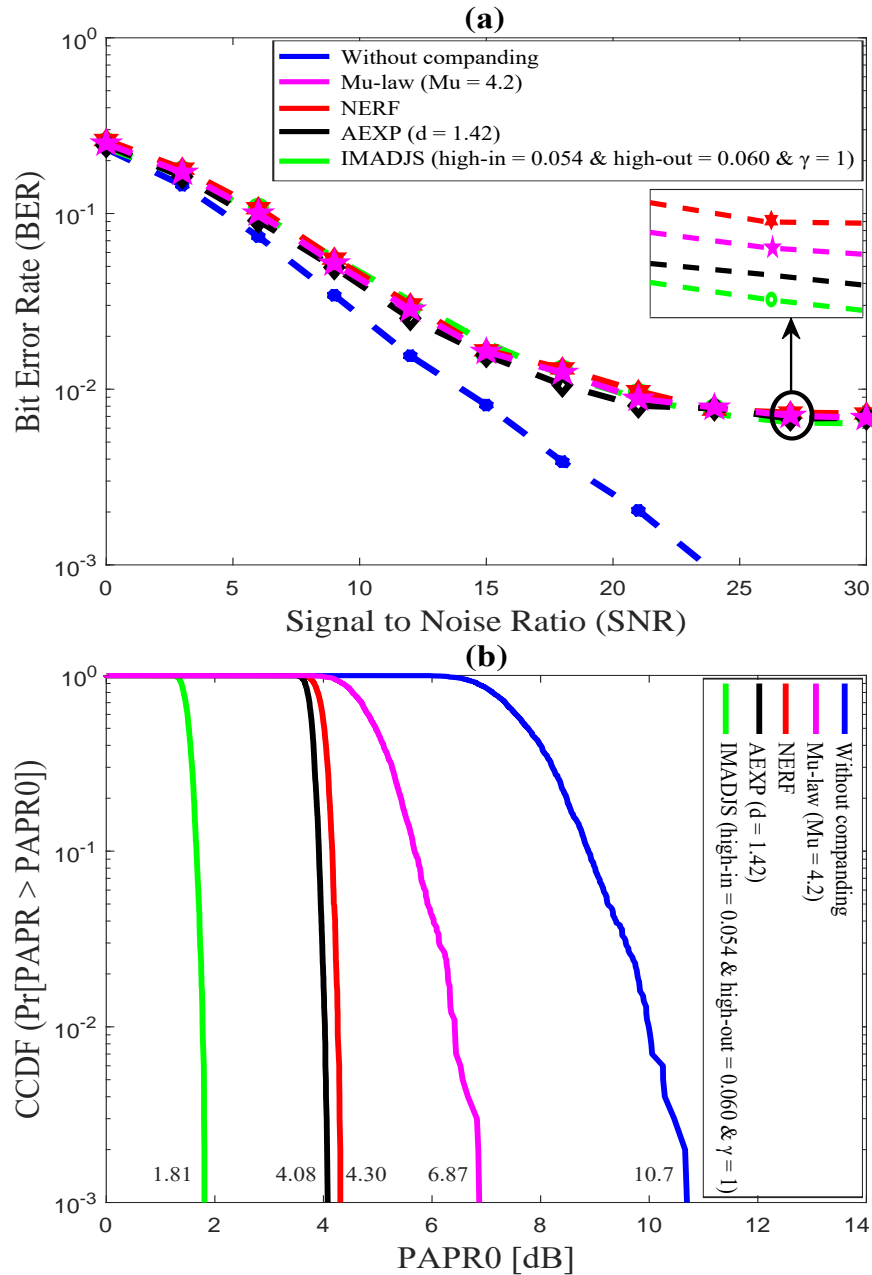


Figure 5.24: Comparing the different companding techniques based on PAPR when they have same BER: (a) same BER and (b) PAPR.

5.3.2 Comparing IMADJS technique with the existing companding techniques based on the average power.

This section presents the simulation results of average power (Avg-pw) for the original signal (without companding) versus the companded signal by using: μ -law, AEXP, NERF and IMADJS companding techniques. To get a fair comparison, the parameters for all techniques are changed to obtain close results in PAPR for all techniques, where $d = 1.3$, $\mu = 28$, $low-in = 0$ $low-out = 0$, $\gamma = 1$, $high-in = 0.093$ and $high-out = 0.1$. According to these parameters, the average power (Avg-pw) for all techniques is portrayed in Figure 5.25. It is observed from Figure 5.25 that, the average power for IMADJS, AEXP and NERF companding techniques are close to the average power of original signal. However, the μ -law companding scheme increases the average power of companded signal, and this is the reason why the μ -law companding technique is the worst in the degradation in BER.

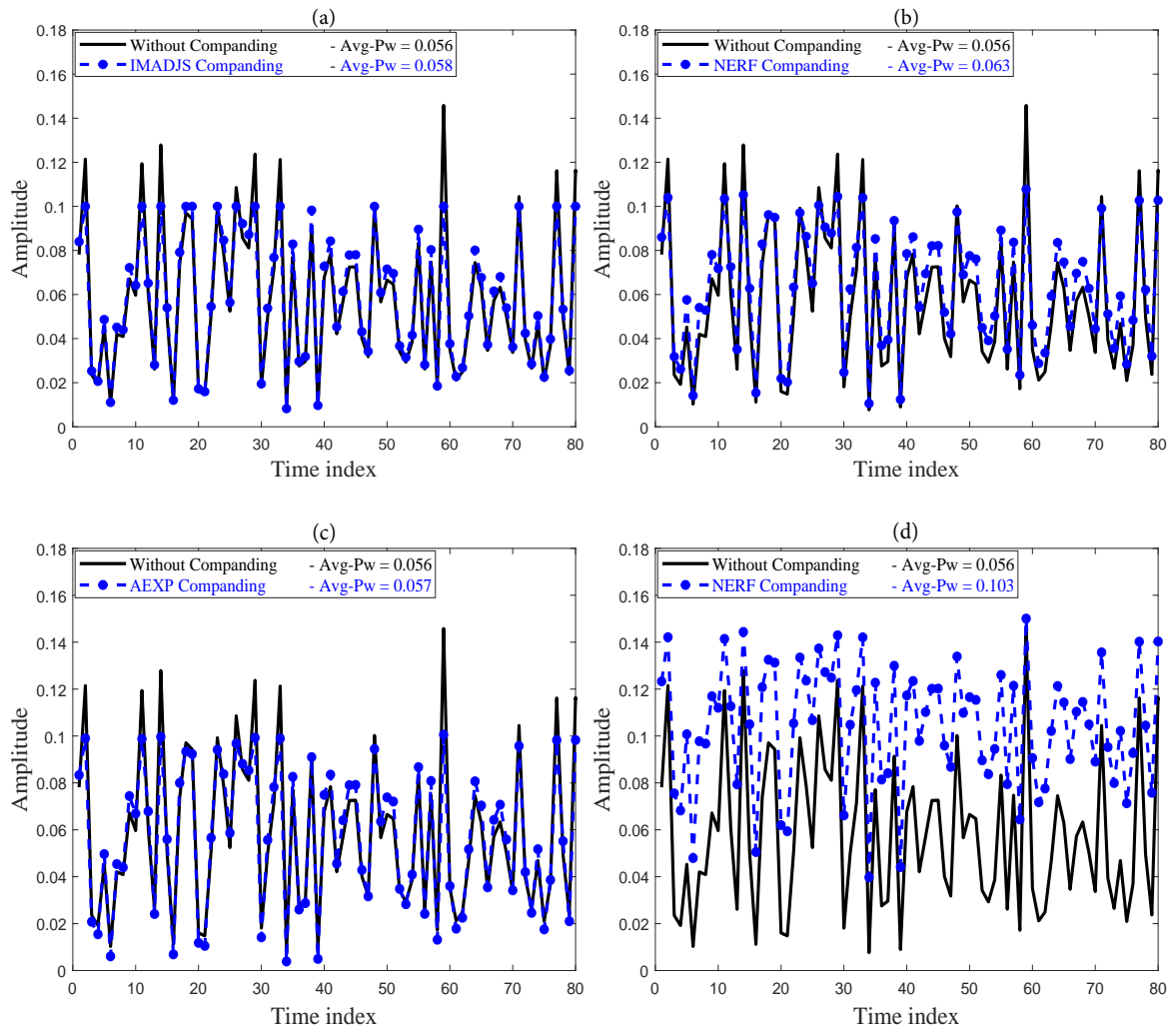


Figure 5.25: Comparing the different companding techniques based on the average power: (a) IMADJS technique, (b) NERF technique, (c) EXP technique and (d) μ -law technique.

5.3.3 Comparing IMADJS technique with the existing companding techniques based on PSD.

This section introduces the effect of companding techniques on the power spectral density (PSD). Many PAPR reduction techniques cause spectrum side-lobes generation. To get a fair comparison, the parameters for all techniques are set to obtain close results in PAPR for all techniques, where $d = 1.3$, $\mu = 28$, $low-in = 0$, $low-out = 0$, $\gamma = 1$, $high-in = 0.093$ and $high-out = 0.1$. According to these parameters, the PSD for all techniques is portrayed in Figure 5.26.

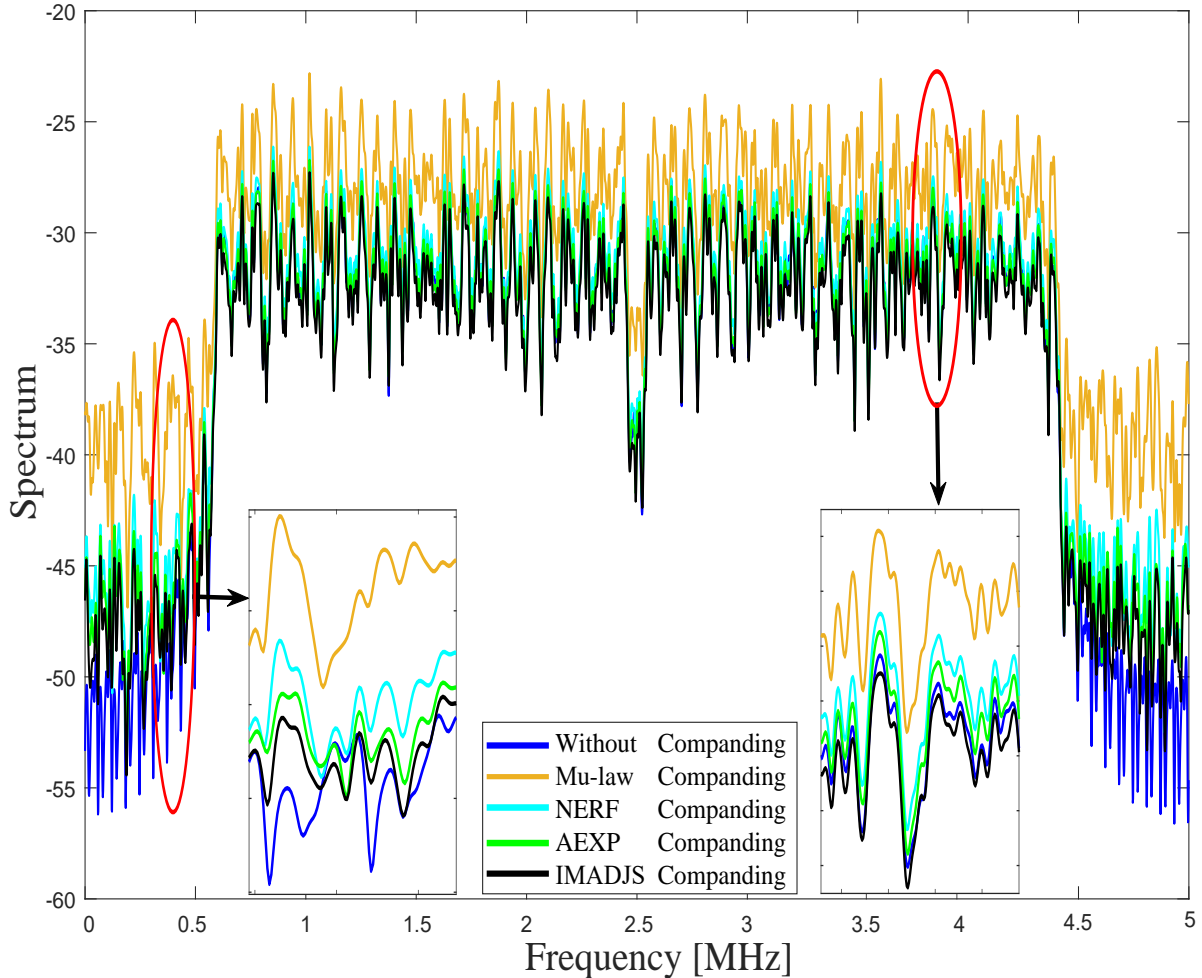


Figure 5.26: PSD for Original signal versus companded signals by using different companding techniques: μ -law, NERF, AEXP and IMADJS.

The new companding technique IMADJS has less effect on the original power spectrum comparing to the other companding schemes such as: AEXP, NERF and μ -law, as seen in Figure 5.26. The companded signals by using the IMADJS technique have a good spectrum characteristic and have nearly no spectral regrowth caused by the PAPR reduction.

It is clear that, the μ -law companding scheme contains high out-of-band component, and the processed signals by the new scheme (IMADJS) have less out-of-band radiation. It is clear from Figure 5.26, the average of out-of-band radiation in IMADJS technique reaches about -50 dB at the frequency 0 MHz, the AEXP and NERF companding techniques reach about -46 dB, while the μ -law companding technique reaches about -37 dB at the frequency 0 MHz. It is the main cause that the IMADJS technique not only increases the small amplitude signals, but also compresses the large amplitude signals while keeping the average power unchanged, which can increase the resistance of small amplitude signals from noise. AEXP, NERF and IMADJS companding techniques have the same principle, where all three techniques increase the small amplitude signals and compress the high amplitude signals. Consequently, they keep the average power before and after companding unchanged. However, the μ -law companding technique increases the average power level and does not change the peak of signals; therefore, the linear operation region in HPA should be larger when the same system performances are requested.

5.3.4 Comparing IMADJS technique with the existing companding techniques based on execution time.

Table 5.6 shows the execution time for four companding techniques (μ -law, IMADJS, NERF and AEXP). Based on the MATLAB program, the IMADJS technique increases the execution time by 1.5% compared to the μ -law companding technique. The NERF technique increases the execution time by 2.5%, while the AEXP technique increases the execution time by 5.4% compared to the μ -law companding technique.

Table 5.6: Execution time for four companding techniques

Method	Execution time using Matlab	Percentage of increasing in the execution time
μ -law	44.7017 s	Using as a reference (Less execution time)
IMADJS	45.3688 s	1.50 %
NERF	45.8183 s	2.50 %
AEXP	47.1264 s	5.40 %

Conclusion and future work

6.1 Conclusion

At the beginning of this study, the transmission impairments were overviewed briefly. Then, the basic principles of the OFDM system have been described with the advantages and drawbacks of OFDM system. This was followed by a detailed overview of the PAPR problem. Next, the companding schemes (such as: A -law, μ -law, AEXP,NERF and IMADJS) were studied, which are highly popular PAPR reduction schemes, due to their good system performance, including PAPR reduction and BER, low implementation complexity and no bandwidth expansion. Each technique was explained separately by its equations and the behavior of the transfer function.

Next, the performance of the companding techniques was studied separately based on the improvement in PAPR and the degradation in BER. Average power of the signal was used as a metric of performance. Companding techniques can be divided into two types: the first type is mainly focuses on enlarging small amplitude signals while keeping peak signals unchanged, such as A -law and μ -law companding techniques. This type increases the average power of the transmitted signals and results in exceeding the saturation region of HPA that may reduce the system performance. A second type of companding scheme has been suggested to overcome the problem of the first type. The second type of companding technique enlarges small signals and compresses large signals simultaneously. This leads to maintain the average power of the signal after companding close to the average power of the signal before companding (Original signal). Absolute exponential (AEXP) companding technique, non-linear error function (NERF) companding technique and the proposed technique (IMADJS) are examples of the second type.

The first simulation part of companding techniques showed that there is always trade-off (balance) between the improvement in PAPR and the degradation in BER. A -law companding technique reduces the high PAPR by increasing the parameter A . Increasing the parameter A enlarges small signals. This increases the average power of the signal, resulting in a reduction in the high PAPR. However, this improvement in PAPR was at the expense of the degradation in BER. Same thing for the μ -law companding technique, where high PAPR decreases by changing the parameter μ . However, this improvement will be at the expense of the degradation in BER. The AEXP companding scheme reduces the high PAPR by changing the degree of companding d . Increasing the degree of companding d enlarges small signals and compresses large signals simultaneously. When the degree of companding d is between [1 , 2], the improvement in PAPR is good compared to the degradation in BER. For d is between [2 , 8], the

improvement in PAPR is large and the degradation in BER is large as well. When the parameter d is greater than 8, the improvement in PAPR is not significant. NERF companding technique enlarges small signals and compresses the peak of the signal and this leads to PAPR improvement, but at the expense of degradation in BER. The proposed technique (IMADJS) has the same principal of AEXP and NERF companding techniques, where it can reduce high PAPR by enlarging small signals and compressing large signals. AEXP, NERF and IMADJS schemes maintain the average power level of the signal before and after companding unchanged, which leads to reduce the degradation in BER compared to the A-law and μ -law companding techniques.

IMADJS companding scheme has five parameters (*low-in*, *low-out*, *high-in*, *high-out* and γ). The effect of each parameter on PAPR and BER has studied separately. The optimum value for *low-in* parameter is zero, because the less PAPR and less BER are achieved at *low-in* = 0. Also, the optimum value for *low-out* parameter is zero, because increasing the *low-out* parameter by small value (0.0015) causes negligible improvement in PAPR. However, this improvement is accompanied by a large deterioration in the BER performance. Accordingly, the best value for *low-out* parameter is zero, because at *low-out* = 0, there is no improvement in PAPR and no degradation in BER. As for *high-in* and *high-out* parameters, decreasing the *high-in* parameter compands large signals, while changing the *high-out* parameter modifies small signals. Consequently, this reduces the high PAPR. However, this improvement is accompanied by deterioration in the BER performance. Based on the above, there is always a trade-off between the improvement in PAPR and the degradation in BER. For the degree of companding (γ), the optimum value for γ is one ($\gamma = 1$), because the least degradation in BER is achieved by using $\gamma = 1$.

The second simulation part has presented a comparative study between the well-known companding techniques and the proposed technique (IMADJS) by sending the data through a multi-path channel. The Rural Urban channel (COST207) with 6 paths was used in this thesis. The comparative study was based on the improvement in PAPR, degradation in BER, average power (Avg-pw) and power spectral density (PSD). To get a fair comparison, the parameters for all techniques are set to obtain close results in PAPR for all techniques, where $d = 1.3$, $\mu = 28$, *low-in* = 0 *low-out* = 0, $\gamma = 1$, *high-in* = 0.093 and *high-out* = 0.1. According to these parameters, the PAPR for all techniques was 4.3 dB. At the same PAPR for all techniques, the least degradation in BER is achieved with the new technique (IMADJS), then AEXP companding technique and NERF companding technique. The worst degradation in BER is achieved by using μ -law companding technique. For comparing the PAPR of all techniques at the same degradation in BER, the parameters for all techniques are set as follows: $d = 1.42$, $\mu = 4.2$, *low-in* = 0 *low-out* = 0, $\gamma = 1$, *high-in* = 0.054 and *high-out* = 0.06. At the same BER for all techniques, the PAPR of IMADJS technique decreased from $PAPR_{(original-signal)} = 10.7$ dB to $PAPR_{(IMADJS)} = 1.81$ dB, the PAPR of AEXP technique decreased to $PAPR_{(AEXP)} = 4.08$ dB, the PAPR of NERF technique decreased to $PAPR_{(NERF)} = 4.3$ dB and the PAPR of A-law technique decreased to $PAPR_{(A-law)} = 6.87$ dB. Consequently, the best improvement in PAPR at the same BER is achieved with IMADJS technique.

For the average power of companding techniques; IMADJS, AEXP and NERF companding techniques almost have the same average power level of the original OFDM signal ($Avg-pw_{(original-signal)} = 0.056$). Where the average power of companded signal by using IMADJS is 0.058 ($Avg-pw_{(IMADJS)} = 0.058$), the average power of companded signal by using AEXP is 0.057 ($Avg-pw_{(AEXP)} = 0.057$) and the average power of companded signal by using NERF is 0.063 ($Avg-pw_{(NERF)} = 0.063$). However, the average power of the μ -law companding technique is greater than the average power of original

OFDM signal, where the average power of companded signal by using μ -law is 0.103 ($Avg-pw_{(\mu-law)} = 0.103$). Increasing the average power eventually distorts the constellation points and making the small points close to the large ones. Consequently, the BER increases as the constellation points get closer.

As for the PSD, the new companding technique (IMADJS) has less effect on the original power spectrum comparing to the other companding schemes such as: AEXP, NERF and μ -law. The μ -law companding scheme contains high out-of-band component. The average of out-of-band radiation of IMADJS technique reaches about -50 dB at the frequency 0 MHz, while the average of out-of-band radiation of original OFDM signal reaches around -52 dB at the frequency 0 MHz. The AEXP and NERF companding technique reach around -46 dB, while the μ -law companding technique reaches about -37 dB at the frequency 0 MHz.

6.2 Future work

The PAPR problem in OFDM is still an ongoing research point, especially for portable devices where the need to minimize the power amplifier linear range is paramount. The IMADJS technique developed in this thesis to reduce the PAPR can be combined with other techniques such as lossy reduction techniques including: Discrete Cosine Transform (DCT), Walsh-Hadamard Transform (WHT), Discrete Hartley transform (DHT) and Discrete Sine Transform (DST). The hybrid methods are considered as better choice for PAPR reduction, because it possesses the advantages of both techniques used in hybridization with slight increase in complexity.

The proposed technique (IMADJS) could be implemented in a complete OFDM transceiver and then implemented in hardware via a FPGA to ascertain whether the latency requirements can be met with the wider bandwidth systems being proposed nowadays, such as LTE and LTE-A.

Bibliography

- [1] A Behrouz Forouzan. *Data communications & networking (sie)*. Tata McGraw-Hill Education, 2007.
- [2] Amir Hadjtaieb. *Performance Analysis of ARQ and Hybrid ARQ over Single-Hop, Dual-Hop, and Multibranch Dual-Hop Networks*. PhD thesis, 2014.
- [3] Muhammad Irfan Ishaq, Yasir Ali Khan, and Muhammad Talha Gul. Precoding in mimo, ofdm to reduce papr (peak to average power ratio), 2012.
- [4] Emad Hassan. *Multi-Carrier Communication Systems with Examples in MATLAB®: A New Perspective*. CRC Press, 2016.
- [5] Ashish Goel. Improved papr reduction in ofdm systems. *Ph.D. dissertation, JAYPEE Institute of Information Technology, India, April, 2013*.
- [6] Gavin Hill. *Peak power reduction in orthogonal frequency division multiplexing transmitters*. PhD thesis, Victoria University, 2011.
- [7] Mathuranathan Viswanathan. Simulation of digital communication systems using matlab. *Mathuranathan Viswanathan at Smashwords*, 2013.
- [8] Ye Geoffrey Li and Gordon L Stuber. *Orthogonal frequency division multiplexing for wireless communications*. Springer Science & Business Media, 2006.
- [9] Rakesh Rajbanshi et al. *Ofdm-based cognitive radio for dsa networks*, 2007.
- [10] Matthias Pätzold, Matthias Patzold, and Mattias Paetzold. *Mobile fading channels*, volume 14. Wiley Online Library, 2002.
- [11] William Stallings and Moumita Mitra Manna. *Data and computer communications*, volume 6. Prentice hall Englewood Cliffs, NJ, 1997.
- [12] A Behrouz Forouzan. *Data communications & networking (sie)*. Tata McGraw-Hill Education, 2006.
- [13] Yong Soo Cho, Jaekwon Kim, Won Young Yang, and Chung G Kang. *MIMO-OFDM wireless communications with MATLAB*. John Wiley & Sons, 2010.
- [14] Thomas Keller and Lajos Hanzo. Adaptive multicarrier modulation: A convenient framework for time-frequency processing in wireless communications. *Proceedings of the IEEE*, 88(5):611–640, 2000.

- [15] Oluyemi Omololu Omomukuyo. *Orthogonal frequency division multiplexing for optical access networks*. PhD thesis, UCL (University College London), 2013.
- [16] Yiyang Wu and William Y Zou. Orthogonal frequency division multiplexing: A multi-carrier modulation scheme. *IEEE Transactions on Consumer Electronics*, 41(3):392–399, 1995.
- [17] William Y Zou and Yiyang Wu. Cofdm: An overview. *IEEE transactions on broadcasting*, 41(1):1–8, 1995.
- [18] Taewon Hwang, Chenyang Yang, Gang Wu, Shaoqian Li, and Geoffrey Ye Li. Ofdm and its wireless applications: A survey. *IEEE transactions on Vehicular Technology*, 58(4):1673–1694, 2009.
- [19] RV Nee and R Prasad. *Ofdm for wireless multimedia communications*. artech house, 2000. *Terrestrial Radio Access (EUTRA) Multiplexing and Channel Coding*, 2012.
- [20] Henrik Schulze and Christian Lüders. *Theory and applications of OFDM and CDMA: Wideband wireless communications*. John Wiley & Sons, 2005.
- [21] Ramjee Prasad. *OFDM for wireless communications systems*. Artech House, 2004.
- [22] Huaiyu Dai and H Vincent Poor. Advanced signal processing for power line communications. *IEEE Communications Magazine*, 41(5):100–107, 2003.
- [23] Jacky S. Chow, Jerry C. Tu, and John M. Cioffi. A discrete multitone transceiver system for hdsl applications. *IEEE journal on selected areas in communications*, 9(6):895–908, 1991.
- [24] Tao Jiang and Yiyang Wu. An overview: Peak-to-average power ratio reduction techniques for ofdm signals. *IEEE Transactions on broadcasting*, 54(2):257–268, 2008.
- [25] Richard van Nee and Ramjee Prasad. *OFDM for wireless multimedia communications*. Artech House, Inc., 2000.
- [26] Guillermo Acosta. Ofdm simulation using matlab. *Smart Antenna Research Laboratory report*, 2000.
- [27] Stephen B Weinstein. The history of orthogonal frequency-division multiplexing [history of communications]. *IEEE Communications Magazine*, 47(11), 2009.
- [28] Bernard Sklar. *Digital communications*, volume 2. Prentice Hall Upper Saddle River, 2001.
- [29] Alina Elena STANCIU, Lăcrămioara-Mihaela NEMȚOI, and Ilona Madalina MOISE. Considerations regarding the spectral efficiency of orthogonal frequency division multiplexing. In *International Conference on DEVELOPMENT AND APPLICATION SYSTEMS*, 2012.
- [30] Faisal Tariq. Impact of papr on link adaption strategies of ofdm based systems. 2007.
- [31] Anil Khatiwada and Hem Dutt Guide Joshi. *PAPR reduction in OFDM System Using Partial Transmit Sequence (PTS) and Precoding Techniques*. PhD thesis, 2014.
- [32] Prasanta Kumar Pradhan. *On Efficient Signal Processing Algorithms for Signal Detection and PAPR Reduction in OFDM Systems*. PhD thesis, 2016.

- [33] Jim Zyren and Wes McCoy. Overview of the 3gpp long term evolution physical layer. *Freescale Semiconductor, Inc., white paper*, 2007.
- [34] SM Abbas, MN Abbas, and SA Mohammed. Slantlet transform-based ofdm scheme. *Journal of Engineering*, 13(3):1638–1647, 2006.
- [35] Rajiv Saxena and Hem Dutt Joshi. Ofdm and its major concerns: a study with way out. *IETE Journal of Education*, 54(1):26–49, 2013.
- [36] Ashish Goel. Improved papr reduction in ofdm systems. 2013.
- [37] Dae-Woon Lim, Seok-Joong Heo, and Jong-Seon No. An overview of peak-to-average power ratio reduction schemes for ofdm signals. *Journal of Communications and Networks*, 11(3):229–239, 2009.
- [38] Athanasios Papoulis and S Unnikrishna Pillai. *Probability, random variables, and stochastic processes*. Tata McGraw-Hill Education, 2002.
- [39] Heung-Gyoon Ryu, Tran Phuong Hoa, Kang Mi Lee, Sang-Woo Kim, and Jin-Soo Park. Improvement of power efficiency of hpa by the papr reduction and predistortion. *IEEE Transactions on Consumer Electronics*, 50(1):119–124, 2004.
- [40] Elena Costa, Michele Midrio, and Silvano Pupolin. Impact of amplifier nonlinearities on ofdm transmission system performance. *IEEE Communications Letters*, 3(2):37–39, 1999.
- [41] R O’neill and LB Lopes. Envelope variations and spectral splatter in clipped multicarrier signals. In *Personal, Indoor and Mobile Radio Communications, 1995. PIMRC’95. Wireless: Merging onto the Information Superhighway., Sixth IEEE International Symposium on*, volume 1, pages 71–75. IEEE, 1995.
- [42] Xiaodong Li and L. J. Cimini. Effects of clipping and filtering on the performance of ofdm. *IEEE Communications Letters*, 2(5):131–133, May 1998.
- [43] Jean Armstrong. Peak-to-average power reduction for ofdm by repeated clipping and frequency domain filtering. *Electronics letters*, 38(5):246–247, 2002.
- [44] Hangjun Chen and Alexander M Haimovich. Iterative estimation and cancellation of clipping noise for ofdm signals. *IEEE Communications Letters*, 7(7):305–307, 2003.
- [45] Xianbin Wang, Tjeng Thiang Tjhung, and CS Ng. Reduction of peak-to-average power ratio of ofdm system using a companding technique. *IEEE transactions on broadcasting*, 45(3):303–307, 1999.
- [46] Tao Jiang, Weidong Xiang, Paul C Richardson, Daiming Qu, and Guangxi Zhu. On the nonlinear companding transform for reduction in papr of mcm signals. *IEEE Transactions on Wireless Communications*, 6(6), 2007.
- [47] Tao Jiang, Yang Yang, and Yong-Hua Song. Exponential companding technique for papr reduction in ofdm systems. *IEEE Transactions on broadcasting*, 51(2):244–248, 2005.
- [48] Xiao Huang, Jianhua Lu, Junli Zheng, Khaled Ben Letaief, and Jun Gu. Companding transform for reduction in peak-to-average power ratio of ofdm signals. *IEEE transactions on wireless communications*, 3(6):2030–2039, 2004.

- [49] Sulaiman A Aburakhia, Ehab F Badran, and Darwish AE Mohamed. Linear companding transform for the reduction of peak-to-average power ratio of ofdm signals. *IEEE Transactions on Broadcasting*, 55(1):155–160, 2009.
- [50] J Hou, JH Ge, and J Li. Trapezoidal companding scheme for peak-to-average power ratio reduction of ofdm signals. *Electronics Letters*, 45(25):1349–1351, 2009.
- [51] Shiann-Shiun Jeng and Jia-Ming Chen. Efficient papr reduction in ofdm systems based on a companding technique with trapezium distribution. *IEEE Transactions on Broadcasting*, 57(2):291–298, 2011.
- [52] Robert W Bauml, Robert FH Fischer, and Johannes B Huber. Reducing the peak-to-average power ratio of multicarrier modulation by selected mapping. *Electronics letters*, 32(22):2056–2057, 1996.
- [53] Leonard J Cimini and Nelson R Sollenberger. Peak-to-average power ratio reduction of an ofdm signal using partial transmit sequences. *IEEE Communications letters*, 4(3):86–88, 2000.
- [54] Seung Hee Han, John M Cioffi, and Jae Hong Lee. Tone injection with hexagonal constellation for peak-to-average power ratio reduction in ofdm. *IEEE Communications Letters*, 10(9):646–648, 2006.
- [55] Brian S Krongold and Douglas L Jones. Par reduction in ofdm via active constellation extension. *IEEE Transactions on broadcasting*, 49(3):258–268, 2003.
- [56] Guosen Yue and Xiaodong Wang. A hybrid papr reduction scheme for coded ofdm. *IEEE transactions on wireless communications*, 5(10):2712–2722, 2006.
- [57] Hong-Jie Chou, Ping-You Lin, and Jung-Shan Lin. Papr reduction techniques with hybrid slm-pts schemes for ofdm systems. In *Vehicular Technology Conference (VTC Spring), 2012 IEEE 75th*, pages 1–5. IEEE, 2012.
- [58] Victor Cuteanu and Alexandru Isar. Papr reduction of ofdm signals using selective mapping and clipping hybrid scheme. In *Signal Processing Conference (EUSIPCO), 2012 Proceedings of the 20th European*, pages 2551–2555. IEEE, 2012.
- [59] T. Sravanti and N. Vasantha. A hybrid technique to reduce papr in ofdm systems. In *2017 Third International Conference on Advances in Electrical, Electronics, Information, Communication and Bio-Informatics (AEEICB)*, pages 416–421, Feb 2017.
- [60] R. Saroj. A cooperative additional hybrid and clipping technique for papr reduction in ofdm system. In *2016 Fifth International Conference on Eco-friendly Computing and Communication Systems (ICECCS)*, pages 53–57, Dec 2016.
- [61] M. Gay, A. Lampe, and M. Breiling. A hybrid papr reduction scheme for ofdm using slm with clipping at the transmitter, and sparse reconstruction at the receiver. In *2014 IEEE 11th International Multi-Conference on Systems, Signals Devices (SSD14)*, pages 1–6, Feb 2014.
- [62] Berna Torun and B Torun. Peak-to-average power ratio reduction techniques for wavelet packet modulation. *MS. thesis*, 2010.
- [63] Seung Hee Han and Jae Hong Lee. An overview of peak-to-average power ratio reduction techniques for multicarrier transmission. *IEEE wireless communications*, 12(2):56–65, 2005.

- [64] Md ANAMUL Islam, N Ahmed, NIZAM UDDIN Ahamed, MATIUR Rahman, and SA Aljunid. Papr reduction in an ofdm system using recursive clipping and filtering technique. *WSEAS Transactions on communications*, 13:291–297, 2014.
- [65] Manju Bala, Mohit Kumar, and Kirti Rohilla. Papr reduction in ofdm signal using signal scrambling techniques. *International Journal of Engineering and Innovative Technology (IJEIT)*, 3(11):140–143, 2014.
- [66] T Jang and Yiyang Wu. An overview of peak-to-average-power ratio reduction techniques for ofdm signals. *IEEE Trans. Broad.*, 54(2):257–268, 2008.
- [67] Xianbin Wang, Tjeng Thieng Tjhung, and Yiyang Wu. On the ser and spectral analyses of a-law companded multicarrier modulation. *IEEE transactions on vehicular technology*, 52(5):1408–1412, 2003.
- [68] T Deepa and R Kumar. Performance analysis of μ -law companding & sqrt techniques for m-qam ofdm systems. In *Emerging Trends in Computing, Communication and Nanotechnology (ICE-CCN), 2013 International Conference on*, pages 303–307. IEEE, 2013.
- [69] Alasdair McAndrew. An introduction to digital image processing with matlab notes for scm2511 image processing. *School of Computer Science and Mathematics, Victoria University of Technology*, 264, 2004.
- [70] Rafael C Gonzalez, Richard E Woods, Steven L Eddins, et al. *Digital image processing using MATLAB.*, volume 624. Pearson-Prentice-Hall Upper Saddle River, New Jersey, 2004.

ملخص الرسالة

تعد تقنية التقسيم الترددي المتعامد (OFDM) من التقنيات متعددة النواقل (Multicarrier) الواعدة لانظمة الاتصالات عريضة النطاق حيث انها تقوم بالتغلب على الاضمحلال الانتقائي التردد للقناة (Frequency selective fading channel). ايضا هذه التقنية تقدم حماية عالية ضد الخفوت الناتج عن تعدد المسارات (Multipath fading) بتحويله الى خفوت مسطح وكذلك حماية ضد الضوضاء (Noise) بذلك تتلاشى الحاجة لطرق تكافؤ القناة المعقدة (Equalizers).

رغم هذه المميزات المتعددة فإن الأنظمة التي تعتمد على التقسيم الترددي المتعامد تعاني من مشكلتين أساسيتين. الأولى هي الحساسية العالية لحدوث إزاحة في تردد الموجة الحاملة (Carrier frequency offsets). أما المشكلة الثانية هي ان الإشارة المرسله بهذه التقنية يكون لها ذروة عالية بالنسبة لمتوسط نسبة الطاقة (PAPR). هذه المشكلة تجعل الإشارة المرسله بتقنية التقسيم الترددي المتعامد حساسة للتشوية الناتج عن التكبير اللاخطي لمكبر القدرة مما يؤدي الى تدهور أداء النظام ككل خاصة معدل الخطأ الرقمي الثنائي (BER).

والغرض من هذه الرسالة هو تحسين أداء النظم اللاسلكية التي تعتمد على تقنية التقسيم الترددي المتعامد من خلال اقتراح بعض الحلول لمشكلة ال PAPR والتي يمكن عرضها كالآتي:

❖ عمل مقارنة لبعض طرق الضغط وفك الضغط (Companding Technique) الموجودة والتي تستخدم لعلاج مشكلة ال PAPR وهذه الطرق يمكن تصنيفها الى صنفين:

● **الصنف الأول:** يعتمد هذا الصنف على رفع الاشارات الصغيرة و هذا يؤدي الى رفع متوسط الطاقة للإشارة مما يؤدي الى تحسين ال PAPR من دون تغيير ذروة الاشارات, لكن هذا الصنف يؤدي الى تدهور أداء النظام خاصة معدل الخطأ الرقمي الثنائي (BER). من أمثلة هذه الطريقة:

A-law companding technique

μ -law companding technique

● **الصنف الثاني:** يعتمد هذا الصنف على ضغط ذروة الاشارة و تكبير الاشارات الصغيرة مما يؤدي الى معالجة مشكلة ال PAPR مع المحافظة على متوسط الطاقة للإشارة بعد معالجتها قريبة من متوسط الطاقة قبل معالجتها, هذا بدوره يؤدي الى المحافظة على أداء النظام من التدهور خاصة معدل الخطأ الرقمي الثنائي (BER). من أمثلة هذه الطريقة:

Absolute exponential companding technique (AEXP)

Non-linear error function companding technique (NERF)

❖ إقتراح طريقة جديدة لمعالجة مشكلة ال PAPR وهذه الطريقة موجودة في معالجة الصور وتستخدم لتحسين الصور وتسمى (Image adjustment function). الطريقة الجديدة تحافظ على متوسط الطاقة للإشارة وبالتالي تحافظ على أداء النظام.

تم دراسة الطرق القديمة والطريقة الجديدة في بيئة ذات ضوضاء كبيرة (Noisy Media). وكانت النتائج كالتالي:

- حصلنا على افضل نتيجة باستخدام الطريقة الجديدة IMADJS حيث أن هذه الطريقة فعالة في البيئة ذات الضجيج العالي.
- عند تثبيت نسبة القدرة العظمى الى القدرة المتوسطة (PAPR) لكل الطرق, تم الحصول على اقل نسبة خطأ (BER) باستخدام الطريقة الجديدة
- عند تثبيت نسبة الخطاء في البتات (BER) لكل الطرق, تم الحصول على اقل قيمة لنسبة القدرة العظمى الى القدرة المتوسطة (PAPR) باستخدام الطريقة الجديدة.



مهندس : عبدالواحد محمد عبدالواحد

تاريخ الميلاد : 1985 \ 03 \ 01

الجنسية : يمني

تاريخ التسجيل : 2015 \ 10 \ 01

تاريخ المنح : 2019 \ \

القسم : هندسة الإلكترونيات والاتصالات الكهربائية

الدرجة : ماجستير العلوم

المشرفون :

أ.د. أمين نصار

أ.د. حسن مصطفى

الممتحنون :

أ.د. السيد مصطفى سعد (الممتحن الخارجي) (أستاذ دكتور - كلية الهندسة - جامعة حلوان)

أ.د. أحمد حسين خليل (الممتحن الداخلي)

أ.د. أمين نصار (المشرف الرئيسي)

أ.د. حسن مصطفى (مشرف)

عنوان الرسالة:

طريقة جديدة لتقليل نسبة القدرة العظمى الى القدرة المتوسطة في نظام
التقسيم الترددي المتعامد

الكلمات الدالة:

التقسيم الترددي المتعامد، نسبة القدرة العظمى الى القدرة المتوسطة، خوارزمية تعديل السطوع بالصور و تقنيات الضغط وفك الضغط.

ملخص الرسالة:

في العمل المقدم، تم استخدام تقنية جديدة لحل مشكلة ارتفاع نسبة القدرة العظمى الى القدرة المتوسطة (PAPR) في انظمة التقسيم الترددي المتعامد (OFDM) حيث ان هذه الطريقة تستخدم لتحسين الصور. حيث ان هذه الطريقة تم تطبيقها لأول مرة لحل مشكلة ارتفاع نسبة القدرة العظمى الى القدرة المتوسطة (PAPR) في انظمة التقسيم الترددي المتعامد (OFDM). الخوارزمية أظهرت كفاءة كبيرة في حل المشكلة مع الحفاظ على اداء النظام خاصة معدل الخطأ الرقمي الثنائي (BER). تم استخدام برنامج الماتلاب لمحاكاة الخوارزمية الجديدة بالاضافة الى التقنيات القديمة، حيث تم مقارنة التقنية الجديدة بالتقنيات السابقة واثبتت كفاءتها خاصة في البيئة عالية الضجيج، حيث تم الحصول على افضل النتائج في تقليل ارتفاع نسبة القدرة العظمى الى القدرة المتوسطة بالاضافة الى المحافظة على اداء النظام.

طريقة جديدة لتقليل نسبة القدرة العظمى الى القدرة المتوسطة
في نظام التقسيم الترددي المتعامد

إعداد
عبدالواحد محمد عبدالواحد

رسالة مقدمة إلى كلية الهندسة - جامعة القاهرة
كجزء من متطلبات الحصول على درجة ماجستير العلوم
في
هندسة الكترونياات والاتصالات الكهربية

لجنة الفحص والمناقشة

المشرف الرئيسي

مشرف

ممتحن داخلي

ممتحن خارجي

اد. أمين نصار

اد. حسن مصطفى

اد. أحمد حسين خليل

اد. السيد مصطفى سعد

(أستاذ دكتور في كلية الهندسة، جامعة حلوان)

كلية الهندسة، جامعة القاهرة

الحيزة، جمهورية مصر العربية

طريقة جديدة لتقليل نسبة القدرة العظمى الى القدرة المتوسطة
في نظام التقسيم الترددي المتعامد

إعداد
عبدالواحد محمد عبدالواحد

رسالة مقدمة إلى كلية الهندسة - جامعة القاهرة
كجزء من متطلبات الحصول على درجة ماجستير العلوم
في
هندسة الكترونياات والاتصالات الكهربية

تحت إشراف

اد. حسن مصطفى

أستاذ دكتور في الإلكترونياات
قسم الإلكترونياات والاتصالات الكهربية
كلية الهندسة، جامعة القاهرة

اد. أمين نصار

أستاذ دكتور في الإتصالات
قسم الإلكترونياات والاتصالات الكهربية
كلية الهندسة، جامعة القاهرة

كلية الهندسة، جامعة القاهرة

الحيزة، جمهورية مصر العربية

2019



Cairo University



طريقة جديدة لتقليل نسبة القدرة العظمى الى القدرة المتوسطة
في نظام التقسيم الترددي المتعامد

إعداد
عبدالواحد محمد عبدالواحد

رسالة مقدمة إلى كلية الهندسة - جامعة القاهرة
كجزء من متطلبات الحصول على درجة ماجستير العلوم
في
هندسة الكترونياات والاتصالات الكهربية

كلية الهندسة، جامعة القاهرة

الحيزة، جمهورية مصر العربية

2019